

**HOLTEC INTERNATIONAL**

**HI-STORM 100 CERTIFICATE OF COMPLIANCE 72-1014**

**LICENSE AMENDMENT REQUEST 1014-1**

**REVISION 2**

**JULY, 2001**

**VOLUME 1 OF 2**

**HOLTEC INTERNATIONAL**

**LAR 1014-1**

**REVISION 2**

**JULY, 2001**

**VOLUME I OF II**

**HI-STORM 100 CASK STORAGE SYSTEM  
DOCKET NO. 72-1014  
TAC NO. L23082**

**HOLTEC RESPONSES TO NRC REQUEST FOR ADDITIONAL INFORMATION**

**LICENSE AMENDMENT REQUEST 1014-1**

**1.0 General Description**

**Question 1.1**

Provide detailed procedures of how a loaded HI-STORM 100S is moved into and out of the Part 50 facility with neither the temporary lid nor permanent lid installed as described on page 1.2-8 of the Safety Analysis Report (SAR). "Users who require specific configuration may move the loaded HI-STORM 100S overpack into or out of the Part 50 facility with neither the temporary nor the permanent lid installed. Before moving the overpack to the ISFSI, the permanent lid should be installed as soon as practicable after the loaded overpack leaves the Part 50 facility."

These evolutions are not described in SAR Chapter 8, "Operating Procedures." This information is not provided and is needed to assure compliance with 10 CFR 72.11.

**Response 1.1**

New subsection 8.1.1.2 has been added to the operating procedures in FSAR Chapter 8 to add required administrative controls pertaining to the movement of the HI-STORM 100 overpack without the permanent lid installed. The new administrative controls will require users to support the overpack from below and maintain slow speed and positive control over the load during movement, in addition to the originally proposed requirement to install the permanent lid as soon as practicable after the overpack leaves the Part 50 facility. Recognition of these administrative controls has also been added to the detailed procedures in the body of Sections 8.1. and 8.3.2. The specifics of how these administrative controls are implemented are necessarily left to the cask users to determine, based on site specific needs and capabilities.

**Question 1.2**

Revise description of multi-purpose canister (MPC)-68F on page 1.2-25 to be consistent with CoC Appendix B and Table 1.2.1. The correct number of allowed damaged fuel canisters (DFCs) containing debris is 4.

This information is needed to assure compliance with 10 CFR 72.11.

**Response 1.2**

The FSAR text in Section 1.2 has been revised as suggested.

**Question 1.3**

Explain and resolve the discrepancy between description of MPC-68FF on page 1.2-26 and the description in table 1.2.1. According to table 1.2.1, the MPC-68FF can only store up to 4 DFCs with Dresden Unit 1 or Humboldt fuel debris, but the description implies that any number of DFCs with this debris can be stored.

This information is needed to assure compliance with 10 CFR 72.11.

**Response 1.3**

The MPC-68FF can accommodate up to eight (8) damaged fuel containers containing fuel debris from *any* BWR plant, including Dresden Unit 1 and Humboldt Bay. This limit is based on the containment analysis performed for transportation of the MPC-68FF. To maintain transportability of the MPC, this limit must also apply in storage. The FSAR text and tables and the proposed CoC revision have been reviewed and modified as necessary to reflect this limit.

**Question 1.4**

Table 1.2.6 on page 1.2-33 does not identify the need for special bolt down procedures for the HI-STORM 100A/100SA when the units are placed in storage at the ISFSI pad. Include this step to the HI-STORM 100 Operations Sequence.

This information is not included and is needed to assure compliance with 10 CFR 72.11.

**Response 1.4**

An item has been added to Table 1.2.6 to recognize the need to torque the nuts onto the studs for users of HI-STORM 100A and HI-STORM 100SA.

**Question 1.5**

Address the apparent conflict between the general verbal description of the basket assembly and the configuration for the MPC-24 series as shown on the drawings with regard to the welding of the baskets. Also revise the title of Figure 3.1.1 to "MPC-68 Fuel Basket Geometry." On page 1.2-3, in the third paragraph, last sentence, it is stated that, "All MPC baskets are formed from an array of plates welded to each other, ..." On page 3.1-3, second paragraph, the last two sentences, it is stated that, "Welding of the basket plates along their edges essentially renders the fuel basket into a multi-flange beam. Figure

U.S. Nuclear Regulatory Commission  
ATTN: Document Control Desk  
Document ID: 5014422  
Attachment 1  
Page 3 of 71

3.1.1 provides an isometric illustration of a fuel basket for the MPC-68 design.” It is noted that the title of Figure 3.1.1 is, “MPC Fuel Basket Geometry.”

The MPC-24 series as shown in Drawing Number 1395, Sheets 1 and 2, the proposed MPC-24E/24EF cross-section shown in Figure 1.2.4A and Drawings 2889 and 2890 each show a corner detail that indicates all basket cells in this series have at least one corner that is not constructed by welding intersecting plates, but is instead a formed or bent corner configuration. In some cases there are only two of the four corners that are fabricated by welding with the other two being formed or bent. In these cases there is at least one corner of the cell that is unsupported by intersecting plates.

This information is needed to assure compliance with 10 CFR 72.11 and 72.236.

#### **Response 1.5**

The RAI is correct in noting that some corner details of the fuel storage cells in the MPC-24, -24E, and -24EF do not include intersecting plate welds. This oversight has been corrected in the FSAR by revisions to FSAR Figure 3.1.1, and Section 1.2.1.1. The title of Figure 3.1.1 has been revised to be “MPC-68 and MPC-32 Fuel Basket Geometry” to correctly include both of the non-flux trap basket designs. FSAR Section 1.2.1.1 has been revised to more accurately describe the flux trap and non-flux trap basket designs.

## **2.0 Principal Design Criteria**

### **Question 2.1**

SAR Table 2.0.5, included in the section of the principal design criteria, addresses the interface between the cask and the pad for the anchored version of the Hi-Storm 100A.

- A.** Clarify if the embedment for the connection of an anchor stud to the concrete pad is cast-in-place exclusively or post-installed.
- B.** Provide sample design parameters for an acceptable embedment to which the anchor studs will be connected for staff audit.
- C.** ACI 349-85, Appendix B, has been shown to be non-conservative in some applications through testing and there are changes that are ready for implementation by the building and construction industry. Justify the continued use of ACI 349-85, Appendix B, as a reference for anchorage to concrete. Explain what design provisions need to be mandated for the designer of the cask concrete pad and the anchorage embedment that would become part of the certificate of compliance under the site-specific parameters and analyses.

This information is required to assure compliance with 10 CFR 72.236.

### **Response 2.1A**

The embedment for the connection of the anchor studs to the concrete pad is required to be cast-in-place, exclusively. This clarification has been added to the "Comment" column of FSAR Table 2.0.5.

### **Response 2.1B**

New FSAR Figure 2.A.1 shows an example of an acceptable fastening detail for HI-STORM 100A (and 100SA). New FSAR Table 2.A.1 provides specific parameters for a typical embedment for use with the design basis high seismic spectra. As further noted in FSAR Appendix 2.A and Section 3.4.3.b of Appendix B to the CoC, the HI-STORM 100A (and 100SA) embedment design at a particular ISFSI site is the responsibility of the ISFSI owner. The governing Code for embedment design is Appendix B of ACI-349-97. The FSAR and CoC has been revised to allow users to follow a later edition of this Code provided a written reconciliation is performed.

### **Response 2.1C**

Appendix B in ACI-349-(85) is essentially unchanged in every version of ACI-349 through 1997 with no major modifications in the design methodology. Versions of ACI-349 Appendix B, through 1997, base the design of the embedment on ductile failure of the steelwork. The

proposed 2001 revision of Appendix B, while encouraging design governed by ductile failure, appears to base all formulas and guidance on test data that resulted in breakout of the concrete rather than failure of the steelwork. We have reviewed the draft of the proposed 2001 revision of ACI-349, Appendix B and the public comments generated subsequent to the initial draft release. We have reached the conclusion that the proposed revision cannot be applied directly to the design of the deep anchors required for the HI-STORM 100A anchored cask in a high seismic environment and therefore should not be specified as the governing design document. Therefore, we propose to specify the 1997 version of Appendix B of ACI-349 as the applicable design code in the CoC. The FSAR text in Appendix 2.A has been revised to refer to ACI-349-97 for deployment of HI-STORM 100A and HI-STORM 100SA. In addition, Appendix 2.A has also been revised to instruct the embedment designer to consider relevant test data in designing the pad embedment for anchored casks. The justification for our position is detailed below:

The detailed formulas provided in the proposed 2001 revision to Appendix B (design procedures in B.5.2 and B.6.2) do not apply to the full range of acceptable embedment designs proposed for the anchored casks as their use is precluded for embedment lengths in excess of 25 inches (because no test data in that range was available to use in the development of the formulas). Therefore, for deep anchors, proposed ACI-349, Appendix B, Section B.4.2 will be the designer's only recourse, which unfortunately contains no design formulas and mandates testing of the embedment, with due consideration of size effects, to verify the formulas used.

However, the Code Committee themselves, in a response to a comment, stated "Unfortunately, it is not reasonable to perform the comprehensive tests required by this section to establish a design model. The committee will continue to review data for such deep fasteners and hope to develop design requirements for inclusion in a future revision." In essence, the proposed 2001 revision to ACI-349 Appendix B offers no guidance for the design of deep embedments (beyond 25 inches) except to perform tests that incorporate size effects. This is in contrast to Appendix B of ACI-349 (97), which provides a rational design basis for all cast-in-place anchors without requiring testing. One of the comments on the proposed 2001 revision to ACI-349, Appendix B (by a former ACI Committee member) notes that there have been no reported failures of a properly designed embedment in accord with previous ACI-349 Appendix B methodology. It is, therefore, appropriate to invoke ACI-349 (97) as the governing code. The FSAR, however, should recognize that additional test data germane to deep anchors, if available, should be factored into the embedment design as would befit a sound engineering practice.

The proposed requirements for HI-STORM 100A anchorage and embedment design in Section 3.4.3.b of Appendix B to the CoC have been revised to remove the "length of stud below the nut" requirement and to add a note allowing site-specific embedment designs, subject to certain limits specified in the CoC and FSAR. Appendix B to ACI 349-97 is the code specified for the cast-in-place embedment design. Later editions of this code may be used if a written reconciliation is performed.

### **Question 2.2**

In proposed Appendix 2.A, on pages 2A-1 and 2A-2, the requirements of ACI-349 are noted as Reference 2.02 for the design and construction of the ISFSI pad. Reference 2.02 is ACI-349-85, a document that has been revised, issued, and become effective twice (1990 and 1997) since the 1985 document became effective. As discussed in the previous RAI, ACI-348-85 [sic] has been revised (ACI 349-01) and became effective on February 1, 2001.

Provide your justification for prescribing the use of an outdated version of the ACI 349 Code, especially in view of the significant changes that have been made in such subject areas as in Chapter 12, Development and Splices of Reinforcement. In providing this justification, indicate how any changes made in the current ACI 349-01 since the 1985 version will have no significant impact on the design of an ISFSI pad.

This information is required to assure compliance with 10 CFR 72.236.

### **Response 2.2**

It is our understanding that the 2001 Edition of Appendix B to ACI-349 was approved by the governing ACI working group in February, 2001, but it is not yet approved by ACI or considered effective. As noted in the previous response, we have replaced references to the 1985 version of ACI-349 with references to the 1997 version, including Appendix B, in the design and analysis of the ISFSI pad for anchored casks. Please note that previously licensed commitments to the 1985 edition of ACI-349 have remained unchanged.

### **Question 2.3**

On page 2A-1, Section 2.A.2, Item 4, it is stated that, "The American Concrete Institute guidelines on reinforced concrete design of ground level slabs to minimize thermal and shrinkage induced cracking shall be followed." This statement identifies an important aspect of the design, construction, and subsequent performance of the important to safety ISFSI pad that is to be provided by the anchored cask user. The statement however, lacks sufficient specificity for the cask user to design, construct, and monitor the ISFSI pad. Based on the Holtec statement it would appear that ACI 360R-92, "Design of Slabs on Grade," ACI 302.1R, "Guide for Concrete Floor and Slab Construction," and ACI 224R-90, "Control of Cracking in Concrete Structures," represent the major documents that should be identified. Provide additional specificity regarding the performance characteristics that are needed for the concrete ISFSI pad such as limits on concrete shrinkage and/or minimum steel areas beyond any that are identified in the ACI 349 code requirements for the 100S.

This information is required to assure compliance with 10 CFR 72.236.

### **Response 2.3**

We concur with the staff that we should identify applicable major documents. ACI 360R-92, ACI 302.1R, and ACI 224R-90 are now identified in Appendix 2A as being documents that should be reviewed and utilized, as applicable, by the ISFSI pad designer for anchored HI-STORM overpacks. Since the detailed design of the ISFSI pad itself is not within the purview of the FSAR, its specification has been appropriately be limited to load combinations and minimum depths and strength requirements for the concrete so that the clear interface between the cask designer and the ISFSI pad designer is preserved.

### **Question 2.4**

Clarify the apparently conflicting requirements for the steel embedments. On page 2A-2 it is stated that, "The steel embedment, including the anchorage bolts, are required to follow the provisions stipulated in ACI 349 [2.02], Appendix B "Steel Embedment" and the associated Commentary on Appendix B." On page 1.2-8 in discussing the anchor studs it is stated that, "during the seismic event the maximum bolt axial stress remains below the limit prescribed for bolts in the ASME Code, Section III, Subsection NF (for Level D conditions)." It appears that these two different code references will not provide consistent requirements. In one case the allowable stress for the embedment steel in tension would be the yield strength or 0.7 times the ultimate strength, whichever is smaller whereas the other would be 0.9 times the yield strength or 0.8 times the ultimate strength, whichever is smaller.

This information is required to assure compliance with 10 CFR 72.236.

### **Response 2.4**

The jurisdictional boundaries have been established by considering the interfaces between the components and the load path. The ISFSI pad concrete (including the amount and placement of steel reinforcement) and all steel embedment in intimate contact with the concrete (cast-in-place) are governed by ACI-349-97, including Appendix B. Above the top surface of the ISFSI pad, the HI-STORM 100A overpack steel structure is governed by ASME III, Subsection NF, as described in the FSAR. The cask anchor studs, which are pre-loaded in their as-installed state, constitute the connecting component between the overpack and the ISFSI pad. The anchor stud interfaces are defined as:

1. an interface with the cast-in-place steel embedment at the loaded surface between each stud and its anchor receptacle, and
2. an interface with the overpack at the loaded surface between the anchor stud nut and the overpack baseplate.

Since the anchor studs are not in intimate contact with the concrete, they are designed to the same Code limits as the overpack steel structure (ASME III, NF). FSAR Table 2.0.5 has been revised to define the interfaces as described above. For additional clarification, we

U.S. Nuclear Regulatory Commission  
ATTN: Document Control Desk  
Document ID: 5014422  
Attachment 1  
Page 8 of 71

have also added text and a figure depicting a representative HI-STORM 100A anchor stud receptacle to proposed FSAR Appendix 2.A (see also Response 2.1B).

### **3.0 Structural Review**

#### **Question 3.1**

A number of editorial issues were identified. Review the issues and make changes as necessary. The SAR should be internally consistent.

- A.** Page 2 of 71 of Attachment 1, "Summary of Proposed Changes," to the Holtec letter, dated October 6, 2000, appears to have some erroneous text. The 3<sup>rd</sup> line of the 2<sup>nd</sup> paragraph under the "Reason for Proposed Changes" for Change No. 2A contains the following words: "...where the heat removal system may not be able to cannot be restored within Completion Times."
- B.** The proposed page 3.6-10 for Revision 1 that continues the List of Appendices Included in Chapter 3 that begins on page 3.6-9 has not been updated to be consistent with the addition of Appendices AO, AP, AQ, AR, and AS identified in the List of Effective Pages for Proposed FSAR Revision 1. The Table of Contents has also not been updated.
- C.** Pages v and vi of the Table of Contents, Revision 1A, indicates that Appendices 3.P, 3.Q, and 3.V have been deleted. On page 3.6-9, Revision 1, under "Appendices Included in Chapter 3," it is indicated that Appendices 3.P, 3.Q and 3.V are included and address the MPC-32, and on pages 10, 11 and 16, Revision 1 of the "List of Effective Pages for Proposed FSAR Revision 1," it is indicated these Appendices are included as Revision 1.
- D.** Page 3.6-9, Revision 1, lists Appendix 3.U as, "HI-STORM 100 Component Thermal Expansions-MPC-24 and 24E." Page vi, Revision 1A, of the Table of Contents lists Appendix 3.U as, "HI-STORM 100 Component Thermal Expansions-MPC-24" and Appendix 3.AQ as "HI-STORM 100 Component Thermal Expansions; MPC-24."
- E.** On page 2A-1 under Section 2.A.2, Item 3, the document "ACI 3449" is identified instead of ACI 349.

#### **Response 3.1A through 3.1E**

The summary of proposed changes document accompanying the amendment request has been revised and is resubmitted with this RAI response. The revised summary of proposed changes includes a correction to the text identified in RAI 3.1A, as well as other changes discussed in our meeting with the SFPO on May 15, 2001 and our letter of May 18, 2001. Modifications in the summary of proposed changes document are indicated with new text in italics, deleted text in strikeout, and revision bar in the right-hand margin.

The other editorial discrepancies (3.1B through 3.1E), pointed out by the staff, have been corrected and the FSAR text revised as required.

### **Question 3.2**

For the new lid concept of the 100S on page 3.AO-4 it is noted that welds on the shear bar of the 100S include a groove weld and a fillet weld. On page 3.AO-2 the weld size is noted to be 0.43125". The welds call out and sizing were not located on Drawings 3068 or 3074 or in the Notes on Drawing 3073 where it would be expected. Indicate where these welds are specified on the drawings, or revise the drawings as necessary.

This information is required to assure compliance with 10 CFR 72.236.

### **Response 3.2**

The staff reviewer is correct. However, based on other questions and comments (see Questions 3.3 through 3.8) pertaining to the HI-STORM 100S lid analyses, changes to the shear bar concept have been made. A complete shear ring has replaced the separate shear bar and a new set of drawings has been issued that replace the existing drawings applicable to the HI-STORM 100S lid. New drawing series 3443 has been developed for the HI-STORM 100S, with the shear ring configuration depicted on sheets 5 and 7. The overpack top plate (Item 11 of Sheet 5) bears against the shear ring attached to the bottom of the overpack lid (Item 31 on Sheet 7) to resist the shear load. The new drawings also reflect the correct weld configuration for this ring as revised to respond to issues raised in the remainder of the questions in this section of the RAI. The calculations appearing in proposed FSAR Appendix 3.AO have been revised accordingly and have been relocated from the FSAR to the supporting calculation package as a part of the proposed Revision 1B of the FSAR. The appropriate additional information regarding this design modification required to respond to balance of these questions has been added to FSAR Section 3.4.

### **Question 3.3**

On Drawing 3073 for the new lid concept of the 100S there is a call out for Item 52, Shear Bar, "See Note 2 and Detail B on Drawing 3074." Drawing 3074 appears to have only a Note 1. Clarify this reference.

This information is required to assure compliance with 10 CFR 72.236.

### **Response 3.3**

The call out refers to Note 2 (on Dwg. 3073) and Detail B on Drawing 3074. As noted in the response to Question 3.2, Drawings 3073 and 3074 are withdrawn and new drawings have been created that reflect the changes made to address the issues raised in Questions 3.4 through 3.8. The appropriate drawing series number is now 3443 and the revised drawings have the proper call outs, where applicable.

### **Question 3.4**

Clarify the design changes and drawing 3074 associated with the 100S lid. Drawing 3074 is indicated to be Revision 0, however it appears that there have been changes made in the design concept during the design process since the remnants of a previous concept to transfer the lid load to the cask body under accident conditions in the area of the lid stud as opposed to the periphery of the lid. A call out for Item 52, the shear bar, is shown pointing to no part within the dotted circle defining Detail C and there is a vertical dimension of 2.25 +/- 1/16 shown in the same highlighted area that apparently does not dimension a current part.

This information is required to assure compliance with 10 CFR 72.236.

### **Response 3.4**

The question correctly points out a discrepancy in the design drawing. The call out for item 52 is in an incorrect location and the dimension noted should not be there. As noted in Response 3.2, the shear bar configuration has been altered from its configuration and replaced by a shear ring. The new HI-STORM 100S drawing series, 3443, correctly dimensions components designed to transfer the shear. The design changes in the HI-STORM 100S lid, resulting from these questions, are made to separate the functions of the studs and the shear resisting components. These design changes ensure that a full shear ring resists all lateral load arising from a non-mechanistic tipover event and that the studs are not exposed to shearing and bending loads. The studs develop only tensile loads to resist a rigid body rotation of the lid relative to the HI-STORM 100S overpack.

### **Question 3.5**

Clarify and make any necessary revisions associated with the inconsistencies with the lid studs for the 100S. On pages 3.AO-3 and 3.AO-4 the calculations show that the four 3-1/4" diameter lid studs in transferring the lateral load from the tipover accident condition will impose such a large bearing stress on the edge of the 0.5" thick lid shield ring that the load cannot be sustained since the bearing stresses will exceed 190,000 psi. The statement is then made that, "This demonstrates that the bolts cannot support the shear load." The design calculation (see Drawing 3074) then proposed to utilize the addition of the approximate quadrants of circumferential shear bars (Item 52) that will be welded to the cask top plate (Item 9). The shear bar is then to resist the total lateral lid load by the edge bearing of the lid shield ring (Item 27) on the shear bar (Item 52). The permitted radial gap between the lid shield ring (Item 27) and the shear bar (Item 52) can be as much as 0.25" as shown on Drawing 3074, Detail Item 52. The hole in the lid shield ring (Item 27) is detailed on Drawing 3074 to be 3-3/4" +/- 1/16" in diameter. With the -1/16" diameter tolerance the hole could have a radius of 1.84375". The stud that passes through this hole is 3-1/4" diameter (radius=1.625") leaving a radial gap between the stud and the edge of the hole in the lid shield ring (Item 27) of 0.21875". This radial gap is less than the 0.25" gap allowed between the lid shield ring and the shear lug. This appears to mean that the

stud will still be loaded before the lid shield ring comes into bearing contact against the shear bar. This condition would negate the design assumptions used in the design calculation in Appendix 3.AO.

This information is required to assure compliance with 10 CFR 72.236.

### **Response 3.5**

The condition noted in Question 3.5 is correct when worst case tolerances are employed. As previously stated, the issues raised, as a whole, required reconfiguring the lid to ensure that the shear load path and the tensile load path do not intermingle. As noted in Response 3.2, the calculation previously contained in proposed new FSAR Appendix 3.AO has been relocated to an internal Holtec calculation package and revised to reflect the design modifications necessitated to respond to these RAI's. The revised calculations reflect the changes to the drawings based on the revised lid configuration noted previous responses. The revised lid configuration is toleranced so that the lid studs never experience a shear load during a non-mechanistic tipover event. There will be no bearing stress experienced in the neighborhood of the stud holes; the shear ring resists all shear force with the studs resisting only tensile loads resulting from resisting any rotation of the lid relative to the overpack. Drawing series 3443 documents the new lid shear ring design details with detailed supporting calculations in the calculation package. The FSAR text contains a revised summary of safety factors for the HI-STORM 100S lid.

### **Question 3.6**

Describe how the load of the 100S lid is to be transferred to the cask body when uniform edge contact without deformation has been assumed between the lid shield ring (Item 27) and the shear bar (Item 52) over one of the four circumferential sector sections of the shear bar. On page 3.AO-4 the calculations for the safety factors for steel bearing stresses and for weld shear stresses are provided to demonstrate the integrity of the lid to cask body connection under the tip over accident condition. It appears that uniform edge contact without deformation has been assumed between the lid shield ring (Item 27) and the shear bar (Item 52) over one of the four circumferential sector sections of the shear bar. Because the edge radius of the shear beam and the lid shield ring can be up to 0.25" in difference, there will not be uniform contact. For radial movement of one with respect to the other, the contact between them will not be described as a surface with an area equal to the thickness of Item 27 times the arc length of Item 52. The contact without deformations will be a line across the thickness of Item 27 because of the different radii. It appears that the assumption needs to be reassessed.

This information is required to assure compliance with 10 CFR 72.236.

### **Response 3.6**

The purpose of the bearing surface is to transfer primary stresses; the analysis assumes ductile behavior of the bearing parts. Therefore, it is assumed that local yielding due to localized initial contact occurs and spreads the load over the total section involved (therefore creating a primary stress state). Having stated that, it would be proper to assume the load resisting area to be the appropriate arc of the lid shield ring rather than the shear bar. Therefore, the original calculation required revision at least to that extent. However, as noted in previous responses, to respond to the totality of issues raised with respect to the lid behavior during a non-mechanistic tipover, modifications to the 100S lid to replace the shear bar with a shear ring eliminates any need for consideration of line contacts between the shear bar and the lid shield ring. The calculation is revised to evaluate the shear transfer between the lid and the shear ring attached to the overpack body. The issue of non-uniform contact is resolved with this design modification by virtue of the tolerances in the revised lid configuration and the recognition that local yielding will occur until the area is sufficient to balance the applied load. The adequacy of the structural configuration is measured by the gross area available to support the load and meet primary stress levels, and not by the local area that is loaded prior to achieving conformal contact.

### **Question 3.7**

Describe the load transfer mechanism of the new 100S lid under the cask tip over accident condition when the tip over rotational axis coincides with the centerline axis of a pair of opposite exhaust vents, making the direction of the gravity loading coincident with the other pair of exhaust vents. The calculation on page 3.AO-4 apparently does not consider this orientation. Provide an expansion of Appendix 3.AO to address this.

This information is required to assure compliance with 10 CFR 72.236.

### **Response 3.7**

During a non-mechanistic tipover event, the lid develops inertia forces directed laterally and longitudinally, with respect to the overpack body. The lateral inertia loads are transferred to shear members that are flush with the top surface of the overpack body. The longitudinal inertia force, together with any overturning moment arising from the offset of the lid centroid from the point of impact during a non-mechanistic tipover, are resisted by the lid studs. In the initial design, the shear load path could not be precisely delineated; as the staff questions in this RAI have indicated, it was possible for the studs to be subject to some shear load. The revised lid configuration and the supporting revised calculation that responds to the issues raised evaluates the performance for the most limiting orientation where gravity is parallel to the longitudinal axis of an inlet exhaust vent. The revised configuration ensures complete separation of the shear resisting members from the tension resisting members. The revised configuration provides appropriate shear transfer surface to resist 100% of the lateral force regardless of the orientation of the lid during a non-mechanistic tipover. Inherent in the revised design and load path is the assumption that the

shear ring is fully functional; that is, the lid does not suffer any rigid body rotation, with respect to the overpack, that would diminish the effectiveness of the shear ring. This is accomplished by demonstrating that the lid studs are capable of providing sufficient tensile load resistance to ensure a resisting moment to balance the overturning moment from lid inertia forces. The safety factors for all segments in the load path are reported in FSAR Section 3.4.4.3.2.2 for the revised HI-STORM 100S lid.

### **Question 3.8**

Explain and justify the assumed behavior considering the rigidity of the volume of the material in the space around the lid bolt holes and clarify the proposed appendix for the 100S. Appendices 3.AC and 3.AP contain conflicting information in the form of statements regarding the shear capability of the four lid studs. At the top of page 3.AO-4 the following statement is made. "This demonstrates that the bolts cannot support the shear load." Apparently as a result of fact, the four peripheral shear bars were introduced into the design. On page 3.AP-1, Section 3.AP.1, Introduction, the following statement is made. "This appendix provides a calculation which shows that the 4 studs holding the lid to the overpack top plate have sufficient capacity to resist any shear load that may be imposed by the lid during the non-mechanistic tipover of the cask." In Section 3.AP.2 Methodology, it is stated that, "The load is shown to be larger than the load causing enlargement of the clearance hole in the lid so the actual bolt load is reduced." In discussing the transfer of any shear load in the studs from the lid to the top of the cask on page 3.AP-2, in the last paragraph, the following statement is made, "Since we have line contact, there will be an immediate local yielding and hole enlargement. Conformance of the bolt and the hole cannot occur prior to the shear bars becoming effective. (text omitted) The bolt hole will begin to substantially open up at the 'flow stress' that is assumed to be the average of yield and ultimate stress."

The assumption that there will be deformation (ovalling) of the hole in the lid shield ring as the radius of the stud and the radius of the hole edge change contact from a line load to some edge area of loading apparently does not consider the fact that for such behavior the contact line on the edge of the hole must move into the edge of the hole. However, in the actual configuration it is not just an edge of 0.5" thickness of steel that is the contact line, but the plate is topped with a steel pipe sleeve as an axial liner in the hole with the entire sealed volume in the annular space being filled with concrete. With this degree of rigidity, the contact line probably extends further axially into the hole than just the thickness of the lid shield ring. The statement made in the middle of page 3.AP-3 that, "It is clear that the bolts cannot resist the entire load because the bolt holes will simply open due to the high stress in the lid material," would appear to only be true if the concrete behind the steel above the inside face of the shield ring were to deform.

This information is required to assure compliance with 10 CFR 72.236.

### **Response 3.8**

New FSAR Appendix 3.AP was included in proposed FSAR Revision 1 with the LAR package to try to address tolerancing issues. The intent of the original design was to have the shear bars resist the entire shear. However, recognizing that the tolerances were such that the studs may contact prior to the shear bars if the worst-case tolerance stack-up were assumed, Appendix 3.AP showed that if all four studs contacted, then the load per stud was less than the allowable load per stud. The appendix further addressed the issue of only one stud contacting before the other studs and before the shear bar. The staff question correctly states that we did not account for the volume of the concrete that would oppose opening of the hole and clearly elucidates the potential difficulties quantifying the load on a stud in the presence of worst-case tolerances.

Accordingly, the questions in this RAI led to a re-design to address this issue. The HI-STORM 100S lid configuration has been revised to ensure that the studs no longer resist the shear imposed by a non-mechanistic tipover event. As such, the issues raised in Question 3.8 are no longer applicable to the component. FSAR Appendix 3.AP is rendered moot by this revised configuration; tensile load requirements for the studs (see Response 3.5) are detailed in the calculation package supporting the safety factors summarized in the FSAR. Stud safety factors in tension are reported as part of the summary table.

### **Question 3.9**

On page 3.1-6 in the section addressing accident conditions, only the free standing HI-STORM 100 is mentioned regarding demonstration that no tip over of a fully loaded HI-STORM 100 overpack is possible under seismic conditions. The HI-STORM 100A is not addressed. Address the HI-STORM 100A in this section.

This information is required to assure compliance with 10 CFR 72.236.

### **Response 3.9**

The following statement has been added to FSAR Section 3.1 addressing accident conditions:

“...The HI-STORM 100A is specifically engineered to be permanently attached to the ISFSI pad. The ISFSI pad engineered for the anchored cask is designated as “Important to Safety”. Therefore, the non-mechanistic tip-over event is not applicable to the HI-STORM 100A...”

### **Question 3.10**

The proposed Revision 1 for Figures 3.1.2 and 3.1.3 adds the configuration of the side drop orientations of the fuel baskets for the MPC-32 configuration to those side drop orientations for the MPC-24 and MPC-68. The proposed revision does not describe any re-analysis for

the MPC-24, yet the orientation with respect to the direction of gravity for MPC-24 from Revision 0 to proposed Revision 1 was changed. Explain the change in the orientation of the baskets for the MPC-24 and why there was no change in the computed stresses reported in Appendix T, for example, in the case of the 45-degree basket orientation with a side drop.

This information is required to assure compliance with 10 CFR 72.236.

**Response 3.10**

There were no new analyses performed for the MPC-24 in proposed Revision 1. The anomaly noted by the staff is due to an improper transcription of the MPC-24 configuration from the CAD drawing to the proposed FSAR figures. This error has been corrected with revised figures to match that in Revision 0, plus the addition of MPC-32.

**Question 3.11**

Proposed Table 3.4.1 is titled, "Finite Elements in Representative MPC Structural Models," and provides the data on the models for the MPC-24 and MPC-68 units with no information on the MPC-32 model regarding the element types used in the three listed model types. Provide the same information for the MPC-32 and leave the title of the table as it currently is, "Finite Elements in MPC Structural Models."

This information is not provided and is needed to assure compliance with 10 CFR 72.236.

**Response 3.11**

FSAR Table 3.4.1 has been revised as requested and now includes the element types for the MPC-32.

## 4.0 Thermal Evaluation

### Question 4.1

Describe the effect of the presence of the heat conduction elements on restricting helium movement in the down-comer region when evaluating the thermo-siphon effect.

The presence of the heat conduction elements in the canister design has been neglected in the thermo-siphon enabled models (i.e., the heat transfer contribution has been eliminated), however, in reality they still remain within the cask. This information is not provided and is needed to assure compliance with 10 CFR 72.236.

### Response 4.1

The reduction in the downcomer flow area due to the presence of the aluminum heat conduction elements has been recognized in the heat transfer (FLUENT) simulations. In fact, the analysis utilized a smaller downcomer flow area than is actually available with the aluminum heat conduction elements in place. Table 4.1.1 below provides numerical data for the case of MPC-24 (extracted from Reference [4.1]) to illustrate the extent of conservatism in the downcomer area used in the thermal analysis.

<b>Downcomer Flow Area:</b>	<b>Value, in<sup>2</sup></b>
Actual in the absence of aluminum heat conduction elements	741.7
Actual in the presence of aluminum heat conduction elements	682.9
Used in the thermal analysis	517.4

Further, we confirm that no credit for conduction through the aluminum heat conduction has been taken in the thermal analysis. Finally, the reduction in the flow area available for convection has been overstated in the thermal model to suppress the contribution of the thermosiphon effect in facilitating heat rejection from the MPC.

Inasmuch as the aluminum heat conduction elements are no longer relied on for heat transfer in the MPCs, and are actually a detraction to the convection mode of heat transfer, we have revised the FSAR and MPC drawings (1392, Sht. 1; 1395, Sht. 1; 1401, Sht. 1, and 2890) to make them an optional item for the users of our system. In other words, they may be installed at the discretion of the ISFSI Owner. The heat transfer calculations, as stated above, comfortably bound both scenarios, namely, where the aluminum heat conduction elements are (i) included or (ii) excluded.

### **Question 4.2**

Describe the effect of the damaged fuel canisters on inhibiting the movement of helium when calculating the heat transfer capabilities from the thermo-siphon effect. Additionally, provide calculations or suitable references, to support the conclusions reached in Section 4.4.1.1.4 with regard to decreased basket conductivities and effects on the overall basket heat dissipation rate (page 4.11).

This information is not provided and is needed to assure compliance with 10 CFR 72.236.

### **Response 4.2**

The damaged fuel canisters add to the flow resistance in the storage cells in which they are located by slightly reducing the net axial flow area (less than 5%), and by interposing bottom and top screens (250 mesh). The net effective thermal resistance of the storage cell (explained in Section 4.4.1.1.4 of the FSAR) is also increased because of the interference in the radiative heat exchange between the SNF and the cell walls by the intervening DFC cell walls.

The DFCs (for other than the low heat emitting Dresden Unit 1 and Humboldt Bay fuel assemblies) are, however, permitted to be stored only in the peripheral cells of an MPC (those adjacent to the MPC shell wall) where the temperature under the all-intact fuel storage scenario is considerably lower than the corresponding temperature at the center of the basket.

Placing the more thermally resistive DFCs in the peripheral cells has the effect of reducing the helium flow through those cells (due to relatively more flow resistance), forcing more helium flow through the inner cells loaded with intact fuel, which would be beneficial in reducing the peak cladding temperature in the central region of the basket. Counteracting this beneficial effect is the net reduction in the overall helium circulation rate due to the overall reduction in the fuel basket conductance (caused by the more resistive DFCs in the peripheral cells). One would heuristically expect the net consequence to be quite minor.

To quantify the effect of DFCs in the peripheral cell locations, the following problem was analyzed.

The MPC-68 basket was assumed to be loaded with DFCs in all of the sixteen peripheral locations, intact fuel in all others. Each fuel assembly (canisterized as well as intact) was assumed to emit heat at the design basis maximum heat load (MPC-68 heat load = 28.19 kW). As in the design basis analysis, the BWR fuel type assumed is also the one that produces minimum basket conductance type (GE 11 - 9x9). Finally, in the FLUENT analysis, to bound the effect of DFCs, the axial flow resistance in the peripheral cells where the DFCs are located, was set equal to ten times the resistance in the cells containing intact SNF. (In reality, the resistance increases to 5.8 times that of the intact fuel) The details of this analysis are archived in Appendix I of the Holtec calculation package [4.2]. The key

results are presented below, side-by-side with the design basis case wherein all cells are loaded with intact SNF.

Case	MPC Heat Load, kW	Peak Cladding Temperature, °F	Maximum Cladding Temperature in the Peripheral Cells, °F
Intact fuel in all cells	28.19	739.9	560.2
Sixteen peripheral cells loaded with DFCs	28.19	740.5	563.2

It is evident from the above results that, thanks to the self-compensating characteristics of the thermosiphon mechanism, the DFCs in the peripheral cells have a negligible effect on the peak cladding temperature (which occurs in the SNF located near the center of the basket). These results indicate that DFCs with 100% of the heat load permitted for intact fuel can be used in the HI-STORM MPCs in quantities limited by the CoC for each MPC type so long as the DFCs are loaded *only* in the peripheral cells.

**Question 4.3**

Provide clarification regarding the temperature range where the postulated conductivity, as noted in SAR Section 4.2 for Holtite is valid. Additionally, verify that the lower bound is appropriate for the temperature range that this material is exposed to during normal and off-normal accident conditions.

Holtite is a composite material consisting of epoxy poly and as delineated elsewhere, B<sub>4</sub>C and Aluminum trihydrate. Thermal conductivity values for polymeric components are provided in the range of 0.05 to 0.2 Bu/ft-hour-°F. The addition of Alumina fillers increases conductivity by up to a factor of 10. Holtec thus considers a postulated lower bound conductivity value of 0.3 Btu/ft-hour-°F in their thermal models for the neutron shield region.

This information is not provided and is needed to assure compliance with 10 CFR 72.11 and 72.236.

### **Response 4.3**

The Holtite™ neutron shielding material is used in the 125 ton HI-TRAC transfer cask lid (See FSAR Figure 1.2.9). For normal and off-normal conditions (FSAR temperature limit of 300°F), a lower bound Holtite thermal conductivity (K) of 0.3 Btu/ft-hr-°F is postulated in the thermal evaluation of HI-TRAC 125 transfer cask. This, as we show below, imputes a large conservative bias to the material's heat dissipation characteristics. In Figure 4.3.1 provided herein, we present a comparison of the Holtite™ measured thermal conductivity data<sup>a</sup> with the FSAR value over a temperature range of 106°F to 306°F. The following observations are applicable:

- i. The FSAR value (K) under-states Holtite™ conductivity by at least 37%.
- ii. The upper limit for which conductivity is measured exceeds the FSAR temperature limit (300°F).
- iii. Holtite™ thermal conductivity rises with decreasing temperatures.

Therefore, the K used is a conservative lower bound value for normal and off-normal conditions (temperatures less than the FSAR limit of 300°F). For a fire accident condition (Section 11.2.4.2.2 of the FSAR), a heat transmission into the cask is conservatively maximized. For the fire accident evaluation, the HI-TRAC lid thermal resistance is completely ignored.

### **Question 4.4**

Provide the conductivity values for temperatures outside the 200° F to 700° F range.

In table 4.2.2 thermal conductivity values are provided for 200° F, 450° F, and 700° F with intermediate values linearly interpolated. Values for ambient conditions for temperatures are below 200° F, notably air temperatures, are not provided.

This information is needed to assure compliance with 10 CFR 72.11 and 72.236.

### **Response 4.4**

In the HI-STORM 100 System, the materials that are exposed to temperatures below 200°F are carbon steel, concrete and air. Because the conductivity of carbon steel drops slightly with rising temperature, a material conductivity at the upper bound temperature of 200°F is conservative. This approach has been employed in the HI-STORM calculations.

---

<sup>a</sup> "Transmittal of Test Results", from Anter Laboratories, Inc. to Dr. Turner (Holtec), November 30, 2000.

For concrete, a conservative lower bound thermal conductivity of 1.05 Btu/ft-hr-°F is postulated in the FSAR (see Table 4.2.2), which is below the typical values reported in the literature (in the range of 1.2 to 2.0 Btu/ft-hr-°F in "Properties of Concrete", Neville, 4<sup>th</sup> Edition, p. 375).

The thermal conductivity data<sup>b</sup> for air in the temperature range that covers ambient to 200°F, obtained from a robust source [4.3] is provided below.

Temperature (°F)	Air Conductivity (Btu/ft-hr-°F)
32	0.0139
212	0.0176

FSAR Table 4.2.2 has been revised to include this information.

The majority of the materials that could potentially reach temperatures in excess of 700°F (Alloy X, fuel cladding, helium and Boral cladding) have thermal conductivities that increase with increasing temperature. For these materials, it is conservative to limit conductivity values to those at 700°F. Only the B<sub>4</sub>C core of the Boral and UO<sub>2</sub> have thermal conductivities that decrease with increasing temperature. Any slight decrease in the fuel basket conductivity that would result from a decrease in the thermal conductivity of B<sub>4</sub>C or UO<sub>2</sub> would be more than offset by the increased conductivity of the other materials and the fourth-order increase in temperature in the contribution of thermal radiation heat transfer.

In the FLUENT analyses where temperatures in excess of 700°F can occur, the conductivity of the MPC fuel basket is input as a second-order (quadratic) polynomial, not linearly interpolated. As this formulation extrapolates the fuel basket conductivity using a second-order function that conservatively neglects the fourth-order behavior of thermal radiation, this is also conservative. Based on this consideration and those in the previous paragraph, it is concluded that thermal conductivity values for temperatures above 700°F were not necessary.

#### **Question 4.5**

As an editorial note, Section 4.3.1.2 page 4.3.6 lists internal rod gas pressure as P<sub>i</sub> and Section 4.3.1.2 page 4.3.7 lists rod internal pressure as P<sub>o</sub>. Clarify this inconsistency.

#### **Response 4.5**

The editorial correction on page 4.3-6 has been made: We have replaced subscript "i" in P<sub>i</sub> with an "o".

---

<sup>b</sup> The thermal calculations employ the data provided herein.

#### **Question 4.6**

Correct the inconsistent statements with regard to crediting the conduction through the aluminum heat conduction elements in the thermal analyses.

Section 4.4.1 "thermal model" states that conduction through the aluminum heat conduction elements is neglected in the thermal modeling analyses. Use of this assumption is not consistent throughout the thermal section. For example Section 4.4.1.1.9 Fluent Model for HI-STORM, Pg 4.4-18 states, "To this 'helium conductance-radiation' based peripheral gap conductivity, the effective conductivity of the aluminum heat conduction elements added to obtain a combined peripheral gap conductivity." This is not consistent with the methodology defined elsewhere in the application.

This information is needed to assure compliance with 10 CFR 72.11 and 72.236.

#### **Response 4.6**

We agree that the heat transfer calculations under vacuum drying conditions had not been revised to remove the recognition of the aluminum heat conduction elements. We have corrected this inconsistency in the revised text in paragraph 4.4.1.1.9. With the above revisions incorporated, now there is complete consistency throughout the FSAR with regard to the exclusion of the aluminum heat conduction elements from all of the HI-STORM thermal analyses. This clean up of the FSAR does not introduce any changes to the conclusions on thermal analysis contained in Section 4.6 of the FSAR. The appropriate calculation package (see [1], Appendix I) has also been updated to reflect the changes incorporated in Subsection 4.4.1.1.9 of the FSAR.

#### **Question 4.7**

Justify that the conclusions regarding fuel cladding temperatures for a MPC placed in the HI-STORM 100S overpack are bounded the HI-STORM 100 overpack fuel cladding temperatures and provide references to the specific calculations that support this assertion. Include a discussion of those pertinent elements of the model that change with regard to convective heat transfer.

This information is not provided and is needed to assure compliance with 10 CFR 72.11 and 72.236(f).

#### **Response 4.7**

A short summary of the thermal evaluation of HI-STORM 100S, including physical changes pertinent to thermal performance was provided in Section II of the "Summary of Proposed Changes" included as Attachment 1 to the LAR package submittal. A statement confirming that the HI-STORM 100S overpack configuration was evaluated and found to be bounded by the HI-STORM 100 overpack evaluation was included in Section 4.4.1.1.9 of proposed

FSAR Revision 1. Thermal calculations in support of the HI-STORM 100S overpack are documented in the Holtec Calculation Package [2], pages 28 & 29. This calculation was submitted to the NRC on November 20, 2000. From a thermal performance standpoint, the HI-STORM 100S overpack is nearly identical to HI-STORM 100. HI-STORM 100S features a slightly smaller inlet duct-to-outlet duct separation and an optional gamma shield cross plate (that acts as a flow straightener). Since the optional gamma shield cross plate flow resistance is bounding, the optional design was conservatively evaluated in the thermal analysis. The results of the thermal analysis show that the peak fuel cladding temperatures calculated for HI-STORM 100 bound those for HI-STORM 100S.

#### **Question 4.8**

For regionalized fuel loading where the inner region heat load limit will govern peak cladding temperature limits for the hot fuel, provide justification and pertinent calculations, or suitable references, in support of the justification as to why the cladding temperature limits for the longer cooled fuel in the periphery region at the interface are not exceeded for all loading combinations and for each basket design.

It was not clear in the discussion provided on page 4.4-30 which loading configuration and temperature limits govern. This information is not provided and is needed to assure compliance with 10 CFR 72.11 and 72.236(f).

#### **Response 4.8**

In regionalized storage, the fuel cladding temperature limit for the longer cooled fuel can and does govern the maximum permissible MPC heat load in certain scenarios, as we explain below.

In the regionalized storage scenario, where the outer region is populated with relatively "old and cold" fuel and the inner region with "hot" fuel, the temperature limits for the outer region fuel (A) are lower than that for inner region fuel (B). The outer region temperature is bounded by the Interface Cladding Temperature (ICT) and the inner region temperature is bounded by the Peak Cladding Temperature (PCT). The ICT and PCT are tracked in the thermal solutions as a function of inner region heat load. The limit (either A or B) that is reached first governs the MPC maximum heat load ( $Q_{max}$ ). *For the MPC-32 and MPC-68,  $Q_{max}$  is governed by the outer region temperature limit.* For these MPCs, ICT equals A and PCT is less than B at  $Q_{max}$ . For the MPC-24 & MPC-24E canisters,  $Q_{max}$  is governed by the inner region heat load. Therefore PCT equals B and ICT is less than A.

**Question 4.9**

With temperatures in excess of 700 °F noted for long term normal storage, clarify if the pressurized water reactor (PWR) and boiling water reactor (BWR) fuel assembly effective thermal conductivity values delineated in tables 4.4.1 through 4.4.3, and 4.4.5 and 4.4.6 are adequate considering that these tables only denote values up to a maximum temperature of 700°F.

This information is not provided and is needed to assure compliance with 10 CFR 72.11 and 72.236.

**Response 4.9**

As discussed in Subsection 4.4.1.1.4 of the FSAR, the fuel effective conductivity tables (Tables 4.4.1, 4.4.2, 4.4.5, 4.4.6, and 4.4.23) provide the means to compare the in-plane heat dissipation capacity of the MPC at three reference temperatures (viz. 200°F, 450°F and 700°F). This is done with due recognition of the fact that heat dissipation is a non-linear function of the coincident temperature principally because radiation heat transfer increases as the fourth power of absolute temperature. FSAR Table 4.4.3 summarizes the MPC in-plane conductivity results. For higher than 700°F co-incident temperatures, MPC thermal conductivity is computed by employing certain polynomial functions in temperature. As a conservative posture, these polynomial functions are limited to second order in temperature and are pegged to the in-plane conductivity results provided in FSAR Table 4.4.3. This means that although radiation heat transfer increases as the fourth power of temperature, the computed rise in the MPC in-plane conductivity is more gradual (quadratic).

**Question 4.10**

Provide an explanation why use of an averaged temperature through the section (footnote to table 4.4.36) is adequate to bound surface temperatures. Justify this method for maintaining adequate thermal margin for the cask materials when considering that surface temperatures may exceed the averaged value. For example, the lid bottom plate and radial shield temperatures are within 3% and 14% respectively of their long term temperature limit using averaged values.

This information is needed to assure compliance with 10 CFR 72.236.

**Response 4.10**

It is recognized that the steel weldment in the HI-STORM overpack serves the structural function while the concrete (deployed without rebars to provide a homogenous continuum and protected from the elements by the enveloping steel structure) is intended to render the radiation shielding function.

Concrete design codes limit the surface and bulk temperature of concrete to mitigate the loss in concrete's compressive strength and to limit the thermal gradients that would add to the structural loading on the reinforced concrete structure. ACI-349-97, for example, recognizes the strength-reducing effect of temperature in concrete (Appendix A, paragraph A.4.3, enclosed). Concrete strength data in the literature (for example, Neville A.M., "Properties of Concrete", 4<sup>th</sup> edition, Addison & Wesley, Table 8.6, enclosed) shows that concrete's compressive strength at 200°C (392 °F) is in the range of 50 to 92% of its room temperature value. However, the key shielding property, namely, density, is scarcely affected. For this reason, the HI-STORM FSAR places a limit of 350 °F on the "section average temperature" of concrete. Surface temperature and associated temperature gradients are meaningful considerations in reinforced concrete subject to structural loadings. In the HI-STORM overpack, there is no mechanistic means for high surface temperatures to produce any deleterious effect. Indeed, according to the technical evidence cited in the above-referenced text by Neville, concrete can withstand temperatures well in excess of 300°C (572 °F) without sustaining any physiological change. However, for conservatism, the section average temperature has been restricted in the HI-STORM FSAR to 350 °F under accident conditions (events of short duration).

Finally, the overpack inner shell, bottom and top lid temperature limits in Table 2.2.3 are incorrectly but conservatively stated. This error in Table 2.2.3 has been corrected in the proposed Revision 1B. The above response supports existing technical information in the HI-STORM FSAR (i.e., not part of the present request for CoC amendment).

#### **Question 4.11**

Provide additional discussion and sensitivity analyses to demonstrate that analysis in the vertical orientation is bounding for cask transport with the HI-TRAC transfer cask. Specifically, will the loss of convective heat transfer be greater than the addition of heat transfer due to more metal to metal surface contact area or will the increased heat transfer due to convective means govern the amount of heat transfer lost due to larger gap resistance?

Section 4.5.2.1 asserts that analysis in the vertical orientation is bounding for cask transport with the HI-TRAC transfer cask. This is in part due to less metal to metal contact between the physically distinct entities and thus gap resistance will be higher than in a horizontally oriented HI-TRAC.

This information is not provided and is needed to assure compliance with 10 CFR 72.236.

#### **Response 4.11**

FSAR Section 4.5.2.1 states that in a vertical configuration, ".. there is apt to be less of metal-to-metal contact between the physically distinct entities, viz., fuel, fuel basket, MPC shell and HI-TRAC. For this reason, the gaps resistance between these parts is higher than in a horizontally oriented HI-TRAC." It does not state that the rate of heat rejection in the

vertical orientation is less effective than the horizontal configuration. The statement in FSAR Subsection 4.5.2.1 is intended to convey the thought that the thermal conductivity of an MPC section is less when the fuel basket has no physical contact with the spent nuclear fuel or the MPC shell (i.e., the vertical configuration). FSAR Section 4.5 reports thermal evaluations of both the horizontal (no thermosiphon) and vertical (thermosiphon enabled) HI-TRAC configurations. The in-plane thermal resistance is bounding for a vertical orientation because of the absence of contact between the fuel and the fuel basket and between the fuel basket and the MPC shell. The horizontal configuration is, therefore, analyzed employing the bounding (vertical configuration) thermal resistance.

#### **Question 4.12**

Provide a technical rationale for why it is acceptable to allow temperature limits for non-fuel clad materials to be exceeded. For users with site-specific design basis which includes an event that results in blockage of air inlets or outlets for an extended period of time, the proposed TS (Appendix B, 3.4.9) only requires verification the fuel clad temperature limits are not exceeded.

This information is not provided and is needed to assure compliance with 10 CFR 72.236.

#### **Response 4.12**

The basis for this proposed TS in the original LAR submittal was Chapter 11 of NUREG-1536 where, for accident conditions, the acceptance criteria include several specific criteria that must be met. In particular, the confinement function, capability of ready retrieval of spent fuel, and subcriticality must be maintained; and the dose to an individual outside the controlled area due to the accident must not exceed the limits of 10 CFR 72.106(b). In addition, structures, systems and components must be adequate to prevent accidents and mitigate the consequences of accidents. In order to provide a contextually complete response to this question, the basis for the previously proposed limit is provided below, along with our proposed modified basis.

#### **Original Basis**

It is implicit from a review of NUREG-1536 and HI-STORM licensing precedent that a minimal amount of damage to the cask system is admissible as a result of an accident, provided the above acceptance criteria are met. For example, the current licensing basis for tornado missiles recognizes that the concrete overpack will sustain some physical damage from the missile impact. Similarly, the current licensing basis for HI-TRAC transfer cask acknowledges the loss of some water in the water jacket during the fire accident. In both of these examples, the shielding design function is impaired to some degree, and the evaluation of the accident described in the FSAR was found to be acceptable. The original licensing basis analysis of the blocked duct event recognizes that the surface concrete temperature may exceed its short term temperature limit before the fuel cladding reaches its short term temperature limit. Because reaching the concrete short term temperature

limit would affect only the shielding design function, the acceptance criterion for evaluating a site-specific event that completely blocks the inlet air ducts was chosen to be fuel cladding temperature, to be consistent with other accident acceptance criteria in the FSAR. A check of the shielding effectiveness of the cask system if the blockage event lasted longer than 33 hours was added to the FSAR to require users determine the extent, if any, of shielding reduction, and the need for corrective actions

### Modified Basis

After further review, we have decided to amend the licensing basis for this new proposed TS to address the component with the most restrictive temperature limit for the blocked duct accident. As part of this review, we have determined that the use of surface concrete temperature is overly conservative based on the design function of the overpack concrete (shielding). Therefore, the *section average* concrete temperature is evaluated, rather than the local (i.e., inner surface) concrete temperature. Any local peaks in inner concrete surface temperature that may occur, above the section average are acceptable based on the logic described above for allowable overpack damage.

We no longer subscribe to the position that only the temperature limits for the fuel cladding should be applied in establishing the permissible duration (say,  $\tau^*$ ) for which all inlet or outlet ducts can be blocked. Specifically, the section average temperature of the shielding concrete (350 °F per Table 2.2.3) should also be considered in establishing  $\tau^*$  (see also Response 4.10 regarding concrete radiation shielding performance at elevated temperatures). The proposed TS (Appendix B, 3.4.9) that calls for the temperature of the fuel cladding as the governing parameter is based on the implicit assumption that the cladding temperature limit will be reached before the corresponding limit for the section average concrete temperature is approached.

To examine the soundness of the above assumption, a transient analysis of a HI-STORM 100 system containing an MPC-68 canister uniformly loaded with SNF emitting a bounding heat load ( $Q=28.74$  kW) was performed. The ambient temperature is assumed to be at the design maximum for normal conditions (80 °F per FSAR Table 2.2.2) and all four bottom ducts are assumed to be blocked. Blocking of the bottom ducts cuts off the thru-flow chimney effect along the HI-STORM annulus. A complete computational fluid dynamics (CFD) model on FLUENT was run to obtain the temperature time-histories of the peak fuel cladding and the section average shielding concrete temperatures. The results are plotted in Figures 4.12-1 and 4.12-2, respectively. From the results plotted in the above-mentioned figures, the soundness of the proposed TS (Appendix B, 3.4.9) is verified. The above transient analysis is archived in Appendix I of the thermal calculation package [2].

FSAR Section 11.2.13.4 has been revised accordingly to address this change in the licensing basis.

**Question 4.13**

Provide the specific changes in annulus geometry and dimensions due to thermal expansion and the effect on the thermo-syphon determinations and subsequent conclusions regarding maximum calculated temperatures.

Explain how tolerances inherent in the fabrication process are addressed regarding the relative contribution to heat transfer effectiveness from the thermo-syphon effect.

Provide a sensitivity analysis, or suitable references, that show fabrication tolerances and changes in annulus dimensions from thermal expansion do not significantly effect the thermo-siphon calculations and results.

This information is not provided and is needed to assure compliance with 10 CFR 72.236.

**Response 4.13**

The MPC annulus features an open downcomer space that is formed between the periphery of the fuel basket and the MPC shell. At the locations of closest approach between the basket and the shell, a 3/16 inch cold condition clearance is provided for accommodating differential thermal growth. Away from these locations, large peripheral spaces (about 9 inches for PWR and 6 inches for BWR) are present in our MPCs to support downcomer helium flow with minimum restriction. In the HI-STORM thermal analyses, the available downcomer flow area is significantly understated. For example, in the MPC-24 canister, (See Response to RAI 4.1), the available downcomer area is 682.9 inch<sup>2</sup> and that employed in the analysis is 517.4 inch<sup>2</sup> (i.e. reduced by more than 100 inch<sup>2</sup>). For other canisters the downcomer area conservatism is on the same order.

Postulating a bounding maximum differential growth of 3/16 inch, the reduction in downcomer area is computed as the product of canister interior circumference and the differential movement as 39.7 inch<sup>2</sup>. Because this is smaller than the above-mentioned downcomer area conservatism, the thermosiphon effect is simulated in a conservative manner in the HI-STORM thermal model.

**Question 4.14**

Provide a justification and bases, or suitable references, for the minimum helium mass required to induce and sustain natural circulation for the MPC designs described in this amendment. Include in your justification a sensitivity study for the helium loading values. Additionally, provide an evaluation, or suitable references, of the long term effects of reduced helium inventory given a minimal helium leakage rate over the licensed period.

This information is not provided and is needed to assure compliance with 10 CFR 72.236.

#### **Response 4.14**

The helium backfill mass in the MPC cavity space defines the fill pressure for an assumed gas temperature and a given cavity volume. The HI-STORM technical specifications stipulate a helium backfill pressure band of 29.1 to 33.1 psig ( 43.8 to 47.8 psia) at a reference gas temperature of 70°F. This is based on a 45.8 psia nominal fill pressure at 70°F with a  $\pm 2$  psi operator fill margin.

As we show by using the example of MPC-32, the quantity of helium provided using the lower bound value in the technical specifications is greater than the amount of helium assumed in the thermal analysis.

The initial fill pressure ( $P_0$ ) is related to the operating condition cavity pressure ( $P$ ) and cavity gas temperature ( $T$ ) by the ideal gas law:  $P/(T + 460) = P_0/(70+460)$ . The minimum helium mass required to sustain natural circulation is defined by the design basis maximum heat load condition, which, for the MPC-32 canister is  $Q = 28.74$  kW,  $P = 5$  atm and the computed  $T$  is 465°F. Using the perfect gas law, the  $P_0$  required to support the thermosiphon effect is computed as 2.865 atm (i.e. 27.4 psig). The technical specification prescribed *minimum* fill pressure is therefore greater than the *lowest* fill pressure required to sustain an adequate level of natural circulation by a respectable margin (about 6%).

The reduction in helium inventory over a 40 year storage life is computed below based on the technical specification maximum leak rate ( $L$ ) of  $5 \times 10^{-6}$  atm-cm<sup>3</sup>/sec. The maximum loss ( $\delta V$ ) is  $L * s/hr * hr/day * days/yr * 40 yr = 6307.2$  cm<sup>3</sup>. The lowest cavity free volume  $V$  (for MPC-68) is  $5.9 \times 10^6$  cm<sup>3</sup>. The helium inventory loss ( $\delta V/V$ ) is therefore quite small (0.11%) over the 40 year design life.

#### **Question 4.15**

Evaluate quantitatively the conservatisms in the thermal model by comparing the results for the limiting case with the results of a best-estimate calculation for same limiting case.

This information is needed to assure compliance with 10 CFR 72.236.

#### **Response 4.15**

FSAR Appendix 4.B provides a discussion of the numerous elements of conservatism embedded in the HI-STORM thermal analysis, and provides an estimated elevation in the computed peak cladding temperature due to each one of them individually. To determine their aggregate effect, a "best estimate" analysis of the HI-STORM system was performed. For this purpose, the design basis analysis for the HI-STORM 100 System containing an MPC-32 was used as the reference case ( $Q = 28.74$  kW). In this "best estimate" analysis the heat load and ambient temperature (80°F) were kept the same.

This best estimate analysis removes most major conservatisms in the solution. However, certain conservatisms, intrinsic to the solution process (and to the limitations in the computer code) remain, such as:

- The heat input to the HI-STORM overpack due to insolation is assumed to correspond to 10CFR71 requirements.
- The thermal conductivity of the overpack concrete is set at the lower bound value set down in the FSAR.
- Turbulation of the helium flow by the SNF gird spacers is ignored (the axial flow in the basket region is assumed to be unmixed laminar).
- The conservatism in the axial flow resistance of the SNF included in the licensing basis model is retained.

The effect of the adjacent casks is modeled using the “hypothetical cylinder” construct explained in Appendix 4.B of the FSAR.

Details of this analysis are documented in Appendix I of the thermal calculation package [2]. Summary results are presented in the table below.

<b>Key Output Data, Thermal Analysis of HI-STORM/MPC-32 at Design Basis Heat Load (Q = 28.74 kW)<sup>c</sup></b>		
<b>Item</b>	<b>Design Basis Case Result from the FSAR</b>	<b>New Realistic Model Analysis</b>
Peak cladding temperature, °F	691	539
Maximum MPC Shell Temperature, °F	341	310
Concrete Section Average Temperature (Active Fuel Mid-Height), °F	134	121

As the above table shows, the peak cladding temperature using the realistic analysis model is slightly above 530°F. The peak cladding temperature would be even lower if helium gas fill pressure is increased and the other remaining conservatisms mentioned above are removed.

<sup>c</sup> Ambient air temperature = 80°F

**Question 4.16**

For the finite element analysis (FEA) models submitted in the thermal section (Chapter 4) of the SAR and as described in Holtec Report No. HI-992252, and Report No. HI-981892 provide the following:

- a) List of the elements, key point options, and real constants used in the FEA models. Provide justifications for the elements, key point options, and real constants used.
- b) An explanation and justification if error functions were disabled for steady state analyses and where those error warnings occurred.
- c) A listing of materials and corresponding material numbers used in the FEA models.

This information is not provided and is needed to assure compliance with 10 CFR 72.236.

**Response 4.16**

There are three finite-element thermal models described in the FSAR. The following table lists these analyses and the corresponding FSAR section.

<b>Thermal Analysis</b>	<b>FSAR Section</b>
Fuel Region Effective Thermal Conductivity	4.4.1.1.2
Modeling of Basket In-Plane Heat Transport	4.4.1.1.4
Fire Analysis for HI-STORM Overpack	11.2.4.2.1

The third of these models, the fire analysis for the HI-STORM overpack, is described in the supporting calculation package HI-981892 as well. Holtec Report HI-992252 does not describe any finite-element models for Holtec cask systems.

The requested element, element key option, real constants, error reporting and materials information for these models are provided in the following. Copies of all ANSYS databases and input script files referenced in the following are included in a CD-ROM being submitted under separate cover.

- a) Elements, Element Key Options and Real Constants

There are three separate ANSYS finite element models used in the fuel region effective thermal conductivity analyses. The next three paragraphs discuss these three finite-element models.

The first model is for a Westinghouse 17x17 OFA fuel assembly with all rods modeled as fuel rods and blackbody radiation in the storage cell of a helium-backfilled MPC. This model contains 9399 2-D thermal plane elements (PLANE55, no key options required), 2316

thermal link elements (LINK32, no key options required) and one radiation substructure matrix element (MATRIX50 with key option 1 = 1 required for radiation). The PLANE55 element type is the only four-noded planar thermal element available in ANSYS. The LINK32 element type is the only 2-D element that can be used to define participating surfaces for radiation in the ANSYS AUX12 radiation processor. The MATRIX50 superelement is the only element available for including radiation in ANSYS using the AUX12 processor. No real constants were required, so none were defined. A single ANSYS Parametric Design Language (APDL) input script (W17OFA.INP) generated the finite-element mesh, applied the thermal properties and loads, and executed the solver to obtain a temperature field solution.

The second model is for a Westinghouse 17x17 OFA fuel assembly with instrument and guide tubes modeled and blackbody radiation in the storage cell of a helium-backfilled MPC. This model contains 18167 2-D thermal plane elements (PLANE55, no key options required), 3876 thermal link elements (LINK32, no key options required) and one radiation substructure matrix element (MATRIX50 with key option 1 = 1 required for radiation). The PLANE55 element type is the only four-noded planar thermal element available in ANSYS. The LINK32 element type is the only 2-D element that can be used to define participating surfaces for radiation in the ANSYS AUX12 radiation processor. The MATRIX50 superelement is the only element available for including radiation in ANSYS using the AUX12 processor. No real constants were required, so none were defined. The finite-element mesh was generated manually and saved in an ANSYS database (W17GTGEO.DB). An APDL input script (W17GT.INP) applied the thermal properties and loads and executed the solver to obtain a temperature field solution.

The third model is for an Atrium-10 fuel assembly with gray-body radiation in the storage cell of a helium-backfilled MPC. This model contains 5564 2-D thermal plane elements (PLANE55, no key options required), 1072 thermal link elements (LINK32, no key options required) and one radiation substructure matrix element (MATRIX50 with key option 1 = 1 required for radiation). The PLANE55 element type is the only four-noded planar thermal element available in ANSYS. The LINK32 element type is the only 2-D element that can be used to define participating surfaces for radiation in the ANSYS AUX12 radiation processor. The MATRIX50 superelement is the only element available for including radiation in ANSYS using the AUX12 processor. No real constants were required, so none were defined. The finite-element mesh was generated manually and saved in an ANSYS database (ATRIUM10.DB). An APDL input script (ATR10HE.INP) applied the thermal properties and loads and executed the solver to obtain a temperature field solution.

There are four separate ANSYS finite element models used in the basket in-plane heat transport analyses. The next four paragraphs discuss these four finite-element models.

The first model is for a helium-backfilled MPC-24. This model contains 7900 2-D thermal plane elements (PLANE55, no key options required), 1836 thermal link elements (LINK32, no key options required) and one radiation substructure matrix element (MATRIX50 with key option 1 = 1 required for radiation). The PLANE55 element type is the only four-noded

planar thermal element available in ANSYS. The LINK32 element type is the only 2-D element that can be used to define participating surfaces for radiation in the ANSYS AUX12 radiation processor. The MATRIX50 superelement is the only element available for including radiation in ANSYS using the AUX12 processor. No real constants were required, so none were defined. The finite-element mesh was generated manually and saved in an ANSYS database (MPC24.DB). APDL input scripts applied the thermal properties and loads and executed the solver to obtain a temperature field solution for four separate sets of conditions. The first script evaluated storage of intact zircaloy clad fuel assemblies (ZRHE24.INP). The second script evaluated storage of damaged stainless steel clad fuel assemblies in damaged fuel containers (SSHE24D.INP). The third script evaluated storage of intact zircaloy clad fuel assemblies with the MPC backfill diluted by gases released from 10% of the fuel rods (V24MG.INP). The fourth script evaluated storage of intact zircaloy clad fuel assemblies with the MPC backfill diluted by gases released from 10% of the fuel rods and a reduced zircaloy emissivity (V24MGZR.INP).

The second model is for a helium-backfilled MPC-68. This model contains 9031 2-D thermal plane elements (PLANE55, no key options required), 635 thermal link elements (LINK32, no key options required) and one radiation substructure matrix element (MATRIX50 with key option 1 = 1 required for radiation). The PLANE55 element type is the only four-noded planar thermal element available in ANSYS. The LINK32 element type is the only 2-D element that can be used to define participating surfaces for radiation in the ANSYS AUX12 radiation processor. The MATRIX50 superelement is the only element available for including radiation in ANSYS using the AUX12 processor. No real constants were required, so none were defined. The finite-element mesh was generated manually and saved in an ANSYS database (MPC68.DB). APDL input scripts applied the thermal properties and loads and executed the solver to obtain a temperature field solution for three separate sets of conditions. The first script evaluated storage of intact zircaloy clad fuel assemblies (ZRHE68.INP). The second script evaluated storage of damaged stainless steel clad fuel assemblies in damaged fuel containers (SSHE68D.INP). The third script evaluated storage of intact zircaloy clad fuel assemblies with the MPC backfill diluted by gases released from 10% of the fuel rods (V68MG.INP).

The third model is for a helium-backfilled MPC-32. This model contains 6991 2-D thermal plane elements (PLANE55, no key options required), 564 thermal link elements (LINK32, no key options required) and one radiation substructure matrix element (MATRIX50 with key option 1 = 1 required for radiation). The PLANE55 element type is the only four-noded planar thermal element available in ANSYS. The LINK32 element type is the only 2-D element that can be used to define participating surfaces for radiation in the ANSYS AUX12 radiation processor. The MATRIX50 superelement is the only element available for including radiation in ANSYS using the AUX12 processor. No real constants were required, so none were defined. The finite-element mesh was generated manually and saved in an ANSYS database (MPC68.DB). APDL input scripts applied the thermal properties and loads and executed the solver to obtain a temperature field solution for two separate sets of conditions. The first script evaluated storage of intact zircaloy clad fuel assemblies

(ZRHE32.INP). The second script evaluated storage of damaged stainless steel clad fuel assemblies in damaged fuel containers (SSHE32D.INP).

The fourth model is for a helium-backfilled MPC-24E. This model contains 7032 2-D thermal plane elements (PLANE55, no key options required), 2120 thermal link elements (LINK32, no key options required) and one radiation substructure matrix element (MATRIX50 with key option 1 = 1 required for radiation). The PLANE55 element type is the only four-noded planar thermal element available in ANSYS. The LINK32 element type is the only 2-D element that can be used to define participating surfaces for radiation in the ANSYS AUX12 radiation processor. The MATRIX50 superelement is the only element available for including radiation in ANSYS using the AUX12 processor. No real constants were required, so none were defined. The finite-element mesh was generated manually and saved in an ANSYS database (MPC24E.DB). APDL input scripts applied the thermal properties and loads and executed the solver to obtain a temperature field solution for two separate sets of conditions. The first script evaluated storage of intact zircaloy clad fuel assemblies (ZRHE24E.INP). The second script evaluated storage of damaged stainless steel clad fuel assemblies in damaged fuel containers (SSHE24ED.INP).

There is only one ANSYS finite element model used in the HI-STORM overpack fire analyses. This model contains 1488 2-D thermal plane elements (PLANE55 with key option 3 = 1 for axisymmetry) and 81 surface effect elements (SURF19, with key options 1=1 for thermal DOF, 3=1 for axisymmetry, 4=1 for no midside nodes, 5=1 for extra node used to define sink temperature, 8=5 for calculating convection coefficient as function of absolute temperature difference, and 9 = 1 for specifying surface to extra node view factor). The PLANE55 element type is the only four-noded planar thermal element available in ANSYS. The SURF19 element type was the only 2-D surface effect element available in ANSYS when the analysis was performed. Real constant set 1 was used to specify the surface-to-extra node view factor = 1.0. APDL input scripts generated the finite-element mesh, applied the thermal properties and loads, and executed the solver to obtain a temperature field solution for two separate evaluations. The first script performed the base evaluation for which results are reported in the FSAR (FIRE8.INP). The second script performed a time step size sensitivity evaluation with the same conditions as the base evaluation but time steps one-half the size (FIRE9.INP).

#### b) Error Reporting During Steady-State Analyses

Error messages were not suppressed during any finite-element model evaluations. Upon completion of each evaluation, the analyst reviewed the error and warning message listing to ensure that no errors messages were generated. The reviews found that no error messages were generated during any of the evaluations.

In the fuel region effective thermal conductivity model evaluations, ANSYS element shape warning messages were generated as a result of high aspect ratio elements between the fuel pellets and the cladding. As a result, the computed temperature solutions were carefully checked and confirmed to be correct.

In the modeling of basket in-plane heat transport, ANSYS solution warning messages were generated as a result of thermal link (LINK32) elements being inactive during solution. These elements are only used to generate the radiation substructure matrix (MATRIX50) and are not needed during solution, so it is appropriate for these elements to be inactive during solution.

In the fire analysis for the HI-STORM overpack, ANSYS solution warning messages were generated as a result of changing material properties between load steps. Both convection and thermal radiation heat transfer to and from the outer surface of the overpack are applied using surface effect elements (SURF19). The convection heat transfer coefficient is specified as a material property, so the differences in convection heat transfer coefficients during and after the fire necessitated changing material properties between load steps.

c) **Materials and Material Numbers**

There are three separate ANSYS finite element models used in the fuel region effective thermal conductivity analyses. The first model is for a Westinghouse 17x17 OFA fuel assembly with all rods modeled as fuel rods. The second model is for a Westinghouse 17x17 OFA fuel assembly with instrument and guide tubes modeled. The third model is for an Atrium-10 fuel assembly. The following table lists the materials and assigned material numbers for these three models.

<b>Finite-Element Model</b>	<b>Material</b>	<b>Material Number</b>
<u>W</u> 17x17 OFA with all fuel rods	Fuel Cladding	1
	Alloy X	2
	Helium	3
	UO <sub>2</sub>	4
<u>W</u> 17x17 OFA with guide tubes	MPC Backfill Gas	1
	UO <sub>2</sub>	2
	Fuel Rod Gas	3
	Fuel Cladding	4
	Gas Inside Guide Tubes	5
	Alloy X	6
	Guide Tubes	7
Atrium-10	MPC Backfill Gas	1
	UO <sub>2</sub>	2
	Fuel Rod Gas	3

Finite-Element Model	Material	Material Number
	Fuel Cladding	4
	Assembly Flow Channel	5
	Alloy X	6
	Water Rod	7

There are four separate ANSYS finite element models used in the basket in-plane heat transport analyses, one for each MPC design (i.e., MPC-24, MPC-68, MPC-32 and MPC-24E). The following table lists the materials and assigned material numbers for these four models.

Finite-Element Model	Material	Material Number(s)
MPC-24	Fuel Space within Cell	1
	Fuel Basket Composite Wall	2
	Alloy X	3
	MPC Backfill Gas	4 and 5
MPC-68	Fuel Space within Cell	1
	Alloy X	2
	Fuel Basket Composite Wall	3
	MPC Backfill Gas	4
MPC-32	Fuel Space within Cell	1
	Fuel Basket Composite Wall	2
	Alloy X	3 and 4
	MPC Backfill Gas	6 through 9
MPC-24E	Fuel Space within 8.75" I.D. Cell	1
	Fuel Basket Internal Composite Wall	2
	Alloy X	3
	MPC Backfill Gas	4
	Fuel Basket Peripheral Composite Wall	5
	Fuel Space within 9.05" I.D. Cell	6

There is only one ANSYS finite element model used in the HI-STORM overpack fire analyses. The following table lists the materials and assigned material numbers for this model.

<b>Material</b>	<b>Material Number(s)</b>
Carbon Steel	1
Concrete	2
Outer Surface Conditions (i.e., emissivity and convection coefficient)	3

**Question 4.17**

For all transient thermal analyses described in the SAR provide the following:

- a) A list of all load steps and load step options.
- b) A list of all time/time step options.
- c) A sensitivity analysis which demonstrates that models are not mesh dependent

For transient analysis in ANSYS, refining mesh sizes may effect the accuracy of the solution. Solutions for transient FEA models should not be mesh dependent. This means that the refining of the element mesh should not affect the solution for transient analysis of a given FEA model.

This information is not provided and is needed to assure compliance with 10 CFR 72.11 and 72.236.

**Response 4.17**

There are six transient thermal analyses described in the FSAR. The following table lists these analyses and the corresponding FSAR section.

<b>Transient Thermal Analysis</b>	<b>FSAR Section</b>
Maximum Time Limit During Wet Transfer Operations	4.5.1.1.5
Cask Cooldown and Reflood Analysis During Fuel Unloading Operation	4.5.1.1.6
Fire Analysis for HI-STORM Overpack	11.2.4.2.1
Fire Analysis for HI-TRAC Transfer Cask	11.2.4.2.2
100% Blockage of Air Inlets	11.2.13
Burial Under Debris	11.2.14

Only the fire analysis for the HI-STORM overpack was performed using the ANSYS finite-element program. The requested load step, time step and mesh sensitivity information for this analysis is provided in the following. Copies of all ANSYS input script files referenced in the following are included on a CD-ROM being submitted under separate cover.

a) Load Steps and Load Step Options

Three load steps were used in the analysis: the pre-fire condition, the fire condition, and the post-fire condition. Each of these loading conditions was applied as a step-changed loads (KBC,1).

The pre-fire condition consists of inner and outer overpack surface temperatures that bound those experienced during the steady-state off-normal hot storage condition. This initial load step was solved with time integration effects disabled (TIMINT,OFF). The fire condition consists of convection and thermal radiation heat input to the outer surface of the overpack from a fire temperature of 1475°F and a fixed inner surface temperature of 300°F. The post-fire condition consists of reducing the ambient temperature to the off-normal hot value of 100°F. Both the fire and post-fire load steps were solved with time integration effects enabled (TIMINT,ON).

b) Time Steps and Time Step Options

The multiple solve method is used to perform time stepping within a load step. Automatic time stepping within a time step was enabled (AUTOTS,ON), with at least 2 and as many as 10 sub-steps per time step (NSUBST,4,10,2). The following table summarizes the time steps used in the evaluation reported in the FSAR.

Load Step	Time Steps
Pre-Fire Condition	Steady-State at t = 0 sec.
Fire Condition	4 steps of 15 sec. each from t = 0 sec. to t = 1 min. 4 steps of 30 sec. each from t = 1 min. to t = 3 min. 1 step of ~37 sec. from t = 3 min to t = 3.622 min.
Post-Fire Condition	1 step of 1.378 min. from t = 3.622 min. to t = 5 min. 3 steps of 5 min. each from t = 5 min. to t = 20 min. 3 steps of 10 min. each from t = 20 min. to t = 50 min. 3 steps of 20 min. each from t = 50 min. to t = 90 min. 7 steps of 30 min. each from t = 90 min. to t = 5 hr.

The ANSYS Parametric Design Language (APDL) input script for this evaluation (FIRE8.INP) is included in Appendix C of Holtec Report HI-981892.

A second evaluation that is not discussed in the FSAR is also presented in HI-981892. This second evaluation (FIRE9.INP) is identical to that reported in the FSAR, except the number of time steps is doubled and the corresponding step sizes are halved. The results of this second evaluation were practically the same as those of the first evaluation, confirming that the time steps used were sufficient to obtain an accurate solution. The comparison between the two evaluations is presented in Table 7.23 of HI-981892.

c) Mesh Sensitivity

To demonstrate that the results of the ANSYS fire transient evaluation presented in the FSAR are not mesh dependent, we have performed an additional evaluation (FIRE10.INP) with the number of elements in each coordinate direction doubled. This increases the total number of elements in the model by a factor of four. Except for the increase in the mesh density, this evaluation is identical to the one reported in the FSAR. This evaluation is archived in Appendix J of Holtec Calculation Report HI-2004407.

The following table presents a comparison of the maximum computed temperatures at the overpack mid-height for these base (i.e., FSAR) evaluation and the increased mesh density evaluation.

Location	Initial Temperature [°F]	Maximum Temperature, Base Run [°F]	Maximum Temperature, Increased Mesh Density Run [°F]	Temperature Rise Difference [%]
Overpack Outer Shell	157	570.27	591.68	5.18
Outer Concrete Surface	157.03	529.58	551.05	5.76
One Inch Into Concrete	158.13	322.56	316.21	-3.86
Two Inches Into Concrete	159.25	262.51	257.29	-5.06
Three Inches Into Concrete	160.38	233.28	229.60	-5.05
Four Inches Into Concrete	161.53	216.48	213.40	-5.61
Five Inches Into Concrete	162.70	205.77	203.29	-5.76
Six Inches Into Concrete	163.89	198.71	196.68	-5.83

As this comparison shows, uniformly doubling the number of elements in all coordinate directions results in a maximum change in the computed maximum temperature rise of less

U.S. Nuclear Regulatory Commission  
ATTN: Document Control Desk  
Document ID: 5014422  
Attachment 1  
Page 40 of 71

than 6%. As stated in the FSAR, less than one-inch of concrete at the outer surface exceeds the short-term temperature limit for concrete (350°F). The same conclusion would be reached based on the results of the increased mesh density evaluation. This comparison confirms that the finite-element mesh used for the fire transient evaluation presented in the FSAR was sufficient to obtain an accurate solution.

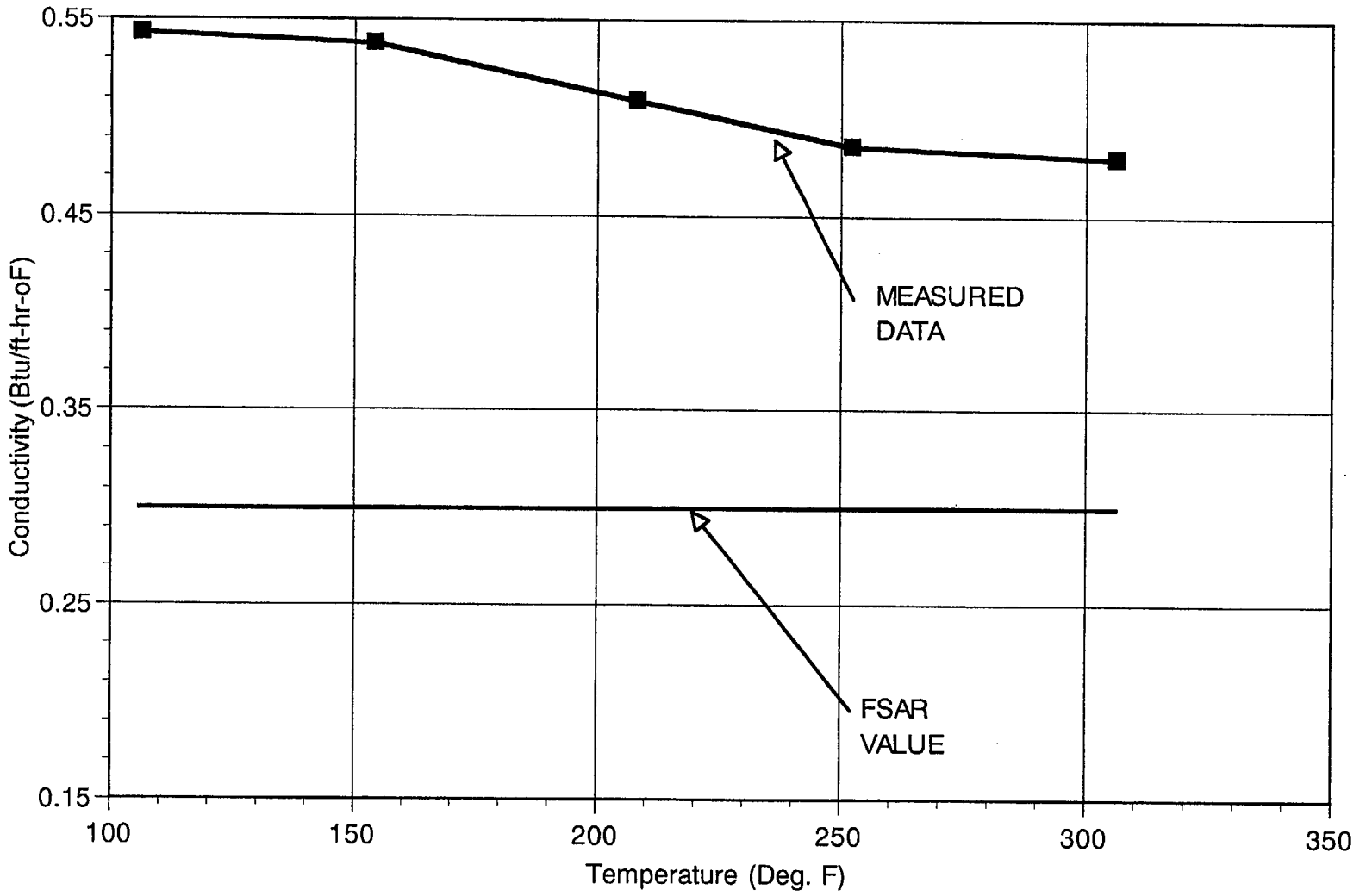


FIGURE 4.3-1: HOLTITE<sup>TM</sup> THERMAL CONDUCTIVITY CONSERVATISM

RAI RESPONSES (LAR 1014-1)

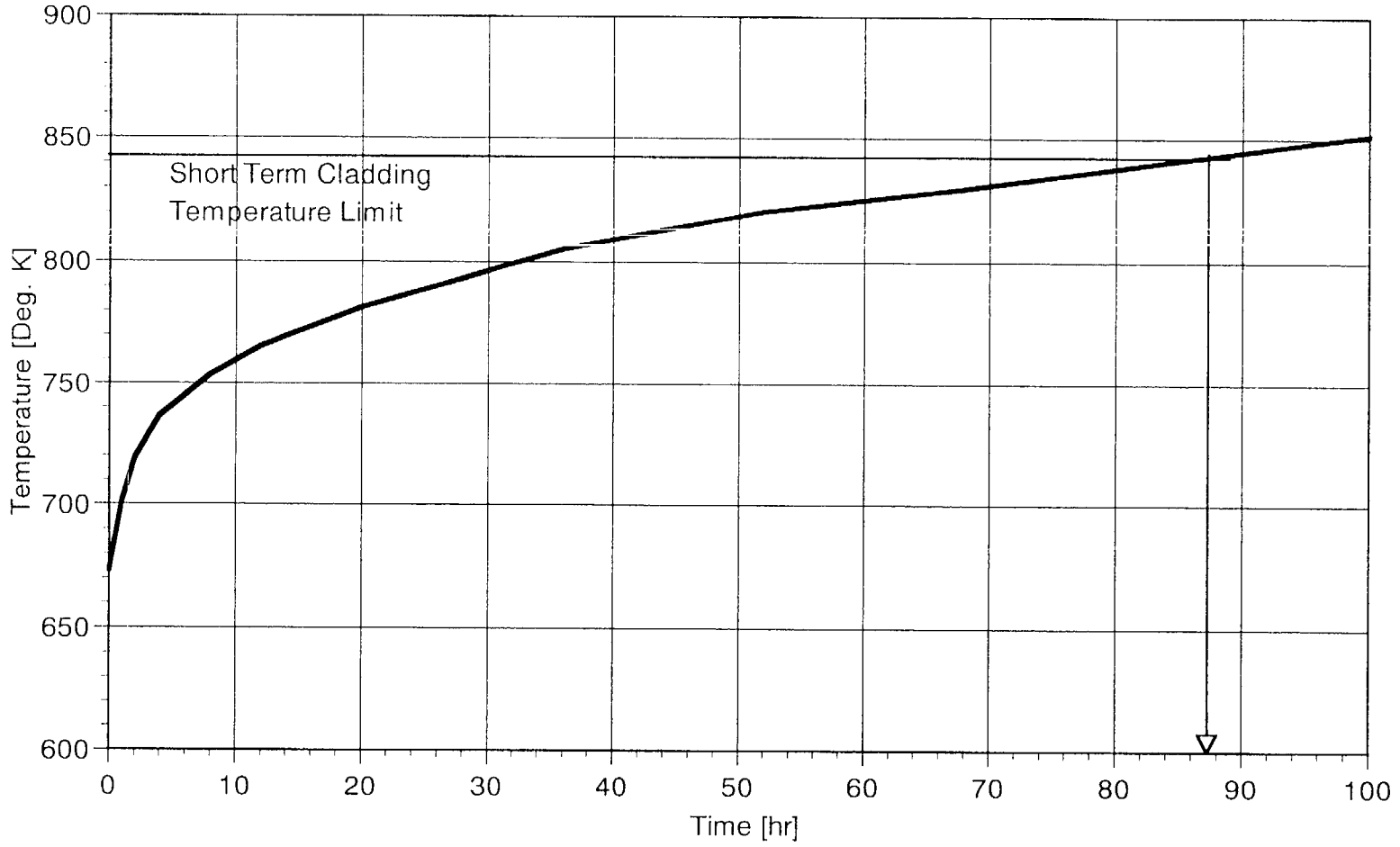


FIGURE 4.12-1: HI-STORM BLOCKED INLET DUCTS TRANSIENT PEAK CLAD TEMPERATURE HISTORY @ 28.74 kW

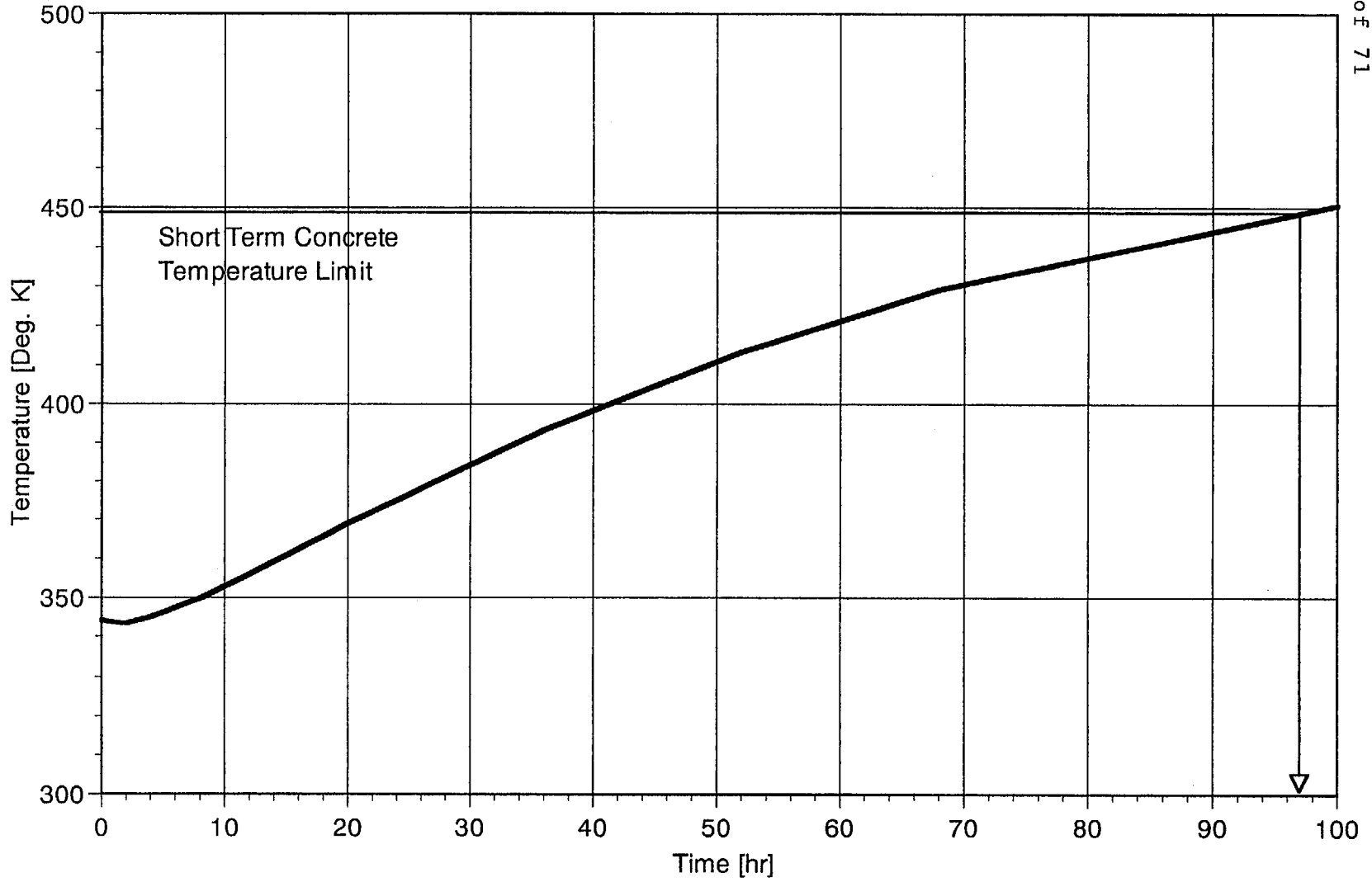


FIGURE 4.12-2: HI-STORM BLOCKED INLET DUCTS TRANSIENT CONCRETE SECTION  
TEMPERATURE HISTORY @ 28.74 kW

## **Appendix 4.A Clad Temperature Limits For High-Burnup Fuel**

10 CFR 72.122(h)(1) requires that spent fuel cladding must be protected from degradation that leads to gross ruptures, or the fuel must otherwise be confined so that degradation of the cladding will not impose operational safety problems. Further, 10 CFR 72.122(l) requires that the storage system must be designed to allow ready retrieval of the spent fuel from the storage system for further processing or disposal. The following questions request information associated with the fuel clad temperature that is not provided in the applications and is needed to assure compliance with the regulations.

### **Preface to the Appendix 4.A Responses**

Recognizing that a number of RAIs have arisen from the compact manner in which the information is provided in Appendix 4.A, additional explanatory material has been added in the proposed Revision 1.B to explain the analysis procedure in more detail and with greater clarity. A subsection containing a summary of the principal conservatisms has also been added to clearly expose the conservatisms built into the solution process. Finally, to resolve certain RAIs in a conclusive manner, it has been necessary to modify the coefficients in the creep equation and utilize a more conservative cladding temperature vs. time curve. The computed peak cladding temperatures (PCT) remain fairly close to the values provided in the previous revision to this appendix. They also remain uniformly above the allowable PCT limits used to compute the heat duty of the system in Chapter 4. Therefore, Chapter 4 analyses are unaffected.

All numerical calculations performed in support of this issue of this appendix are archived in the calculation package, Holtec Report [2], under Appendix H.

### **Question 4.A.1**

Explain why none of the BWR temperatures in Table 4.A.2, Rev. 1A, match those in Appendix F (pages F-4 to F-25) for spent fuel having burnups greater than 45 GWd/MTU (hereafter referred to as high burnup fuel).

### **Response 4.A.1**

The reason why the allowable PCTs in Table 4.A.2 are less than the computed values in Appendix F of the calculation package was explained in an earlier revision (Revision 0) of Appendix 4.A. In summary, whenever the calculations in Appendix F yielded a greater value of the allowable PCT for high burnup SNF than the corresponding value for moderate burnup fuel previously adopted in the HI-STORM FSAR, then the lower value was also prescribed as the allowable PCT for high burnup fuel.

### **Question 4.A.2**

Demonstrate the acceptability of the rod hoop stress equation as stated in Appendix F of

the calculation package, HI-2002407 for determining creep stain in storage. This equation does not appear to account for the stress in the fuel rods at ambient temperature. Additionally, the equation appears to be in error because the hoop stress appears to approach zero for long times.

#### **Response 4.A.2**

The Appendix F<sup>d</sup> rod hoop stress equation was constructed to model the reduction in rod stress as a function of fuel decay heat attenuation in dry storage starting from a conservatively bounding stress at the *beginning* of dry storage. As a conservative posture, the creep modeling in this Appendix completely ignored the reduction in stress and temperature over the 40 year dry storage time except for a short initial period (~1 yr). For this short initial period in dry storage, certain leading order effects were included in the stress model and long term effects (i.e. monotonic approach of rod temperature towards ambient temperature) neglected. Because of the narrow range application of this stress model, this is not suitable for long time extrapolations.

#### **Question 4.A.3**

Provide examples of temperature and stress values versus time in dry storage used to determine the temperature limits in Table 4.A.2, Rev. 1A, for PWR and BWR fuel at 60 GWd/MTU with 6 and 10 year cooling before dry storage. The example calculations are necessary to understand the application of these equations for temperature and stress.

#### **Response 4.A.3**

The requested calculations are provided in explicit detail in Appendix H of the calculation package [2] using the Holtec creep model provided in proposed Revision 1B of the HI-STORM FSAR.

#### **Question 4.A.4**

Provide an explicit calculation of the integrated primary strains (0 to 10,000 hours) using the Holtec creep equation from Appendix G for one cooling time, e.g., 6 years. Attempts to duplicate the calculated primary strains (identified as "creep strain after 10,000 hours" in Appendix F) presented in Appendix G was not possible.

---

<sup>d</sup> In support of Revision 2 to the LAR and these RAI responses, Appendix F to the calculation package has been superseded by Appendix H.

#### **Response 4.A.4**

The integration of creep equation (Eq. 14 in Appendix 4.A) to compute accumulated strain for six years old fuel is provided in explicit detail in Appendix H of the Calculation Package. Pursuant to RAI 4A.11, the primary-creep to secondary-creep interface is assumed to occur at 0.5% strain (not 10,000 hours) in this revision of the FSAR.

#### **Question 4.A.5**

Justify that the data used to derive critical strain energy density (CSED) approach is bounding for fuel greater than 63.5 GWd/MTU. Rashid's paper (page 6) indicates that test were conducted between burnup levels between 25 - 63.5 GWd/MTU. Additionally, Rashid's paper (page 11) states that test were conducted on samples that contained incipient hydrides. Hydrides have been postulated by some researchers to be the limiting condition for cladding integrity.

#### **Response 4A.5**

The CSED approach discussed in Rashid's paper provides the logical framework to justify a higher creep limit than the 1% limit set forth in ISG-11, and adopted in our FSAR. As we discuss in the last paragraph of subsection 4.A.3 of the Appendix, the 1% creep strain limit can be viewed as a conservative specification for burnups up to 68.4 GWD/MTU.

#### **Question 4.A.6**

Justify why the high density hydride rim and blister (due to spallation) is not considered in the metal loss for creep to failure.

#### **Response 4.A.6**

Any form of corrosion that produces non-adherent (flaked or spalled) metal layers unable to withstand hoop stress levels typical of fuel cladding in dry storage (50 to 150 MPa) should be considered to be lost for load (pressure) bearing purposes. Material that remains integral to the fuel cladding metal mass but has developed localized areas of increased strength (such as due to hydriding), on the other hand, should be considered available for the load-bearing function.

#### **Question 4.A.7**

Justify that the information used in the Holtec Report HI-20022407 calculation package pertaining to fuel heat decay attenuation for short cooled fuel between 50-60 GWd/MTU is bounding for all fuel greater than 60 GWd/MTU that will be stored in the cask.

Page G-3, states that these calculations employ certain information pertaining to fuel heat attenuation for short cooled fuel between 50-60 GWd/MTU.

#### **Response 4.A.7**

To accommodate this RAI, the reference fuel decay heat curve has been changed to 70 GWD/MTU burnup for both PWR and BWR fuel. The governing SNF type for both PWR and BWR genre (B&W 15x15 type for PWR and GE 7x7 type for BWR SNF) were used to generate the decay heat curves.

#### **Question 4.A.8**

Demonstrate that the available corrosion reserve and reduced oxide thickness, and hydrides due to oxidation do not compromise the material properties and structural integrity of the cladding to withstand the expected loads encountered during storage under normal, off-normal, and accident conditions.

#### **Response 4.A.8**

Environmental conditions, other than the variation in ambient temperature, are of little consequence to the spent nuclear fuel stored in a helium (inert) environment in a hermetically sealed pressure vessel (MPC) installed in a large steel weldment filled with concrete (HI-STORM overpack). Analyses presented in Chapter 3 of the SAR underscore the structural isolation of the SNF from the environmental loadings. The net effect of the ambient temperature variation is to produce a corresponding variation (albeit smaller) in the fuel cladding temperature. As discussed in Subsection 2.2.2.2 of the FSAR, the normal temperature has been accordingly set at a value (80°F), which bounds the average ambient temperature for all locations in the United States. No new failure modes due to the daily or seasonal temperature variations have been identified in the literature.

The additional material thickness designated as the corrosion reserve, if not consumed by corrosion, will reduce the cladding stress levels and accordingly, retard the rate of creep. In other words, the presence of the "corrosion reserve" material in un-degraded form is uniformly beneficial.

#### **Question 4.A.9**

Demonstrate that the two sets of data from the FRG-2 reactor and compared to the Holtec creep model in FSAR Figures 4.A.2 and 4.A.3 are independent and from two different creep tests. This is because both data sets show nearly identical creep strain, have the same temperature and stress levels, and the specimens came from the same reactor. Therefore, it appears that they are the same data just presented in two different references (see below).

Two sets of data from the FRG-2 reactor in Germany, from H Spilker et al. ("Spent LWR Fuel Dry Storage in Large Transport and Storage Casks After Extended Burnup," Journal of Nuclear Materials 250,1997, 63-74) and G Kasper et al. ("Spalproductfreisetzung und Post-

Pile-Kreichverhalten trohen gelagerter, abgebrannter Brennstabe," BMFT-KWA 2100BO, 1985) have been referenced and used to verify the Holtec creep model in Section 4.A, Revision 1A. However, examination of these two references (similar authors with their arrangement different) and the data, it appears that they are the same creep tests with only differences in the number of data points and total time to which the data is presented, i.e., 6,000 hours and 8,000 hours.

#### **Response 4A.9**

The Holtec creep model is compared with the creep data reported by Spilker et. al. (1997 paper in the Journal of Nuclear Materials) and the creep data reported by Kaspar et. al. (1985 KWO report). The two sources report creep test data on irradiated FRG-2 reactor cladding samples. The creep test conditions for the Spilker data and the Kaspar data, however, are different. The test conditions are listed below:

Spilker et. al. Creep Test Data:

Temperature	: 400°C
Stress	: 70 MPa
Time	: 1000 to 6000 hrs

Kaspar et. al. Creep Test Data:

Temperature	: 380°C (0 to 1000 hrs)
	395°C (>1000 hrs)
Stress	: 86 MPa
Time	: (1000 to 8000 hrs)

#### **Question 4.A.10**

Compare the Holtec creep model predictions to the creep strain data that are more applicable to the temperature and stress for dry storage. Suggested creep data that are more applicable are from R. E. Einziger and R. Kohli, "Low-Temperature Rupture Behavior of Zircaloy-Clad Pressurized Water Reactor Spent Fuel Rods under Dry Storage Conditions," Nuclear Technology, 67:107, 1984 with data at 323 °C and 150 MPa from cladding irradiated in the Turkey Point reactor; and from G Kaspar et al., Spalproductfreisetzung und Post-Pile-Kreichverhalten trohen gelagerter, abgebrannter Brennstabe, BMFT-KWA 2100BO, 1985, Erlangen, Germany with data at 350 °C and 50 MPa from cladding irradiated in the KWO reactor in Germany.

The Holtec post-irradiation creep equation may underestimate strains at low temperature and stresses below 200 MPa because the activation energy for creep of 250 kJ/mole is high, particularly for the creep mechanisms active in the temperature and stress range for dry storage. The Holtec creep equation is normalized to post-irradiation creep data in the range of 380 to 420°F and very high stress data at 300°F which may be the reason why the activation energy is too high.

#### **Response 4.A.10**

We agree with the staff that the coefficients in the creep equation were selected to provide conservative results in comparison to Goll et. al. data which are of a short duration, relatively high temperature (300 °C to 370 °C) and very high stress. The creep equation configured to conservatively bound the Goll et. al. data (which are of questionable relevance to the dry storage conditions compared to other data presented in the FSAR) indeed fails to provide a similarly conservative prediction for the low temperature Einziger, et al. data because of the high activation energy coefficient, as surmised by the staff.

The coefficients in the creep equation have been adjusted to bound the data from Einziger, Kasper et al. cited in the RAI. Subsections 4.A.5 and 4.A.6 of the revised appendix contain the relevant information on the comparison of the creep equation (with revised coefficients) with all test data available to us at this time.

#### **Question 4.A.11**

Provide the experimental evidence (creep data) that demonstrates that Zircaloy cladding creep remains in the primary creep stage, i.e., decreasing creep rate with time, for up to 1% creep strain or 10,000 hours, as applied in the Holtec creep model.

Most of the creep data in the temperature and stress range relevant to dry storage conditions indicate that primary creep saturates at less than 0.5% strain and much less than 10,000 hours. The assumption that the secondary creep rate (i.e., steady-state creep rate with time), is equal to the primary creep rate at 10,000 hours or 1% creep strain (whichever is achieved first) will most likely cause an under prediction of the secondary creep strain rate. As defined in this application for dry cask storage conditions, the 10,000 hour limit will always determine the secondary creep rate. Therefore, it is difficult to conclude that the creep approach, as submitted, will be conservative for dry cask storage applications.

#### **Response 4.A.11**

Our assumption of transition from primary to secondary creep regime at 10,000 hours was based on the limited data available in the literature. However, we agree that the transition point should be logically pegged to an accumulated creep strain value rather than a fixed time duration. Accordingly, we have modified the creep model to set the incipience of secondary creep at 0.5% strain.

#### **Question 4.A.12**

Clarify whether the secondary creep rate calculated at 10,000 hours is assumed to remain constant for all dry storage time periods beyond this point for determining total accumulated strain even though temperature and stress are decreasing beyond this point.

Page 4.A.11 and Equation (16) appear to imply that the secondary creep rate is assumed to be constant after it is calculated at the 10,000 hours time in dry storage and does not take into account the decrease in temperature and stress beyond the 10,000 hours time; however, the text is not entirely clear on this point.

#### **Response 4.A.12**

In the revised formulation, the secondary creep rate is assumed to initiate at  $\epsilon^* = 0.5\%$  ( $\epsilon^*$  is accumulated strain). In the secondary creep phase, the rate of creep is constant for constant stress & temperature. However, the rate of creep will decrease as stress and temperature continue to decrease throughout the storage period. This is further explained in Appendix H of the calculation package [4.2] and in Subsection 4.A.7 in the FSAR.

#### **Question 4.A.13**

Provide an estimate of the non-conservative error that is introduced in Equation 14 in Appendix 4A, Rev. 1, by the assumption that there is a linear relationship between fuel temperatures versus the decrease decay heat with time. Further, confirm that the  $T(\theta)$  and  $T_0$  terms in Equation 14 are relative delta temperatures above ambient temperature.

The above assumption of linearity between decay heat and temperature introduces a non-conservative estimate of fuel temperatures with decreasing decay heat because part of the heat transfer process is non-linear with decreasing temperature, (e.g., heat transfer due thermal radiation decreases with temperature to the fourth power).

#### **Response 4.A.13**

In our estimate, the amount of non-conservatism introduced by assuming a linear relationship between the fuel cladding temperature and heat generation rate was quite small because the temperature values for only the first 10,000 hours of storage were used in the creep analysis (the temperature and stress were assumed to remain constant thereafter as stated in response to RAI 4.A.12).

However, as discussed in Subsection 4.A.6, even this small amount of non-conservatism has been eliminated in the revised creep analysis by computing the fuel cladding and in-rod gas temperatures explicitly as a function of the heat load using the design basis thermal model described in Chapter 4 of the HI-STORM FSAR. Complete details are provided in

Subsection 4.A.6. Detailed computations are archived in the Calculation Package [2], Appendix H.

**Question 4.A.14**

Justify that the allowable temperatures given in Table 4.5.9, "Peak Cladding Temperature in Vacuum," will not result in major annealing of the cladding.

**Response 4.A.14**

As discussed in Section 4.5.2.2 of the FSAR and in revised LCO 3.1.1 in Appendix A to the CoC, we require a closed-forced helium flow system to de-moisturize the MPCs that are loaded with at least one high burnup fuel assembly and backfill them with helium. This will eliminate the potential for annealing of the cladding as well as the threat of hydride reorientation. Therefore, the thermal analysis performed for vacuum conditions does not apply to high burnup fuel.

**Question 4.A.15**

Describe the quantitative effects nitrogen will have on highly spalled zircaloy fuel cladding during the moisture removal process. In the discussion, consideration should be given to (1) the reaction rate of nitrogen with the cladding, and (2) formation of nitric acid. Additionally, revise Chapter 8 of the SAR to specify the purity of the nitrogen gas used for moisture removal.

Page 8.1-19 of the SAR discusses how the MPC employs forced helium or nitrogen recirculation to remove residual moisture from the MPC fuel cavity. If nitrogen is used the possibility of creating nitric acid due to the radiolytic decomposition of water needs to be evaluated along with the impact of nitrogen reaction with the Zircaloy components in the fuel assemblies.

**Response 4.A.15**

The use of nitrogen in the MPC drying process has been removed from the FSAR as an option in this revision of the proposed FSAR.

**Question 4.A.16**

Demonstrate that the moisture removal process ensures that the maximum quantity of oxidizing gases is limited to 1 gram-mole per cask. This 1-gram-mole limit reduces the amount of oxidants below levels where any cladding degradation can occur.

#### **Response 4.A.16**

The helium drying system is designed to remove moisture in the MPC down to a partial pressure of less than 3 torr. The proposed acceptance limit in the technical specifications (SR 3.1.1.1) has been modified from a dew point to an exit gas temperature corresponding to less than the 1 gram-mole limit for moisture content in the MPC. A calculation to demonstrate that this residual moisture is below the 1-gram-mole limit is provided below. The residual gram moles of water is computed by the Ideal Gas Law as follows:

$$n = PV/(RT)$$

where:

n	=	Gas quantity in lb-mol
P	=	Residual Moisture Pressure (3 torr)
V	=	MPC cavity free volume (Upper bound 250 ft <sup>3</sup> )
R	=	Gas Constant 555 mm Hg ft <sup>3</sup> /(lb-mol °R)
T	=	Absolute Gas Temperature (Lower bound 660°R)

Therefore, n computes as  $2.05 \times 10^{-3}$  lb-mole which is 0.93 gram moles. LCO 3.1.1 in Appendix A to the CoC has been revised to replace the dew point limit with the saturation temperature of water at 3 torr (21°F).

#### **Question 4.A.17**

Justify why strain hardening applies in the Holtec creep equation at temperatures and stresses where coble creep may be the controlling creep mechanism for irradiated cladding.

Coble creep may be the active creep mechanism in irradiated cladding at stresses below 200 MPa and temperatures below 400°C. Further, coble creep does not appear to have a mechanism that would allow for strain hardening because coble creep does not require dislocation motion.

#### **Response 4.A.17**

The precise phenomenological processes that act and interact during the creep of irradiated cladding and their relative contribution to the overall creep rate cannot be stipulated with certainty at this time. Our vehicle for predicting the creep strain rate must follow classical procedure as outlined in Subsection 4.A.6. By benchmarking the proposed creep equation with test data, we have followed a solution approach that is well established in the mechanics of visco-plastic media for nearly a century. Our effort at constructing the creep equation is doubtless hindered by the paucity of test data, but it is also helped by the fact that (i) we seek to develop a *bounding*, rather than a *predictive*, relationship and (ii) the range of parameters, namely temperature (300 to 400°C) and stress (50 to 150 MPa) are well defined for our problem.

U.S. Nuclear Regulatory Commission  
ATTN: Document Control Desk  
Document ID: 5014422  
Attachment 1  
Page 53 of 71

**REFERENCES:**

- [4.1] "TN-24P Benchmarking and HI-STAR/HI-STORM Thermal Modeling Calculation Package", Holtec Report HI-992278, Rev. 1.
- [4.2] "Thermal-Hydraulic Calculations for the HI-STAR/HI-STORM Amendments", Holtec Report HI-2002407, Rev. 3.
- [4.3] "Rohsenow, W.M. and Hartnett, J.P., "Handbook of Heat Transfer", McGraw Hill, (1950).

## 5.0 Shielding Evaluation

### Question 5.1

Revise the SAR (Chapters 5 and 8) to show the gamma cross shield plates as mandatory auxiliary equipment.

The dose rates for dose point locations 1 and 3, in Tables 5.1.1 through 5.1-6, assume the gamma cross shield plates are installed.

This information is not provided and is needed to assure compliance with 10 CFR 72.236.

### Response 5.1

In Section 5.3.1, the following wording has been changed from:

“The HI-STORM 100S offers optional gamma shield cross plates, detailed on drawings in Chapter 1, which offer more plates in the ducts. These optional gamma shield cross plates could further reduce the dose rate at the vent openings by as much as a factor of two.”

to:

“Figure 5.3.19 shows two designs for the gamma shield cross plates to be used in the inlet and outlet vents. The designs in the top portion of the figure are mandatory for use in the HI-STORM 100 and 100S overpacks during normal storage operations and were assumed to be in place in the shielding analysis. The designs in the bottom portion of the figure may be used instead of the mandatory designs in the HI-STORM 100S overpack to further reduce the radiation dose rates at the vents. These optional gamma shield cross plates could further reduce the dose rate at the vent openings by as much as a factor of two.”

FSAR Figure 5.3.19 has been added in response to this RAI.

Chapter 8 of the FSAR already states in Sections 8.1.1 and 8.1.7 that the gamma shield cross plates are installed in the overpack. Therefore, the current wording in Chapter 8 in conjunction with the changes in Chapter 5 are sufficient and no further changes to Chapter 8 are necessary, with the following exception: Item 16.f of Section 8.1.7 will be reworded in the following manner to remove an ambiguity that was inadvertently introduced. (See also RAI 8.3).

Original text:

“If necessary, install the HI-STORM exit vent gamma shield cross plates, thermocouples, and vent screens.”

U.S. Nuclear Regulatory Commission  
ATTN: Document Control Desk  
Document ID: 5014422  
Attachment 1  
Page 55 of 71

Modified text:

"Install the HI-STORM exit vent gamma shield cross plates, temperature elements (if used), and vent screens."

### **Question 5.2**

Justify the acceptability of fuel with burnups greater than 45 GWd/MTU for PWR, and 34 GWd/MTU for BWR spent fuel, considering the uncertainties with source term determinations associated with high burnup fuel.

The application does not provide benchmark data for SAS2H to provide adequate validation of the isotopic depletion calculations for burnups above 45 GWd/MTU for PWR, and 34 GWd/MTU for BWR spent fuel. This information is needed to assure compliance with 10 CFR 72.236.

### **Response 5.2**

There have been numerous comparisons of experimental isotopic data and decay heat data for both PWRs and BWRs to calculated values using SAS2H and ORIGEN-S. Many of these comparisons have been performed in the US and have been published by ORNL. The majority of this data is for burnups below 45 GWD/MTU with one data point above 45 GWD/MTU. There is an ongoing effort, according to ORNL, to obtain data for burnups above 45 GWD/MTU. In fact, there is already a limited amount of data available (with more data hopefully becoming available in the near term) and calculated comparisons to this data are currently under way at ORNL. Some of these new comparisons should be published before the end of 2001. The comparisons that have been published have all shown generally good agreement between calculations and measurements and there is no reason to expect that the on-going comparisons with higher burnup fuel will not achieve similarly good agreement. In addition, the Japanese have published isotopic data and results (using their SWAT code system, JAERI report JAERI-Tech 2000-071) which also show generally good agreement between measurements and calculation. Although this is not SAS2H and ORIGEN-S, the results appear to indicate that nothing "unusual" is going on in the high burnup regime.

NUREG/CR-6700, "Nuclide Importance to Criticality Safety, Decay Heating, and Source Terms Related to Transport and Interim Storage of High Burnup LWR Fuel", analyzes various isotopes and their relative contribution to decay heating and dose rate for radiation shielding. These results indicate that the important nuclides for decay heating and radiation shielding are approximately the same at low and high burnups. This implies that the physics of depletion as it relates to decay heat and radiation shielding is similar between low and high burnups. Therefore, the validation of isotopics below 45 GWD/MTU would suggest that equally good agreement should be obtained between SAS2H calculations and measurement for burnups above 45 GWD/MTU.

The following text has been added to Section 5.2 of the SAR to discuss the validations of SAS2H that have been performed.

“SAS2H has been extensively compared to experimental isotopic validations and decay heat measurements. References [5.2.8] through [5.2.12] present isotopic comparisons for PWR and BWR fuels for burnups ranging to 47 GWD/MTU and reference [5.2.13] presents results for BWR measurements to a burnup of 57 GWD/MTU. A comparison of calculated and measured decay heats is presented in reference [5.2.14]. All of these studies indicate good agreement between SAS2H and measured data. Additional comparisons of calculated values and measured data are being performed by various institutions for high burnup PWR and BWR fuel. These new results, when published, are expected to further confirm the validity of SAS2H for the analysis of PWR and BWR fuel.”

The following references have been added.

- [5.2.8] O. W. Hermann, et al., “Validation of the Scale System for PWR Spent Fuel Isotopic Composition Analyses,” ORNL/TM-12667, Oak Ridge National Laboratory, March 1995.
- [5.2.9] M. D. DeHart and O. W. Hermann, “An Extension of the Validation of SCALE (SAS2H) Isotopic Predictions for PWR Spent Fuel,” ORNL/TM-13317, Oak Ridge National Laboratory, September 1996.
- [5.2.10] O. W. Hermann and M. D. DeHart, “Validation of SCALE (SAS2H) Isotopic Predictions for BWR Spent Fuel,” ORNL/TM-13315, Oak Ridge National Laboratory, September 1998.
- [5.2.11] “Summary Report of SNF Isotopic Comparisons for the Disposal Criticality Analysis Methodology,” B00000000-01717-5705-00077 REV 00, CRWMS M&O, September 1997.
- [5.2.12] “Isotopic and Criticality Validation of PWR Actinide-Only Burnup Credit,” DOE/RW-0497, U.S. Department of Energy, May 1997.
- [5.2.13] B. D. Murphy, “Prediction of the Isotopic Composition of UO<sub>2</sub> Fuel from a BWR: Analysis of the DU1 Sample from the Dodewaard Reactor,” ORNL/TM-13687, Oak Ridge National Laboratory, October 1998.
- [5.2.14] O. W. Hermann, et al., “Technical Support for a Proposed Decay Heat Guide Using SAS2H/ORIGEN-S Data,” NUREG/CR-5625, ORNL-6698, Oak Ridge National Laboratory, September 1994.

## **6.0 Criticality Evaluation**

### **Question 6.1**

Provide a detailed description of the calculational model used for the MPC-32 PWR basket in Section 6.3.1 of the SAR. Justify any differences in calculational techniques used for each of the MPC basket designs.

The description in the SAR is not detailed enough to complete the review. Specifically, the discussion in Section 6.3.1 of the SAR concerning the use of CASMO-3 to determine reactivity effects due to manufacturing tolerances appears to apply to all of the different basket configurations, but CASMO-3 results are not given for the MPC-32.

This information is required for the staff to assess compliance with the nuclear criticality safety requirements specified in 10 CFR 72.124 and 72.236.

### **Response 6.1**

The same calculational techniques and level of detail in the criticality models is used for all MPCs including the MPC-32. Reactivity effects are evaluated using CASMO-3 (2-dimensional, infinite lattice) and MCNP (3-dimensional, full cask models). For the MPC-24 and MPC-68, both codes were used. For the MPC-32, only the more detailed MCNP models were used and are documented. Additional discussions have been provided in FSAR Section 6.1 and Section 6.3.1 to clarify these issues.

### **Question 6.2**

Provide a detailed description of the calculational models used for the MPC-24E and MPC-24EF PWR baskets in Section 6.3.1 of the SAR.

The description in the SAR is not detailed enough to complete the review. Specifically, Section 6.3.1 of the SAR discusses the modeling assumptions used for the reduced width of the periphery Boral panels for the MPC-24 basket, but it is not clear that the same modeling assumptions apply to the MPC-24E and -EF baskets.

This information is required for the staff to assess compliance with the nuclear criticality safety requirements specified in 10 CFR 72.124 and 72.236.

### **Response 6.2**

A discussion has been added to Section 6.3.1 regarding the modeling assumptions for the peripheral Boral panels for the MPC-24E and -24EF baskets. FSAR Figure 6.3.4.A has been updated.

### **Question 6.3**

Provide SCALE inputs for the following cases:

- a) the most limiting normal and accident cases for the MPC-24E/ MPC-24EF, and
- b) the most limiting normal and accident cases for the MPC-32.

The inputs used in the SCALE calculational models are not provided. This information is required for the staff to assess compliance with 10 CFR 72.124 and 72.236.

### **Response 6.3**

The following three Holtec-proprietary criticality input files (MCNP) are provided under separate cover:

- MPC-24E/EF with intact fuel (Assembly 15x15F, 4.5 wt% <sup>235</sup>U),
- MPC-24E/EF with intact and damaged fuel (configuration with highest calculated reactivity) and
- MPC-32 (Assembly Class 15x15F, 5.0 wt% <sup>235</sup>U, 2600 ppm soluble boron)

These input files apply to both normal and accident conditions.

### **Question 6.4**

Provide a justification that uneven draining is not credible with the mesh size used in the damaged/failed fuel cans. Alternatively, a criticality analysis considering uneven flooding for the MPC-24E and -24EF should be provided.

Statements in the SAR Section 6.4.2.2 regarding the credibility of uneven flooding are not justified. Uneven draining may be possible for screens with a mesh size of 350 or less because the water surface tension may be capable of supporting water and uneven draining in the canister may be more reactive than a fully flooded cask. In previous reviews the staff safety evaluation report noted that the assumptions regarding uneven flooding being not credible were not justified.

This is required for the staff to assess compliance with 10 CFR 72.124 and 72.236.

### **Response 6.4**

Additional criticality analyses have been performed in response to this RAI and are summarized in FSAR Chapter 6 assuming uneven draining when Damaged Fuel Containers (DFCs) are present in the MPCs. These analyses have been performed for all MPCs which may contain DFCs; MPC-24E, MPC-24EF, MPC-68, MPC-68F, and MPC-68FF. The analyses demonstrate that the preferential flooding condition is bounded by the fully flooded condition already analyzed. FSAR Section 6.4.2.4 was updated, and FSAR

U.S. Nuclear Regulatory Commission  
ATTN: Document Control Desk  
Document ID: 5014422  
Attachment 1  
Page 59 of 71

Table 6.4.4 was added.

**Question 6.5**

Explain in further detail, and justify, the analysis performed in Section 6.4.4.2.2 to determine the optimum moderation and maximum reactivity for damaged fuel and fuel debris. The description does not state if the analysis was performed on a cask basis or if some other configuration was used.

This information is not provided and is required for the staff to assess compliance with 10 CFR 72.124 and 72.236.

**Response 6.5**

The analyses in FSAR Section 6.4.4.2.2 were performed on a cask basis, i.e. for an MPC-24E/-24EF with 20 intact assemblies and 4 DFCs, and for a MPC-68/-68FF with 52 intact assemblies and 16 DFCs. Appropriate clarification of the modeling approach has been added to this FSAR section and to FSAR Section 6.4.4.2.

## **7.0 Confinement Evaluation**

### **Question 7.1**

Revise the exposure-to-dose conversion factors (DCFs) in the spreadsheet in Appendix 7.A of the application to use the most limiting value for each radionuclide and each organ. Alternatively, justification should be provided if the most limiting value is not used. For example, the DCF for a less restrictive lung-clearance class is used (SR-90, RU-106, Y-90, CD-113M, SN-119M, S3-125, TE-125M, CE-144, PR-144, PM-147, PU-238, PU-239, PU-240, PU-241 and PU-242).

This information is not provided and is needed to assure compliance with 10 CFR 72.104 and 72.236.

### **Response 7.1**

The exposure-to-dose conversion factors (DCFs) in the spreadsheet of Appendix 7.A have been revised to use the most limiting value for each radioisotope and each organ. Tables 7.3.2 through 7.3.5 and Table 7.3.8 have been revised to reflect the changes to the DCFs.

### **Question 7.2**

Revise the confinement analysis to include the DCF values for Rh 106m, or justify the omission of Rh-106m and the use of the zero DCF values for Rh 106.

The spreadsheet in Appendix 7.A lists the DCF for the radionuclide Rh 106 as zero. It is not clear that Rh 106 is the appropriate radionuclide to be considered, since Rh-106m would be more likely to occur due to the decay of Ru-106.

This information is needed to assure compliance with 10 CFR 72.11.

### **Response 7.2**

As described in Section 7.3.1 of the HI-STORM FSAR, the inventory for isotopes was calculated with the SAS2H and ORIGEN-S modules of the SCALE 4.3 system. Therefore, the isotope Rh-106m is "omitted" from the inventory of isotopes because the SCALE 4.3 system calculates a zero inventory for this isotope. This is consistent with two independent sources (References 7.1 and 7.2) that both indicate that  $^{106}\text{Ru}$  decays 100% to the ground state  $^{106}\text{Rh}$  and not to the metastable state  $^{106\text{m}}\text{Rh}$ .

The DCF value for the radionuclide  $^{106}\text{Rh}$  is listed as zero in Appendix 7.A because there is no DCF value listed for  $^{106}\text{Rh}$  in EPA Federal Guidance Report No. 11. In such cases, we have historically used a zero DCF. The EPA guidance additionally states that the DCF for some daughter products are zero (i.e., not included in the tables) because they are incorporated into the DCF of the parent. Since  $^{106}\text{Ru}$  is the parent of  $^{106}\text{Rh}$  and the dose

contribution of  $^{106}\text{Ru}$  is included in Appendix 7.A, the dose contribution of  $^{106}\text{Rh}$  is accounted for in this manner. Additionally, Holtec has contacted Dr. Keith Eckerman, the primary author of EPA Federal Guidance No. 11 and he has confirmed that due to the short half-life of  $^{106}\text{Rh}$  (29.9 seconds) it cannot effectively be included in the ICRP 30 respiratory model used to determine the DCFs and the DCF of the parent nuclide  $^{106}\text{Ru}$  suitably accounts for the radiological effect of the daughter nuclide,  $^{106}\text{Rh}$ . The way in which Holtec interpreted the EPA guidance document is consistent with the author's intent.

### **Question 7.3**

Provide the imbedded formulas that are used to calculate the results presented in the spreadsheet in Appendix 7.A. Also provide the assumptions used for the constants used in the spreadsheet that are not listed in Appendix 7.A, such as cask diameter and cask length, fuel rod and assembly specifications, etc., used for the analysis.

This information is not provided and is needed to assure compliance with 10 CFR 72.11.

### **Response 7.3**

The imbedded formulas used in the spreadsheet in Appendix 7.A have been added in a revision to the Holtec-proprietary confinement calculational package, to be submitted to the NRC under separate cover. Calculation of the MPC cavity volume is detailed in a Holtec internal calculation package using dimensional information from the design drawings in FSAR Section 1.5. The results of these volumetric calculations are summarized in Tables 4.4.12 (MPC-24), 4.4.13 (MPC-68), 4.4.24 (MPC-32) and 4.4.25 (MPC-24E) of the HI-STORM FSAR. A previous revision of the Holtec calculation package containing the detailed MPC cavity volume calculations was submitted to the NRC on July 29, 1999 (Holtec Report No. 971788). Appendix H of that report contains the detailed MPC cavity volume calculations. An updated version of this calculation can be provided to the NRC, if needed. All other constants used in Appendix 7.A are explained in Section 7.2 (normal and off-normal conditions) and Section 7.3 (hypothetical accident conditions).

### **References:**

- 7.1 Richard B. Firestone, et. al, "Table of Isotopes" (CD-Rom Edition), Version 1.0, March 1996.
- 7.2 U.S. EPA, Federal Guidance Report No. 12, *External Exposure to Radionuclides in Air, Water and Soil*, EPA 402-R-93-081, 1993.

## 8.0 Operating Procedures

### Question 8.1

Clearly state which steps and sequences in Chapter 8 are optional. Additionally, all statements implying that 10 CFR 72.48 evaluations are not necessary and should be removed.

These statements are too open-ended and can not be evaluated by the staff. The information is needed to assure compliance with 10 CFR 72.11. The following are examples of statements that should be removed.

Page 8.0-1, "Users may add, modify the sequence of, perform in parallel, or delete steps as necessary provided that the intent of this guidance is met, and the requirements of the CoC are met. Such changes are within the scope of this chapter and do not require a 72.48 evaluation."

Page 8.0-2, "Users may select alternate configurations, equipment, and methodology to accommodate their specific needs provided that the intent of this guidance is met and the requirements of the CoC are met. Such changes are within the scope of this chapter and do not require a 72.48 evaluation."

### Response 8.1

We have reviewed Chapter 8 and made revisions, as necessary, to indicate optional versus mandatory steps and sequences.

The statements regarding changes not requiring a 72.48 evaluation have been removed from the FSAR as suggested. However, the other proposed changes are clarifications to previously approved text already contained in the FSAR that allow users to develop appropriate site-specific procedures and use alternate equipment. Specifically, the third paragraph of Section 8.0 in the current, approved FSAR states, in part:

"The procedures contained herein describe acceptable methods for performing HI-STORM 100 loading and unloading operations. Users may alter these procedures to allow alternate methods and operations to be performed *in parallel or out of sequence* [emphasis added] as long as the general intent of the procedure is met.....In some cases, the figures are artists rendition(s). Users may *select alternate configurations, equipment and methodology to accommodate their specific needs* [emphasis added].....User-developed procedures and the design and operation of any alternate equipment must be reviewed by the Certificate holder prior to implementation."

The clarifications we have proposed include adding the phrases "modify the sequence of, perform in parallel" and "and the requirements of the CoC are met" to the first paragraph of Section 8.0, and clarifying the above paragraph as follows (changed text shown in italics):

"The procedures contained herein describe acceptable methods for performing HI-STORM 100 loading and unloading operations. *Unless otherwise stated, references to the HI-STORM 100 apply equally to the HI-STORM 100 and the HI-STORM 100S.* Users may alter these procedures to allow alternate methods and operations to be performed in parallel or out of sequence as long as the general intent of the procedure is met.....In some cases, the figures are artists rendition (sic). Users may select alternate configurations, equipment and methodology to accommodate their specific needs *provided that the intent of this guidance is met and the requirements of the CoC are met.* .....User-developed procedures and the design and operation of any alternate equipment must be reviewed by the Certificate holder prior to implementation."

These proposed clarifications do not change the intent of the previously licensed text. Based on our experience with loading HI-STAR 100 Systems at Plant Hatch and Dresden Unit 1 and with loading HI-STORM 100 Systems at Plant Hatch, recognition of this flexibility in the text of Chapter 8 is necessary for the development of site procedures that meet the clients' needs while assuring the safety intent of the guidance in FSAR Chapter 8 is maintained. Users evaluate applicability of 10 CFR 72.48 and process screenings or full evaluations, as appropriate, during development of their implementing procedures as they relate to the information contained in Chapter 8.

### **Question 8.2**

Clearly specify which "other configurations" of the HI-TRAC cask may be used for fuel transfer. The following statement is not specific enough to perform an evaluate.

Page 8.1-1, "Users may opt to use other configurations (e.g., a single lid) as long as there is sufficient crane capacity, available room to perform the operating and that appropriate measurers are available to prevent contamination of the MPC external shell. Any alternate configuration must be evaluated by the certificate holder on a site-specific basis to ensure that the design margins for criticality, shielding, structural, and thermal remain adequate and that all appropriate operation and safety features are maintained."

The information is needed to assure compliance with 10 CFR 72.11.

### **Response 8.2**

This text was added to the HI-STORM 100 FSAR in support of changes to the HI-TRAC transfer cask being undertaken under the provisions of 10 CFR 72.48. Based on the needs of our client users, Holtec has developed an alternate design concept for facilitating the transfer of the MPC between the HI-TRAC transfer cask and the HI-STORM or HI-STAR overpack.

Because this change is being made under 10 CFR 72.48, no drawings or other figures related to this change are included in our license amendment request package. The FSAR text changes are included because other portions of this section are modified in support of changes the NRC is reviewing as part of this LAR (e.g., HI-STORM 100S).

As a lesson learned, Holtec now separates the electronic document files for pending FSAR changes in support of license amendment requests from those approved in support of changes made under 10 CFR 72.48. Both sets of "living" FSAR documents are reviewed by our engineering personnel in evaluating new changes. However, to avoid confusion in the future, only those FSAR changes for which NRC review and approval is being requested will be included in future license amendment requests. When certificate amendments are issued, the associated FSAR changes are integrated into the electronic documents containing the changes approved under 10 CFR 72.48 to create an accurate living FSAR. Approved changes (either via 72.48 or certificate amendment) are included in the periodic FSAR updates, as required by the Part 72 regulations.

### **Question 8.3**

Clearly state in the applicable SAR sections, that installation of the vent screens is mandatory.

There are places in the SAR that imply that the screen vents are optional. The following is an example on page 8.1-28, "If necessary, install the HI-STORM exit vent gamma cross plates, thermocouples and vent screens."

This information is needed to assure compliance with 10 CFR 72.236.

### **Response 8.3**

We agree that the current proposed wording is unclear, in that it could be interpreted that installation of the vent screens (and the gamma shield cross plates) is optional. The "if necessary" provision of the cited text was intended to apply only to thermocouples. The installation of gamma shield cross plates and vent screens is mandatory. This procedural step has been revised to clarify that installation of the vent screens is mandatory. In addition, the term "thermocouples" has been replaced with "temperature elements" here and elsewhere in the FSAR, to allow users the flexibility to use other instruments, such as

U.S. Nuclear Regulatory Commission  
ATTN: Document Control Desk  
Document ID: 5014422  
Attachment 1  
Page 65 of 71

resistance temperature detectors (RTDs). The specific revised wording is provided in the response to RAI 5.1

## **9.0 Acceptance Tests and Maintenance Program**

### **Question 9.1**

Revise SAR Section 9.1.5.3 to include the areal density numerical value for boron and that a visual examination for defects for the Boral plates will be performed. Alternatively, a justification can be provided that an examination is not needed.

This information is not provided and is needed to assure compliance with 10 CFR 72.236.

### **Response 9.1**

The minimum required Boral® areal density (e.g., <sup>10</sup>B loading) for each MPC model is currently in Section 3.2 of Appendix B to the CoC and FSAR Table 1.2.2. To add clarity new Table 2.1.15 has been added with this same information. The text in FSAR Section 9.1.5.3 has also been revised to refer to this new table. FSAR Section 9.1.5.3 and Table 9.1.1 have also been revised to reflect the Boral visual inspection programs implemented by the Boral manufacturer and the MPC fabricator, as discussed below.

The Boral manufacturer conducts 100% visual examination of the neutron absorber plates. Each plate is inspected for damage (e.g., scratches, cracks, burrs, pealed cladding) and for foreign material embedded in the plate surfaces. Specific criteria are established for acceptance or rejection of any visual inspection observations.

The MPC fabricator performs visual inspection of the Boral plates on a lot sampling basis. The sample size is determined in accordance with MIL-STD-105D. The selected Boral plates are inspected for inclusions, cracks, voids, delamination, and surface finish.

Applicable supplier procedures that contain these visual inspection requirements are subject to Holtec's review and approval before they can be used in manufacturing. To provide additional defense-in-depth, Holtec will add specific verbiage elaborating on the visual inspection requirements in the applicable procurement specifications as part of the next scheduled revision to these documents.

### **Question 9.2**

Revise SAR Section 9.1.6 to include thermal acceptance testing and criteria for the Boral absorber plates. To assure performance of the plates thermal safety function as described in SAR section 4.3.2, the thermal conductivity should be verified through ASTM E1225, ASTM E1461, or by an equivalent method. Alternatively, a justification should be provided to demonstrate that thermal acceptance testing is not required.

This information is not provided and is needed to assure compliance with 10 CFR 72.236.

## **Response 9.2**

Boral<sup>®</sup> is a patented industry product with over 40 years of use in neutron attenuation in reactors, spent fuel pools, and dry spent fuel storage casks. The developer of Boral (DOE and Brooks & Perkins in the 50's) performed detailed investigations to quantify Boral's mechanical properties. The properties were published in a series of technical papers through the 60's and the 70's. Holtec relied on the Boral Manufacturer's (AAR Corporation, which acquired Brooks & Perkins in the early 80's) data in our fuel rack design work. In the early 90's, concurrent with the initiation of our cask research and development program, we also performed independent verification of key properties of Boral germane to dry storage.

Toward that end, in March, 1993 a series of Boral<sup>®</sup> panels were submitted to an independent lab for analysis of their thermophysical properties by AAR. Tests were undertaken in order to establish the thermal diffusivity from which calculations were made to determine thermal conductivity. Tests were also conducted to establish thermal expansion values for Boral. In the 1994 time frame the Boral manufacturer submitted information to Holtec describing the results of this testing program. This proprietary information was originally included in the HI-STAR 100 transportation Safety Analysis Report (Docket 71-9261) in 1995, but was later removed from that document due to its proprietary status. There is no indication in this information as to the specific test standards used by the laboratory in conducting these tests.

Holtec has reviewed ASTM E1225-99, "Standard Test method for Thermal Conductivity of Solids by Means of the Guarded-Comparative-Longitudinal Heat Flow Technique", and ASTM E1461-92, "Standard Test Method for Thermal Diffusivity of Solids by the Flash Method". ASTM E1225 is not applicable because the thermal conductivity of Boral was calculated (rather than measured directly), based on measured values of specific heat, density, and thermal diffusivity. A review of the test technique used to measure Boral thermal diffusivity (discussed below) indicates that the "flash" method was used in a manner equivalent to that described in ASTM E1461.

A summary of the methods used in the test program are described here.

Thermal conductivity ( $\lambda$ ) values were obtained from the specific heat ( $C_p$ ), bulk density ( $d$ ), and thermal diffusivity ( $\alpha$ ) test results according to the following relation:

$$\lambda = \alpha C_p d$$

Specific heat was measured using a standard Perkin-Elmer Model DSC-2 Differential Scanning Calorimeter with sapphire as the reference material. The standard and sample were subjected to the same heat flux as a blank and the differential powers required to heat the sample and standard at the same rate, were determined using the digital data

acquisition system. From the masses of the sapphire standard and sample, the differential power, and the known specific heat of sapphire, the specific heat of the sample were computed. The experimental data were visually displayed as the experiment progressed. All measured quantities were directly traceable to NBS standards.

Thermal diffusivity was determined using the laser flash diffusivity method. In the flash method, the front face of a small disc-shaped sample is subjected to a short laser burst and the resulting rear face temperature rise is recorded and analyzed. The apparatus consists of a Korad K2 laser, a high vacuum system including a bell jar with windows for viewing the sample, a tantalum or stainless steel tube heater surrounding a sample holding assembly, a thermocouple or an ir. detector, appropriate biasing circuits, amplifiers, A/D converters, crystal clocks and a minicomputer-based digital data acquisition system capable of accurately taking data in the 40 microsecond and longer time domain. The computer controlled the experiment, collected the data, calculated the results and compared the raw data with the theoretical model.

A dual pushrod dilatometer (Theta Dilatronics I1), was used to measure linear thermal expansion from 100 to 1300K. The differential expansion between the sample and a known standard reference material was measured as a function of temperature. The expansion of the sample was computed from this differential expansion and the expansion of the standard. The measurements were made under computer control and linear expansion is calculated at pre-selected temperature intervals. The expansion was able to be monitored with the graphics terminal during the measurement process. Six standard reference materials for expansion were obtained from NBS and these included materials with low, moderate and large expansions. For the purposes of calibration and checkout, one NBS standard was measured against another NBS standard.

## Test Results

The density values of the A1 skin and core material were found to be 2.65 and 2.53 gm/cm<sup>3</sup>, respectively.

The specific heat of both the cladding and core material increased monotonically with temperature, with the core having the higher values.

The aluminum cladding had a higher thermal conductivity than the core material. The test results showed that the thermal conductivity of the aluminum cladding ranged from 1.600 W/cm-K at 25°C to 1.864 W/cm-K at 500°C. The core material conductivity ranged from 0.865 W/cm-K at 25°C to 0.768 W/cm-K at 500°C. The overall temperature-dependent thermal conductivity of the composite Boral material was determined for the temperature range of interest using common heat transfer formulas for calculating such values, given the thermal conductivities and thicknesses of the constituent materials. This overall thermal conductivity for Boral was used in the thermal analyses supporting the HI-STORM 100 System design.

U.S. Nuclear Regulatory Commission  
ATTN: Document Control Desk  
Document ID: 5014422  
Attachment 1  
Page 69 of 71

Each manufactured plate of Boral is inspected and tested by the manufacturer to assure the chemical composition and other design specification requirements are met. Based on this inspection and testing program and on the many years of successful service in wet and dry spent fuel storage applications, periodic thermal acceptance testing of Boral is not deemed necessary.

## **12.0 Technical Specifications**

### **Question 12.1**

Revise definition of non-fuel hardware in CoC Appendix B to delete "other similarly designed devices with different names," or provide information in the SAR on these items.

This information is not provided and is needed to show compliance with 10 CFR 72.236.

### **Response 12.1**

The proposed definition of non-fuel hardware in Appendix B of the CoC and in Table 1.0.1 of the FSAR has been modified. The modifications are to add other common terms used to identify the hardware we have specifically analyzed (or have bounded by our analysis) to authorize this material for storage in the HI-STORM 100 System. Additional examples of non-fuel hardware include Wet Annular Burnable Absorber Rods (WABAs), Rod Cluster Control Assemblies (RCCAs), Control Element Assemblies (CEAs), water displacement guide tube plugs, and orifice rod assemblies.

### **Question 12.2**

Revise Section II. B of Table 2.1-1, CoC Appendix B, to state that fuel debris is not authorized in the MPC-68 to be consistent with the other MPC formats. Revise Section VI. A.1 of Table 2.1-1, CoC Appendix B, to renumber lettering.

This information in the submittal appears to be erroneous and should be corrected.

### **Response 12.2**

These changes to the CoC have been made as suggested.

### **Question 12.3**

Explain the discrepancy between Section VI. B. of Table 2.1-1, CoC Appendix B, and Table 1.2.1 of the SAR. Table 1.2.1 allows the storage of up to 68 damaged Dresden Unit 1 or Humboldt fuel assemblies whereas the CoC does not.

This information is needed to show compliance with 10 CFR 72.11.

### **Response 12.3**

FSAR Table 1.2.1 and CoC Appendix B have been revised to consistently state that up to 68 D-1 or Humboldt Bay damaged fuel assemblies in damaged fuel containers are authorized for storage in either an MPC-68 or MPC-68FF.

U.S. Nuclear Regulatory Commission  
ATTN: Document Control Desk  
Document ID: 5014422  
Attachment 1  
Page 71 of 71

**Question 12.4**

Revise note 6 of Table 2.1-2 CoC Appendix B to include the two rod pitches.

This information is not provided and is needed to show compliance with 10 CFR 72.236.

**Response 12.4**

The note has been revised as suggested.

RAI 4.10 Enclosure  
6 Total Pages

**ACI 349-97**  
**ACI 349R-97**

**Code Requirements  
for Nuclear Safety Related  
Concrete Structures (ACI 349-97)  
and Commentary—ACI 349R-97**

Reported by ACI Committee 349



**international**

**american concrete institute**

P.O. BOX 9094  
FARMINGTON HILLS, MICHIGAN 48333

# APPENDIX A—Thermal Considerations

## A.1—Scope

**A.1.1** Nuclear safety related reinforced concrete structures shall conform to the minimum provisions of this Code and to the special provisions of this appendix for structural members subjected to time-dependent and position-dependent temperature variations.

**A.1.2** The provisions of this appendix apply to concrete structures which are subjected to normal operating conditions as well as thermal accident conditions and which have restraint such that thermal strains would result in thermal stresses.

**A.1.3** The design provisions of this appendix are based on the strength design method. The assumptions, principles, and requirements specified in 10.1 and 10.2 are applicable for both normal operating and accident conditions.

**A.1.4** This appendix does not address temperature requirements during curing, nor does it address temperature and shrinkage reinforcement.

## A.2—Definitions

**Base temperature**—The temperature at which a concrete member is cured.

**Temperature distribution**—The variation of the total temperature across a section at a point in time.

**Mean temperature distribution**—A uniform distribution of temperature across a section evaluated to be an average of the temperature distribution.

**Gradient temperature distribution**—The temperature distribution minus the mean temperature distribution across a section at a point in time.

**Thermal strain**—Strain produced by thermal expansion or contraction due to a thermal gradient and the difference between the base and mean temperature.

**Thermal stress**—Stress produced by restraint of thermal strain.

## A.3—General design requirements

**A.3.1** The effects of the gradient temperature distribution and the difference between mean temperature distribution and base temperature during normal operation or accident conditions shall be considered.

**A.3.2** Time-dependent variations of temperature distributions shall be considered in evaluating thermal strains for both normal operating conditions and accident conditions.

**A.3.3** Thermal stress shall be evaluated considering the stiffness of the member and the rigidity of the section and the degree of restraint of the structure. The evaluation may be based on cracked section properties, provided the following conditions are met:

- a) The tensile stress for any section exceeds the tensile stress at which the section is considered cracked.
- b) Redistribution of internal forces and strains due to cracking are included.
- c) All concurrent loads, as specified in 9.2, are considered.
- d) The coefficient of thermal expansion may be taken as  $5.5 \times 10^{-6}$  per deg F unless other values are substantiated by "tests."

**A.3.4** When thermal stress is combined with the stress due to other loads to determine a design stress, the magnitude of the design stress must not be less than the magnitude of the stress due to other loadings alone unless the following are considered:

- a) The effect of cracking in the tensile zone of flexural members on reduction of the flexural rigidity and on the redistribution of stress,
- b) The reduction of long term stresses due to creep, and
- c) Stress combinations that reduce the magnitude of the stress due to other loads utilizing actual temperatures and temperature distributions which act concurrently with the other loads.

## A.4—Concrete temperatures

**A.4.1** The following temperature limitations are for normal operation or any other long term period. The temperatures shall not exceed 150 F except for local areas, such as around penetrations, which are allowed to have increased temperatures not to exceed 200 F.

**A.4.2** The following temperature limitations are for accident or any other short term period. The temperatures shall not exceed 350 F for the surface. However, local areas are allowed to reach 650 F from steam or water jets in the event of a pipe failure.

**A.4.3** Higher temperatures than those given in A.4.1 and A.4.2 above may be allowed for concrete if tests are provided to evaluate the reduction in strength and this reduction is applied to design allowables. Also, evidence shall be provided which verifies that the increased temperatures do not cause deterioration of the concrete either with or without load.

# Properties of Concrete

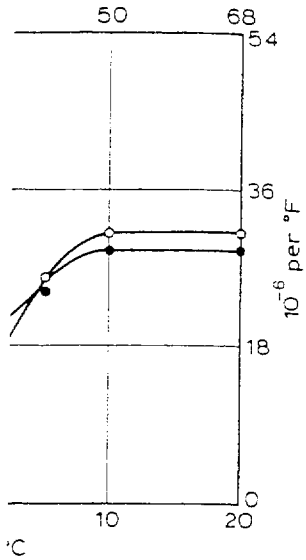
Fourth Edition

**A. M. NEVILLE**

CBE DSc(Eng) DSc PhD FStructE FAmSocCE FIARB PEng FRSE  
Principal and Vice-Chancellor, University of Dundee;  
Formerly Head, Department of Civil Engineering, University of  
Leeds; Dean of Engineering, University of Calgary, Canada



with Addison Wesley Longman  
Educational Low-Priced Books Scheme  
funded by the British Government



Thermal expansion and temperature of concrete (water/cement ratio of 0.40) stored and conditions of humidity<sup>8,107</sup>

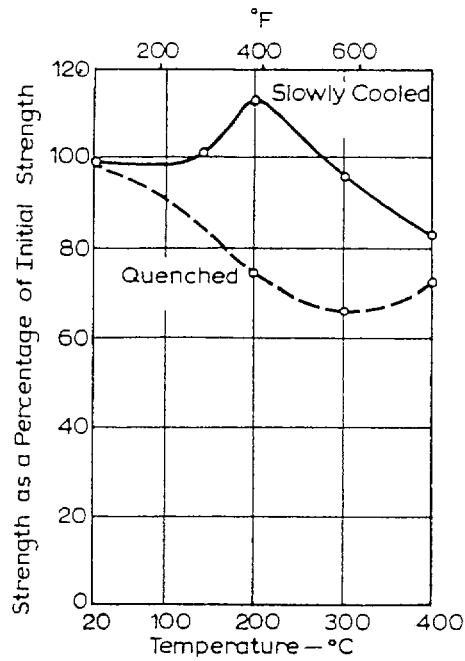
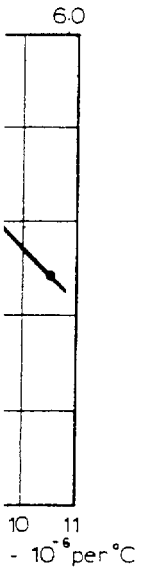


Fig. 8.16 Effect of the rate of cooling on the strength of concrete made with a sandstone aggregate and previously heated to different temperatures<sup>8,93</sup>

**Strength of concrete at high temperatures and resistance to fire**

Reports on tests intended to establish the effect of exposure to high temperature, up to about 600 °C (1100 °F), give widely varying results. The reasons for this include: differences in the stress acting upon, and in the moisture condition of, the concrete while being heated; differences in the length of exposure to the high temperature; and the differences in the properties of the aggregate. In consequence, globally valid generalizations are difficult. Moreover, the knowledge of the strength of concrete may be required for different practical conditions of exposure; for instance, in the case of fire, the exposure to the high temperature is only of a few hours' duration but the heat flux is large and so is the mass of concrete subjected to it. Conversely, in cutting concrete by a thermic lance, the exposure to high temperature is only of a few seconds' duration and the heat flux applied is very low. In what follows, test data from several investigations will be referred to, and these have to be interpreted in the light of the foregoing comments.

The compressive and splitting tensile strengths of concrete, made with limestone aggregate, exposed to a high temperature for 1 to 8 months are shown in Fig. 8.17.<sup>8,45</sup> The specimens tested were 100 mm by 200 mm (4 in. by 8 in.) cylinders, moist-cured for 28 days, then stored in the laboratory for 16 weeks. They were then heated at the rate of up to 20 °C per hour (36 °F per hour) under conditions such that loss of water from the concrete could take place. From Fig. 8.17, it can be seen that, relative to the strength prior to the exposure to the high



Thermal expansion of concrete and the temperature required to produce a 75 per cent reduction in strength

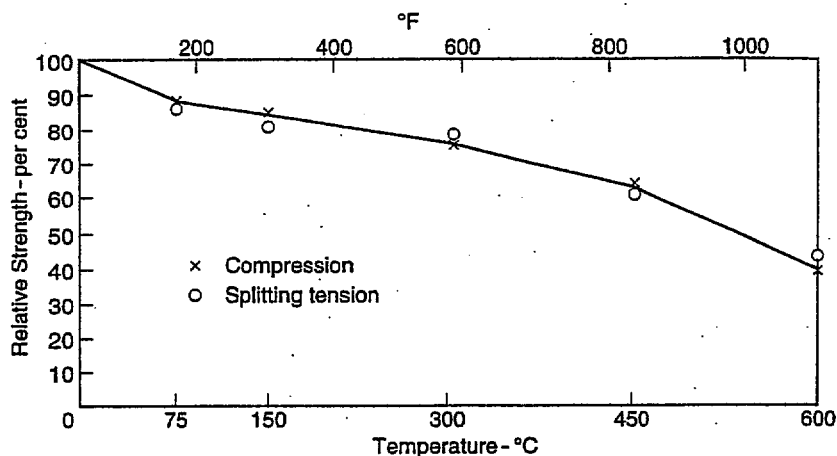


Fig. 8.17 Influence of exposure to a high temperature on the compressive and splitting-tensile strengths of concrete, made with a water/cement ratio of 0.45, expressed as a percentage of strength before exposure (based on ref. 8.45)

temperature, there is a steady loss in strength with an increase in temperature. The relative loss in compressive strength is very slightly smaller at the water/cement ratio of 0.60 than at the water/cement ratio of 0.45; this trend does not necessarily continue down to the water/cement ratio of 0.33.<sup>8.42</sup> However, leaner mixes appear to suffer a relatively lower loss of strength than richer ones.<sup>8.95</sup>

The influence of the water/cement ratio on the loss of strength is not noticeable in the splitting tensile strength; the loss in this strength is similar to that in the compressive strength.<sup>8.45</sup> It can be added that no effect of the length of exposure (between 1 and 8 months) was observed. Also, there was no difference in the relative loss of strength between concrete made with Portland cement only and concrete containing fly ash or ground granulated blastfurnace slag.<sup>8.45</sup>

Further tests by the same researchers<sup>8.42</sup> have shown that an increase in the length of exposure to a temperature of 150 °C (302 °F) or higher, from 2 to 120 days, increases the loss of compressive strength. However, the major part of the loss occurs early.<sup>8.42</sup> Tests<sup>8.44</sup> on concrete with basalt aggregate showed that the major part of the loss of strength occurs within 2 hours of the rise in temperature. It should be noted, however, that the exposure temperature is not necessarily the same as the temperature within the concrete so that it has to be emphasized once again that the details of the test method influence the measured output of the tests, but these details cannot always be fully appreciated from the published description of the tests. All these factors lead to a broad band of the loss of strength as a function of temperature, as shown in Table 8.6.

Lightweight aggregate concrete exhibits a much lower loss of compressive strength than normal weight concrete: a residual strength of at least 50 per cent after exposure to 600 °C was reported.<sup>8.112</sup>

Tests<sup>8.48</sup> on high strength concrete (89 MPa) suggest a higher relative loss of strength than is the case with normal strength concrete. What is more important with respect to high performance concrete, which contains silica fume, is the

Table 8.6 Compressive Strength at Room Temperature (based on

Maximum temperature, °C

Range of residual strength, per cent

occurrence of explosive spalling observed by Hertz<sup>8.47</sup> in concrete 300 °C (570 °F) even at a relatively short time, which is an order of magnitude confirmed in tests on concrete with a water/cement ratio of 0.26.<sup>8.43</sup> This might seem small but, on the other hand, the

It can be stated more generally: the lower the permeability of the concrete, the lower the temperature. An associated observation is that the loss of strength at higher temperatures is greater in saturated concrete than in dry concrete at the time of application of the load.

The influence of moisture content on the strength of concrete, where excessive moisture content causes explosive spalling. In general, moisture content is a determining factor in the structural behavior of concrete members, moisture movement is more pronounced at high temperature, while loss of water is more pronounced in thin members.

One of the changes which occur at high temperature (750 °F) is the decomposition of calcium hydroxide as a consequence of drying.<sup>8.7</sup> If, however, the re-hydration of lime can be prevented, the strength subsequently to the fire. From the tests on concrete mix, which remove calcium hydroxide, it is seen that the

While it is the behaviour of concrete that the behaviour of concrete may mask the true behaviour of concrete specimens of hydrated cement paste with a water/cement ratio of 0.30 and with a water/cement ratio of 0.45, compression while hot, showed a progressive decrease in strength. The strength at 120 °C (248 °F) is to be approximately equal to the strength at 300 °C (572 °F). However, at still higher temperatures a progressive decrease in strength is ascribed by Dias and his colleagues to the pressure (see p. 37) and densification of the concrete, which may be limited by the difficulty of effecting

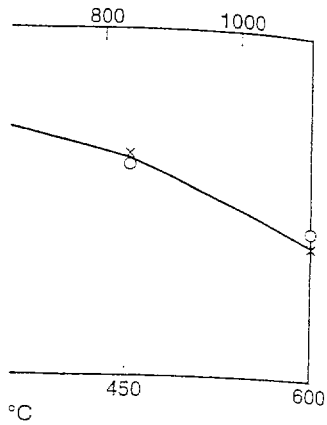


Figure 8.6 shows the compressive and splitting-tensile strength as a percentage of the 28-day strength at room temperature, expressed as a function of maximum temperature (based on ref. 8.44).

with an increase in temperature. The strength is very slightly smaller at the water/cement ratio of 0.45; this trend does not appear to be very different from that of a water/cement ratio of 0.33.<sup>8.42</sup> However, the loss of strength is not noticeable in concrete with a water/cement ratio of 0.45. However, the loss of strength is not noticeable in concrete with a water/cement ratio of 0.33.<sup>8.42</sup> However, the loss of strength is not noticeable in concrete with a water/cement ratio of 0.45. However, the loss of strength is not noticeable in concrete with a water/cement ratio of 0.33.<sup>8.42</sup> However, the loss of strength is not noticeable in concrete with a water/cement ratio of 0.45.

It is shown that an increase in the temperature of 120 °F (or higher, from 2 to 120 °F) results in a very slight loss of strength. However, the major part of the loss of strength is due to the loss of water from the concrete. In concrete with a water/cement ratio of 0.45, the loss of strength is not noticeable within 2 hours of the rise in temperature. In concrete with a water/cement ratio of 0.33, the loss of strength is not noticeable within 2 hours of the rise in temperature. In concrete with a water/cement ratio of 0.45, the loss of strength is not noticeable within 2 hours of the rise in temperature.

Such lower loss of compressive strength of at least 50 per cent

suggest a higher relative loss of strength in concrete. What is more important is that concrete which contains silica fume, is the

Table 8.6 Compressive Strength as a Percentage of 28-day Strength at Room Temperature (based on ref. 8.44)

Maximum temperature, °C	20	200	400	600	800
Range of residual strength, per cent	100	50-92	45-83	38-69	20-36

occurrence of explosive spalling associated with high temperature. This was observed by Hertz<sup>8.47</sup> in concrete heated to temperatures in excess of about 300 °C (570 °F) even at a relatively slow rate of rise in temperature of 60 °C per hour, which is an order of magnitude lower than in a fire. Explosive spalling was confirmed in tests on concrete containing silica fume and having a water/cement ratio of 0.26.<sup>8.43</sup> This might seem surprising as the volume of water involved is small but, on the other hand, the permeability is extremely low.

It can be stated more generally that the risk of explosive spalling is higher the lower the permeability of the concrete and the higher the rate of rise in temperature. An associated observation is that the loss in strength at higher temperatures is greater in saturated than in dry concrete, and it is the moisture content at the time of application of load that is responsible for the difference.<sup>8.101</sup>

The influence of moisture content on strength is apparent also in fire tests on concrete, where excessive moisture at the time of fire is the primary cause of spalling. In general, moisture content of the concrete is the most important factor determining its structural behaviour at higher temperatures.<sup>8.111</sup> In massive concrete members, moisture movement is extremely slow so that the effects of a high temperature, while loss of water is prevented, may be more serious than in thin members.

One of the changes which occurs as the temperature rises to about 400 °C (or 750 °F) is the decomposition of calcium hydroxide so that lime is left behind in consequence of drying.<sup>8.7</sup> If, however, after cooling, water ingresses into concrete, the re-hydration of lime can be disruptive; thus the damage manifests itself subsequently to the fire. From this standpoint, inclusion of pozzolanas in the mix, which remove calcium hydroxide, is beneficial.

While it is the behaviour of concrete that is of practical interest, the overall behaviour of concrete may mask some of the changes which occur in small specimens of hydrated cement paste. Tests<sup>8.46</sup> on paste specimens having a water/cement ratio of 0.30 and wet-cured for 14 weeks, heated and tested in compression while hot, showed a decrease in strength with an increase in temperature up to 120 °C (248 °F). At higher temperatures, the strength was found to be approximately equal to the original value. This strength is maintained up to 300 °C (572 °F). However, at still higher temperatures, there is a severe and progressive decrease in strength. The unimpaired strength at intermediate temperatures is ascribed by Dias *et al.*<sup>8.46</sup> to the disappearance of the disjoining pressure (see p. 37) and densification of the gel. In concrete, such changes would be limited by the difficulty of effective drying.

## **LAR 1014-1 SUMMARY OF PROPOSED HI-STORM 100 CHANGES<sup>1</sup>**

### **SECTION I – PROPOSED CHANGES TO CERTIFICATE OF COMPLIANCE 1014**

#### **Proposed Change No. 1**

Certificate of Compliance, Appendix A, LCO 3.1.1, SR 3.1.1.2, and Table 3-1:

The MPC helium backfill *density* limit is revised to *include an alternative* maximum helium backfill *pressure* range as shown in the attached marked-up LCO and table. The pressure range is established at a reference temperature of 70 degrees F.

#### **Reason for Proposed Change**

The existing units of g-mole/liter for this TS limit was found, in practice, to be cumbersome to implement. Therefore, a change in favor of a simpler requirement is warranted. Pressure is a readily measurable parameter in the field. *The density limit remains as an option in the CoC to accommodate HI-STORM users who have loaded MPCs under previous versions of the CoC.*

#### **Justification for Proposed Change**

The proposed change to the MPC helium backfill TS requires the users to backfill the MPC within a range of helium pressures. This ensures the presence of *the correct amount of helium* in the MPC free space. Helium backfill *density or pressure* in the range specified by the CoC is consistent with the governing thermal analyses. Helium backfill pressure within this pressure range at a reference temperature of 70 degrees F ensures the proper mass of helium to support MPC internal convection heat dissipation.

#### **Propose Change No. 1A**

Certificate of Compliance, Section 1.b

*This CoC Section is revised to describe the additional MPC models to be authorized under this amendment for storage in the HI-STORM 100 System.*

---

<sup>1</sup> Proposed changes marked with a "\*" have previously been submitted under License Amendment Request (LAR) 1008-1 for HI-STAR 100 (Docket 1008, 11/24/99). These changes have been reviewed by the NRC (SFPO) and approved under Amendment 1 or 2 to the HI-STAR 100 CoC..

***Reason and Justification for Proposed Change***

*This change is editorial to assure the CoC text accurately describes the various MPC models.*

**Proposed Change No. 2**

Certificate of Compliance, Appendix A, SR 3.1.2.1 and LCO 3.1.3:

- a. Revise the Surveillance Requirement acceptance criterion to 126 degrees F.
- b. Revise the Completion Time for LCO 3.1.3, Required Action A.2 from 24 hours to 22 hours

**Reason and Justification for Proposed Changes**

The revised delta T limit and Completion Time are necessary due to the higher heat duty for the cask system as discussed elsewhere in this section (see Proposed Change No. 28). The higher heat duty is based on credit being taken for internal convection heat dissipation inside the MPC. These changes ensure fuel cladding temperatures are maintained below established limits for all heat loads, up to and including the design basis maximum.

**Proposed Change No. 2A**

Certificate of Compliance, Appendix A, LCO 3.1.2, associated Bases B3.1.2, and CoC Appendix B, new Section 3.4.9

- a. Revise the Conditions, Required Actions, and Completion Times as shown on the attached CoC mark-ups.
- b. *Revise the Bases for LCO 3.1.2 as shown in the attached FSAR mark-ups to clarify the intent of the LCO.*
- c. *Add requirements through new Subsection 3.4.9 in CoC Appendix B to address site-specific design basis events that could block the overpack inlet air ducts for longer than the Completion Time of LCO 3.1.2.*

**Reason for Proposed Changes**

- a. Two editorial corrections are made to the LCO to a) correct a typographical error in the Required Action numbers for Condition B and b) to change the case of the word "operable" to lower case since

“operable” is not a defined term in the HI-STORM 100 technical specifications.

- b. *The LCO is not intended to apply to known design basis event that could cause blockage that lasts longer than the entire completion time of the Required Actions. The LCO is intended to apply to short term blockages of the air ducts that have a reasonable expectation of occurring and where access is achievable to facilitate removal of the blockage in a relatively short period of time (e.g., one operating shift or less).*
- c. *In concert with Proposed Change 2A.b, CoC requirements were deemed necessary to assure site specific design basis events that blocked the air ducts were addressed appropriately, and on a case by case basis.*

#### **Justification for Proposed Changes**

- a. *Editorial changes.*
- b. *The circumstances driving the need for clarification of this LCO were identified by a general licensee planning to use the HI-STORM 100 System where the overpack inlet ducts would be completely submerged during a design basis flooding event. The duration of the flood may exceed the current Completion Times for the Required Actions, placing this licensee in violation of the technical specifications. The LCO is not intended to address long-term duct blockage event, which are necessarily site-specific.*
- c. *New requirements added to Appendix B, Section 3.4.9 address the long-term blockage of the inlet air ducts. In an event such a flood, high water levels would prevent access to the affected casks by personnel and equipment needed to address the situation. The water level will rise and fall with few, if any means for plant personnel to intervene and mitigate the situation or accelerate the process. In such a case, users may take into consideration the actual fuel decay heat to determine what, if any actions need to be taken to assure the short term fuel cladding temperature limits will not be exceeded. The specific analyses and/or actions are necessarily plant-specific and would be expected to take place within the plant’s emergency response to the event.*

*Holtec has performed thermal analyses of the blocked duct accident and found that the fuel cladding temperature does not reach its short term limit*

*and all cask components remain below their respective component temperature limits for the 72-hour duration of the event.*

### **Proposed Change No. 3**

#### **Certificate of Compliance, Appendix A, LCO 3.2.1:**

- a. Revise the HI-TRAC dose rate acceptance criteria as shown on the attached mark-ups of the LCO.
- b. *Delete Figure 3.2.1-1 and revise SR 3.2.1.1 accordingly.*

#### **Reason for Proposed Change**

- a. The addition of the MPC-32 basket, higher fuel burnups and non-fuel hardware have increased the dose rates for the loaded HI-TRAC 100 and HI-TRAC 125 transfer casks.
- b. *The figure includes details of the transfer cask design that are not necessary for performing the surveillance necessary to demonstrate LCO compliance. The SR requires revision to recognize the deletion of the figure.*

#### **Justification for Proposed Change**

- a. The HI-TRAC dose rates are based on conservative, design basis source terms, using relatively low cooling times and high burnups. Users, simply through the nature of core operating cycles, will likely not have any one MPC loaded with design basis fuel. Users will determine the actual (lower) expected dose rates based on their particular fuel characteristics prior to fuel loading. The purpose of this LCO is simply to provide a limit above which users should suspect that a fuel assembly (or multiple fuel assemblies) not meeting the CoC has been loaded into the MPC, and they must take the action required by the Technical Specifications. Users' radiation protection/ALARA programs and operating procedures will control the use of temporary shielding and specific operating activities, as appropriate to ensure doses are ALARA. Note that the FSAR currently recommends that users choose the 125-ton HI-TRAC transfer cask because it provides better shielding. However, users with lower capacity cranes will need to perform an ALARA evaluation to either upgrade their crane capacity or implement temporary shielding to ensure occupational exposures are ALARA.

- b. *The existing figure contains depictions of design features of the transfer cask that are not necessary for users to perform SR 3.2.1.1. The SR has been re-worded to direct users to the proper locations for taking the dose rate measurements necessary to demonstrate compliance with the LCO. This change eliminates information from the technical specification that is not germane to complying with the LCO.*

**Proposed Change No. 3A**

**Certificate of Compliance, Appendix A, LCO 3.2.2**

*A note is proposed to be added to modify the applicability of this LCO. The LCO is not required to be applicable to the transfer cask if the MPC transfer into the HI-STORM overpack occurs inside the Part 50 facility.*

***Reason for Proposed Change***

*This change eliminates an unnecessary LCO requirement for a cask component not being used by some HI-STORM 100 System users.*

***Justification for Proposed Change***

*The intent of this LCO is to assure that a transfer cask containing a loaded MPC that leaves the Part 50 facility meets the loose contamination limits specified in the LCO. For users that perform the MPC transfer inside the Part 50 facility, the loaded transfer cask does not leave the Part 50 facility. Handling and storage of the empty transfer cask is therefore governed by the users' Part 50 program for control of contaminated equipment. This change avoids creating a conflict between Part 50 and Part 72 requirements.*

**Proposed Change No. 4**

**Certificate of Compliance, Appendix A, LCO 3.2.3:**

- a. The LCO acceptance criteria for the side of the overpack and the inlet and outlet vents are increased to 50 and 45 mrem/hr, respectively.
- b. The LCO Applicability is revised to delete "TRANSPORT OPERATIONS."
- c. Required Action A.2 is revised to substitute a written evaluation in lieu of an analysis.
- d. *Delete Figure 3.2.3-1 and revise SR 3.2.3.1 accordingly.*

### **Reason for Proposed Changes**

- a. Both dose rate limits are increased due to the addition of the MPC-32 basket, higher burnup fuel, and non-fuel hardware. The inlet and outlet vent duct dose rate limit is also slightly increased due to the new HI-STORM 100S overpack design and high burnup fuel.
- b. The dose rate acceptance criteria are not required to be met until the overpack is in its final storage configuration and in its designated storage location at the ISFSI. Therefore, having this LCO applicable during TRANSPORT OPERATIONS is not appropriate.
- c. This change is proposed to provide appropriate flexibility for user in evaluating the nonconforming condition.
- d. *The figure includes details of the transfer cask design that are not necessary for performing the surveillance necessary to demonstrate LCO compliance. The SR requires revision to recognize the deletion of the figure.*

### **Justification for Proposed Change**

- a. In both cases, the higher dose rate acceptance criteria are a result of increasing the number of PWR fuel assemblies in the MPC with the addition of MPC-32, adding high burnup fuel, as well as adding non-fuel hardware to the contents of the PWR MPCs. The duct dose rates are also affected by the design changes made to create the HI-STORM 100S, which include shortening the overall length of the HI-STORM overpack (see Proposed Change No. 33). This involved changes to the lid design, which incorporates the outlet ducts directly into the lid, and shortening the pedestal upon which the MPC rests. These changes moved the MPC closer to the top of the inlet ducts and closer to the bottom of the outlet ducts.

While these changes increase dose rates somewhat, they remain low. Further, use of the 32-assembly MPC will reduce the total number of MPCs to be loaded by a given PWR user, thereby reducing the total occupational dose over an entire loading campaign. Increasing the dose rate limits will not jeopardize the ability of the system to meet the 10CFR72.104 requirements for off-site dose. In addition, each site will perform an evaluation considering their specific fuel to demonstrate compliance with 10CFR72.104 prior to utilizing the HI-STORM 100 system.

- b. In its final storage configuration, the overpack has its *mandatory design* gamma shield cross plates installed in the inlet and outlet ducts. If the overpack is transported while supported from the bottom (e.g., with air pads) these shielding devices cannot be installed until the overpack is at its final storage location. This change is also consistent with the current Surveillance Requirement Frequency, which does not require measuring dose rates until within the first 24 hours after the beginning of STORAGE OPERATIONS. By definition, STORAGE OPERATIONS begin when the overpack is at the ISFSI.
- c. A written evaluation may include an analysis but does not necessarily need to. Depending upon the circumstances and magnitude of the high dose rates, an evaluation may include something less than an analysis and the user should have the option of performing the appropriate type of evaluation for the situation. This proposed change makes HI-STORM consistent with the dose rate LCO for HI-STAR (LCO 2.2.1).
- d. *The existing figure contains depictions of design features of the transfer cask that are not necessary for users to perform SR 3.2.3.1. The SR has been reworded to direct users to the proper locations for taking the dose rate measurements necessary to demonstrate compliance with the LCO. This change eliminates information from the technical specification that is not germane to complying with the LCO.*

### **Proposed Change No. 5**

#### **Certificate of Compliance, Appendix A, LCO 3.3.1:**

This new LCO is added to provide limits for the minimum soluble boron concentration during wet loading and unloading operations for the MPC-32 with relatively higher enriched fuel in the MPC-24, MPC-24E, and MPC-24EF.

#### **Reason for Proposed Change**

Many PWR users need to load fuel up to 5% initial enrichment. In order to authorize storage of any reasonably enriched PWR fuel in the MPC-32 and relatively higher enriched PWR fuel in the MPC-24, MPC-24E, and MPC-24EF (discussed later in Section I), credit for soluble boron in the MPC water during wet loading and unloading operations was taken in the criticality analyses. Since this is a licensee-controlled operational activity related to reactivity, a new technical specification LCO is being created to establish appropriate limits, actions, and surveillance requirements for boron concentration during these operations.

## **Justification for Proposed Change<sup>2</sup>**

Criticality calculations have been performed demonstrating that for the listed conditions (maximum enrichment and minimum soluble boron concentration) for each MPC, the cask system is in compliance with the regulatory requirement of  $k_{\text{eff}} < 0.95$  for all PWR fuel array/classes. The maximum  $k_{\text{eff}}$  calculated for the HI-TRAC is 0.9447 for the MPC-24, 0.9399 for the MPC-24E and MPC-24EF, and 0.9470 for the MPC-32. In the HI-STORM storage configuration, where no water is present inside the MPC, the maximum  $k_{\text{eff}}$  is below 0.52 for all PWR fuel array/classes and MPC models. Additional results, including results from the HI-STAR TSAR, which are directly applicable to the HI-TRAC, can be found in Tables 6.1.2 and 6.1.4 through 6.1.6 in Section 6.1 of the Proposed *Rev. 1* of the FSAR (see Attachment 6).

## **Proposed Change No. 6**

### **Certificate of Compliance, Appendix A, Sections 5.1 and 5.2:**

Delete the training program and pre-operational testing and training exercise requirements entirely.

### **Reason and Justification for Proposed Changes**

Part 72 training requirements are governed directly by the regulations at 10 CFR 72.144(d), 72.190, and 72.192, and through licensees' Quality Assurance programs. Both the regulations and the QA program require licensees to have trained and qualified personnel performing activities important to safety. Therefore, it is unnecessary to duplicate training requirements in the CoC. Further, while the Systematic Approach to Training (SAT) is a commonly used training program development technique, it is inappropriate to impose SAT on licensees via the CoC. All topical areas to be included in the licensees' dry spent fuel storage training program, including the pre-operational testing and training exercises currently in the CoC, are already part of the HI-STORM 100 FSAR, Chapter 12 and, as such, are required to be implemented by licensees. This change is consistent with those being proposed generically by the industry through the NEI technical specification improvement effort.

---

<sup>2</sup> This justification is focused on the criticality aspects of soluble boron. Refer to the new Bases for LCO 3.3.1 proposed to be added to FSAR Chapter 12, Appendix 12.A (Proposed Change No.41 ) for discussion of the Required Actions and Surveillance Requirements, Frequencies, etc.

### **Proposed Change No. 7**

#### **Certificate of Compliance, Appendix A, Section 5.3:**

Move "Special Requirements for First Systems in Place" from the TS to the CoC proper as new Item 9. Re-number existing Item 9 as new Item 10.

#### **Reason and Justification for Proposed Change**

This is an administrative change. One-time requirements are more appropriately located as conditions to the CoC (similar to Part 50 license conditions) rather than technical specifications. This change is consistent with those being proposed generically by the industry through the NEI technical specification improvement effort.

### **Proposed Change No. 8**

#### **Certificate of Compliance, Appendix A, Section 5.5 and Table 5-1:**

- a. The Cask Transport Evaluation Program description has been re-formatted and revised as shown in the attached CoC mark-up pages to modify Table 5-1 and add Subsection 5.5.b to distinguish between the transport of free-standing overpacks and overpacks to be deployed in high-seismic regions (HI-STORM 100A).
- b. The Cask Transport Evaluation Program description, at Subsections 5.5.a.1 and 5.5.a.2, has been revised as a conforming change to support the change to Design Features Section 3.4.6 to eliminate the specific ISFSI pad design criteria (see Proposed Change No. 32).
- c. New specification item 5.5.a.3 is added to address the transport of the loaded TRANSFER CASK or free-standing OVERPACK from the FUEL BUILDING to the ISFSI. The new section allows lifting of the loaded TRANSFER CASK or OVERPACK to any height necessary provided the lift device is designed in accordance with ANSI N14.6 and includes redundant drop protection features.
- d. *Note 1 in Table 5-1 is modified for clarity to replace "transfer lid" with "cask/lid assemblage."*

### **Reason for Proposed Changes**

- a. This change is necessary because there is no specific (generic) drop height or reference ISFSI pad established for the HI-STORM 100A overpack design. Each user must determine a lift height on a site-specific basis, except as provided for in Subsection 5.5.b.2. Subsection 5.5.b.2 allows for no lift height to be established if the cask is lifted with appropriately designed lift devices.
- b. This is a conforming change. References to ISFSI pad design criteria are no longer meaningful, as these criteria (in Design Features Section 3.4.6) are being deleted from the CoC as part of this LAR (see Proposed Change No. 32).
- c. This change is proposed based on user feedback which indicated there were no requirements established for onsite transport of the TRANSFER CASK or OVERPACK that address lifting the TRANSFER CASK or OVERPACK above the lift height limits outside the scope of the Cask Transfer Facility (CTF). This flexibility may be required at some sites based on the transport path between the FUEL BUILDING and the ISFSI.
- d. *Clarification.*

### **Justification for Proposed Change**

- a. The HI-STORM 100A overpack design includes unique design features that make the existing, free-standing drop and tipover analyses (and the lift heights in Table 5-1) not applicable. Each ISFSI pad on which a HI-STORM 100A is deployed will be designed site-specifically accounting for the unique seismic spectra for the site. Therefore, the lift heights for the HI-STORM 100A overpack design will also be determined site-specifically, if required, based on the type of handling device contemplated for use (per Specification 5.5.b.1). If lift devices designed in accordance with ANSI N14.6 and having redundant drop protection features are used, drop events are not credible and, therefore, no lift height limit need be established.
- b. Conforming change in support of the removal of ISFSI pad design criteria from the CoC.
- c. A lift device designed in accordance with ANSI N14.6 and having redundant drop protection features ensures that a drop of the TRANSFER CASK or OVERPACK is not a credible event. This change provides necessary flexibility for users with non-compliant transport path conditions (e.g., a portion of the path that is harder than the "pre-approved" pad design

parameters described in FSAR Table 2.2.9). This change is consistent with HI-STAR 100 LCO 2.1.3.b.

*d. Editorial.*

### **Proposed Change No. 9**

#### **Certificate of Compliance, Appendix B, Section 1.0, and Tables 2.1-2 and 2.1-3:**

The definitions of DAMAGED FUEL ASSEMBLY and INTACT FUEL ASSEMBLY are revised as shown in the attached marked-up CoC changes. The terms “No. of Fuel Rods”, “Clad OD”, “Clad ID”, and “Pellet Diameter” are all revised for clarity.

#### **Reason for Proposed Change**

The revised definitions and terms more accurately reflect the criticality analyses and eliminate potential unintended CoC compliance problems for licensees.

#### **Justification for Proposed Changes**

The criticality analyses were performed for a large variety of fuel assembly arrays and classes. Where appropriate to the fuel assembly array/class, fuel rods were modeled in all fuel rod locations. However, situations may arise for licensees where a particular fuel assembly may not, and may never have had, fuel rods in all fuel rods locations. In such cases, it is important to ensure the fuel rod locations are filled with dummy fuel rods that occupy space (in lieu of moderator) at least as large as the fuel rod modeled there. Further, fuel assemblies with missing fuel rods *not* replaced with dummy rods are to be classified as DAMAGED FUEL ASSEMBLIES. DAMAGED FUEL ASSEMBLIES must meet the fuel specifications of Tables 2.1-2 and 2.1-3. The current “No. of Fuel Rods” requirement in these tables clearly cannot be met by this type of DAMAGED FUEL ASSEMBLY. The wording change for this term eliminates this potential compliance problem.

## **Proposed Change No. 10**

### **Certificate of Compliance, Appendix B, Section 1.0:**

The definition of DAMAGED FUEL CONTAINER (DFC)<sup>3</sup> in Appendix B is revised to include three additional DFCs in addition to the previously approved Holtec DFC designed exclusively for Dresden Unit 1 and Humboldt Bay fuel. The new DFC designs are: 1) a Transnuclear (TN) DFC currently containing Dresden Unit 1 (D-1) fuel\*, 2) a Holtec generic PWR DFC, and 3) a Holtec generic BWR DFC. Detailed drawings for the TN/D-1 DFC are contained in Holtec LAR 1008-1 for HI-STAR 100 submitted to the NRC on November 24, 1999. Sketches of the TN/D-1 DFC and the two new Holtec-designed DFCs are included as proposed new FSAR Figures 2.1.2, 2.1.2B and 2.1.2C (see Attachment 6). In all cases, only outline sketches showing key DFC dimensions and general fabrication details are included in proposed FSAR *Revision 1*. Detailed design drawings of the Holtec DFC are being removed from the FSAR with this amendment request. This change is consistent with previously approved changes for the HI-STAR 100 System under LAR 1008-1.

### **Reason for Proposed Changes**

#### **TN/D-1 DFC**

There are a significant number of Dresden Unit 1 fuel assemblies meeting the HI-STORM fuel specifications which are currently stored in TN DFCs. Authorizing this fuel for storage in the HI-STORM 100 system without having to remove it from the TN/D-1 DFCs and load it into the Holtec DFCs will avoid imposing undue burden on the general licensee with no additional safety benefit. Implementation of this change will allow Dresden Unit 1 to complete decommissioning of the plant in a timely manner. Further, the fuel in the TN/D-1 DFCs is currently located in the Dresden Unit 2/3 spent fuel pool. Removal of this fuel is necessary to maintain full core offload capability and allow D-2/3 to continue operation.

#### **Holtec Generic PWR and BWR DFCs**

The current HI-STORM CoC authorizes only damaged fuel and fuel debris from the Dresden Unit 1 and Humboldt Bay plants for storage in HI-STORM 100. Many other customers have informed Holtec that some of their fuel would be classified as damaged fuel or fuel debris. These new generic DFC designs allow

---

<sup>3</sup> The terms Damaged Fuel Container and Damaged Fuel Canister are used interchangeably throughout this document and "DFC" is applicable to both.

for storage of a much broader scope of damaged fuel and fuel debris for both PWR and BWR fuel.

### **Justification for Proposed Changes**

#### **TN/D-1 DFC**

The justification for this proposed change is provided below, arranged by technical discipline, as applicable. Supporting changes to the FSAR are summarized in Section II of this attachment and included in Attachment 6.

#### **Structural Evaluation**

The TN/D-1 DFC was previously approved for use in the TN-9 transportation package. In addition, the TN/D-1 DFC has been structurally evaluated by Holtec International and found to meet all design requirements for storage in the HI-STORM 100 system. The details of this evaluation are contained in proposed new FSAR Appendix 3.AR, included in Attachment 6. All required safety margins are greater than zero or, in other words, the factors of safety are greater than 1.0.

The FSAR Chapter 3 NUREG-1536 compliance matrix has been revised to address the new DFCs and the supporting appendix. Since all required text changes are confined to the new appendix, no new chapter text is required.

#### **Thermal Evaluation**

Storage of D-1 damaged fuel and fuel debris meeting the specifications of the CoC is permitted in the HI-STORM MPC-68, MPC-68F, and MPC-68FF when encased in a DFC. The thermal characteristics of the TN/D-1 DFC and the Holtec DFC were compared in support of this amendment request. The TN/D-1 DFC is a square shaped canister box fabricated from 12 gage stainless steel plates. A bounding thermal calculation has been prepared in support of this amendment to determine the most heat resistive fuel from the Low Heat Emitting (LHE) group of assemblies encased in a DFC. It is noted that in this configuration, interruption of radiation heat exchange between the fuel assembly and the fuel basket by the DFC boundary renders the DFC configuration as the bounding case when compared with the absence of a DFC. Both canister designs were evaluated and the one exhibiting lower heat dissipation characteristics was adopted for analysis.

For the LHE group of assemblies, the low decay heat load of D-1 fuel (approximately 8 kW) guarantees large thermal margins to permit safe storage of D-1 fuel in the TN/D-1 DFC. The HI-STORM temperature field for this case was calculated and is reported in proposed revisions to HI-STORM FSAR Chapter 4

at Subsection 4.4.1.1.13 (see Attachment 6). Substantial cladding thermal margins are demonstrated by the analysis.

#### Shielding Evaluation

Storage of D-1 damaged fuel and fuel debris meeting the specifications of the CoC is permitted in the HI-STORM MPC-68, MPC-68F, and MPC-68FF when encased in a DFC. Sections 5.4.2 and 5.4.5 of the HI-STORM FSAR, *Revision 0* discuss the post-accident shielding evaluation for D-1 and Humboldt Bay damaged fuel. These sections assume that the damaged fuel assemblies and fuel debris collapse to a height of 80 inches. This dimension was calculated based on the inside dimension of the DFC and the dimensions of the fuel assemblies. Since the TN/D-1 DFC has a smaller inside dimension than the Holtec DFC, the analysis in Sections 5.4.2 and 5.4.5 of the HI-STORM FSAR is applicable and conservative. In addition, the shielding analysis does not take credit for the DFC container in determining the acceptability of storing the approved damaged fuel and fuel debris. Therefore, the use of the TN/D-1 DFC does not affect the shielding analysis and no changes to the Chapter 5 of the FSAR are necessary as a result of this proposed change.

#### Criticality Evaluation

The TN/D-1 DFC was analyzed with the same set of contents used for the analysis of the Holtec DFC documented in *Rev. 0* of the HI-STORM 100 FSAR. This set includes 6x6 and 7x7 fuel assemblies with various numbers of rods missing, a collapsed assembly and dispersed fuel powder. The maximum  $k_{\text{eff}}$  values for both DFCs are listed in proposed *Revision 1* FSAR Table 6.4.5 (Attachment 6). There is no significant difference in reactivity between the two DFCs. For only one case (collapsed assembly), the reactivity for the TN/D-1 DFC is increased marginally ( $\Delta k = 0.0012$ ) compared to the Holtec DFC. In all other cases, the reactivity for the TN/D-1 DFC is below the reactivity of the Holtec DFC with the same contents. Therefore, with the TN/D-1 DFC used instead of the Holtec DFC, the cask system is still in compliance with the regulatory requirement of  $k_{\text{eff}} < 0.95$  for all authorized contents.

### HOLTEC GENERIC PWR DFC

#### Structural Evaluation

The proposed Holtec generic PWR DFC design (see new FSAR Figure 2.1.2B) is a square shaped tube fabricated from 0.075-inch stainless steel. An appropriate cover is included that permits lifting of the unit. The structural evaluation of the generic DFC design for PWR fuel is based on the same design criteria used for the approved Holtec DFC for Dresden/Humboldt Bay fuel. Structural analyses

have been performed for the lifting condition (where NUREG-0612 stress limits are applicable) and for a handling accident leading to an end impact (ASME Code Level D limits are applicable). Positive safety margins are achieved. The results are presented in Appendix 3.AS (see Attachment 6).

#### Thermal Evaluation

The proposed PWR DFC design (see proposed FSAR Rev.11 Figure 2.1.2B in Attachment 5) is a square shaped tube fabricated from 0.075-inch stainless steel. Bounding thermal calculations have been prepared in support of this amendment to determine the most heat resistive Zircaloy and stainless steel clad fuels encased in DFCs. In this configuration, interruption of thermal radiation heat exchange between the fuel assembly and the fuel basket by the DFC renders the DFC configuration as bounding when compared with non-canistered assemblies. Storage of damaged PWR fuel assemblies in generic DFCs is evaluated in proposed FSAR *Revision 1*, Subsection 4.4.1.1.4 (see Attachment 6). The MPC-24E/24EF is designed with four enlarged fuel storage cells to accommodate the DFC. The CoC requires damaged fuel to be stored only in these particular fuel storage locations to preserve the assumptions of the analysis. At least 20 of the 24 fuel storage locations will be occupied by intact fuel assemblies. Therefore, the overall effect of DFC storage on the basket heat dissipation rate is quite small. Conservatively, a 5% reduction MPC heat rating is specified for accommodating damaged, Zircaloy clad fuel. Stainless steel clad fuel storage is evaluated in FSAR Subsection 4.3.2 for a bounding storage configuration (within a DFC).

#### Shielding Evaluation

The Holtec generic PWR DFC is designed to accommodate any PWR fuel assembly that can physically fit inside the DFC. Damaged fuel assemblies under normal conditions, for the most part, resemble intact fuel assemblies from a shielding perspective. Under accident conditions, it cannot be guaranteed that the damaged fuel assembly will remain intact. As a result, the damaged fuel assembly may begin to resemble fuel debris in its possible configuration after an accident.

Since damaged fuel is identical to intact fuel from a shielding perspective, no specific analysis is required for damaged fuel under normal conditions. However, a generic shielding evaluation was performed to demonstrate that fuel debris under normal or accident conditions, or damaged fuel in a post-accident configuration, will not result in a significant increase in the dose rates around the 100-ton HI-TRAC. Only the 100-ton HI-TRAC was analyzed because it can be concluded that if the dose rate change is not significant for the 100-ton HI-TRAC, then the change will not be significant for the 125-ton HI-TRAC or the HI-STORM overpacks, both of which provide more shielding than the 100-ton HI-TRAC.

Fuel debris or a damaged fuel assembly which has collapsed can have an average fuel density that is higher than the fuel density for an intact fuel assembly. If the damaged fuel assembly were to fully or partially collapse, the fuel density in one portion of the assembly would increase and the density in the other portion of the assembly would decrease. This scenario was analyzed with MCNP-4A in a conservative, bounding fashion to determine the potential change in dose rate as a result of fuel debris or a damaged fuel assembly collapse. The analysis consisted of modeling the fuel assemblies in the four peripheral damaged fuel locations in the MPC-24E (or MPC-24EF) and the 16 peripheral locations in the MPC-68 (including the MPC-68FF) with a fuel density that was twice the normal fuel density and correspondingly increasing the source term for these locations by a factor of two. A flat axial power distribution was used which is approximately representative of the source distribution if the top half of an assembly collapsed into the bottom half of the assembly. Increasing the fuel density over the entire fuel length, rather than in the top half or bottom half of the fuel assembly, is conservative and provides the dose rate change in both the top and bottom portion of the cask.

The results of this analysis indicate that the dose rates in the top and bottom portion of the 100-ton HI-TRAC increase slightly while the dose rate in the center of the HI-TRAC actually decreases a little bit. The increase in the top and bottom is due to the assumed flat power distribution. These results indicate that the potential effect on the dose rate is not very significant for the storage of damaged fuel and/or fuel debris. This conclusion is further reinforced by the fact that the majority of the significantly damaged fuel assemblies in the spent fuel inventories are older assemblies from the earlier days of nuclear plant operations. Therefore, these assemblies will have a considerably lower burnup and longer cooling times than the assemblies analyzed in this amendment request. Section 5.4.2 of proposed FSAR *Revision 1* (see Attachment 6) provides the discussion and a presentation of the results of the damaged fuel analysis.

#### Criticality Evaluation

Criticality calculations have been performed for the MPC-24E and MPC-24EF loaded with intact fuel, damaged fuel, and fuel debris (up to 4 DFCs per basket) with a maximum enrichment of 4.0 wt%  $^{235}\text{U}$ . The calculations use a bounding approach to account for the possible wide variation of fuel distribution inside the DFC, based on the analysis of arrays of bare fuel rods. Additionally, typical damaged fuel conditions such as missing rods or collapsed assemblies are analyzed for selected array/classes. The analyses are presented in Section 6.4.4.2 of the Proposed *Rev. 1* of the FSAR (see Attachment 6). The maximum calculated  $k_{\text{eff}}$  for the HI-TRAC is 0.9486, which demonstrates that the cask system is in

compliance with the regulatory requirement of  $k_{\text{eff}} < 0.95$  for all PWR fuel array/classes.

## **HOLTEC GENERIC BWR DFC**

### **Structural Evaluation**

The proposed Holtec generic BWR DFC design (see new FSAR Figure 2.1.2C) is a square shaped tube fabricated from 0.035-inch stainless steel. An evaluation of structural integrity under lifting and handling accident conditions has been performed, similar to that performed for the generic PWR DFC. Positive safety margins are achieved. Structural integrity results are reported in Appendix 3.AS (see Attachment 6).

### **Thermal Evaluation**

Bounding thermal calculations have been prepared for the Holtec generic BER DFC design to determine the most heat resistive Zircaloy and stainless steel clad fuels encased in DFCs. In this configuration, interruption of thermal radiation heat exchange between the fuel assembly and the fuel basket by the DFC renders the DFC configuration as bounding when compared with non-canistered assemblies. Storage of damaged BWR fuel assemblies in generic DFCs is evaluated in proposed FSAR *Revision 1*, Subsection 4.4.1.1.4 (see Attachment 6). The MPC-68 and MPC-68FF are analyzed assuming damaged fuel is stored in up to 16 peripheral fuel storage cells in DFCs. The CoC requires damaged fuel to be stored only in these particular fuel storage locations to preserve the assumptions of the analysis. At least 52 of the 68 fuel storage locations will be occupied by intact fuel assemblies. Therefore, the overall effect of DFC storage on the basket heat dissipation rate is quite small. Conservatively, a 5% reduction MPC heat rating is specified for accommodating damaged, Zircaloy clad fuel. Stainless steel clad fuel storage is evaluated in FSAR Subsection 4.3.2 for a bounding storage configuration (within a DFC).

### **Shielding Evaluation**

See justification for Holtec Generic PWR DFC.

### **Criticality Evaluation**

Criticality calculations have been performed for an MPC-68 loaded with intact fuel, damaged fuel, and fuel debris (up to 16 DFCs) Maximum enrichments of up to 4.0 wt%  $^{235}\text{U}$  for the damaged fuel/fuel debris and up to 3.7 wt%  $^{235}\text{U}$  for the intact fuel were analyzed. The calculations use a bounding approach to account for the possible wide variation of fuel distribution inside the DFC, based on the

analysis of arrays of bare fuel rods. Also, typical damaged fuel conditions such as missing rods or collapsed assemblies are analyzed for selected array/classes. The analyses are presented in Section 6.4.4.2 of the Proposed *Rev. 1* of the FSAR. The maximum calculated  $k_{eff}$  is 0.9328, which demonstrates that the cask system is in compliance with the regulatory requirement of  $k_{eff} < 0.95$  for all PWR fuel array/classes.

### **Proposed Change No. 11**

#### **Certificate of Compliance, Appendix B, Subsection 2.1.1 and Table 2.1-1:**

- a. The wording of Item 2.1.1.a is revised to add the words “and NON-FUEL HARDWARE” and “and other referenced tables.”
- b. Item 2.1.1.c is revised to add a clarification that this requirement applies only to uniform loading.
- c. New Item 2.1.1.e is added; the note in Table 2.1-1, Item II.C is revised; and the word “Zircaloy” is removed from Table 2.1-1, Items II.A.1 through 4 to reflect the authorization for loading of LaCrosse BWR fuel assemblies in stainless steel channels (array/class 10x10D and 10x10E) in the MPC-68. Similar provisions are made for storage of stainless steel channels in the MPC-68FF (see Proposed Change No. 21).

#### **Reason for Proposed Changes**

- a. This change is provided to clarify that PWR fuel may be stored with non-fuel hardware as discussed in Proposed Change Number 14, and to clarify that Table 2.1-1 incorporates other tables by reference.
- b. Without this clarification, regionalized fuel loading would not be possible with damaged fuel assemblies and fuel debris due to this limitation on decay heat.
- c. LaCrosse plant has stainless steel channels and is a Private Fuel Storage, LLC (PFS) member. HI-STORM 100 is one of the storage cask designs referenced in the PFS Part 72 license application.

#### **Justification for Proposed Changes**

- a. Clarification to recognize that non-fuel hardware (as defined in Table 2.1-1) is authorized for loading with PWR fuel. The second change is editorial.

- b. For the regionalized fuel storage configuration described in proposed FSAR subsection 4.4.1.1.9, low heat emitting fuel is arrayed away from the central region occupied by hotter fuel. The note is added so that the regionalized loading strategy is not unduly restricted by a stipulation designed for uniform loading.
- c. The justification for this change is presented by technical discipline below.

#### Structural Evaluation

As the CoC does not permit the total weight of the fuel assembly plus the non-fuel hardware to exceed the design basis weights (BWR -700 lb., PWR -1680 lb.), there are no new structural evaluations nor changes to existing evaluations required.

#### Thermal Evaluation

Zircaloy and stainless steel have comparable thermal conductivities, the latter being approximately 10% greater than the former. The thermal analysis presented in *Revision 0* of the FSAR and proposed *Revision 1* utilize the thermal properties of Zircaloy. Even though the thermal conductivity of the stainless steel channels is greater than that of a Zircaloy channel, the aggregate impact of the thermal properties of the fuel channel on the overall basket conductivity is quite modest. As a result, small differences in the thermal properties (e.g., conductivity, emissivity, etc.) of stainless steel and Zircaloy channels produce a second order effect on the thermal performance of the storage system. Therefore, the analyses using Zircaloy channel properties are also considered to be applicable to stainless steel channels.

#### Shielding Evaluation

The LaCrosse nuclear plant used two types of channels for their BWR assemblies: stainless steel and Zircaloy. Since the irradiation of Zircaloy does not produce significant activation, there are no restrictions on the storage of these channels and they are not explicitly analyzed in the shielding evaluation. The stainless steel channels, however, can produce a significant amount of activation, predominantly from Co-60. LaCrosse has thirty-two stainless steel channels, a few of which have been in the reactor core for approximately the lifetime of the plant. Therefore, the activation of the stainless steel channels was conservatively calculated to demonstrate that they are acceptable for storage in the HI-STORM 100 system. For conservatism, the number of stainless steel channels in an MPC-68 or MPC-68FF is being limited to sixteen and Appendix B to the CoC requires that these channels be stored in the inner sixteen locations.

The activation of a single stainless steel channel was calculated by simulating the irradiation of the channels with ORIGEN-S using the flux calculated from the LaCrosse fuel assembly. The mass of the steel channel in the active fuel zone (83 inches) was used in the analysis. For burnups beyond 22,500 MWD/MTU, it was assumed, for the purpose of the calculation, that the burned fuel assembly was replaced with a fresh fuel assembly every 22,500 MWD/MTU. This was achieved in ORIGEN-S by resetting the flux levels and cross sections to the 0 MWD/MTU condition after every 22,500 MWD/MTU.

LaCrosse was commercially operated from November 1969 until it was shut down in April 1987. Therefore, the shortest cooling time for the assemblies and the channels is 13 years. Assuming the plant operated continually from 11/69 until 4/87 (approximately 17.5 years or 6388 days), the accumulated burnup for the channels would be 186,000 MWD/MTU (6388 days times 29.17 MW/MTU from Table 5.2.3 of *Revision 0* of the HI-STORM FSAR). Therefore, the cobalt activity calculated for a single stainless steel channel irradiated for 180,000 MWD/MTU was calculated to be 667 curies of Co-60 for 13 years cooling. This is equivalent to a source of  $4.94\text{E}+13$  photons/sec in the energy range of 1.0-1.5 MeV.

In order to demonstrate that sixteen stainless steel channels are acceptable for storage in an MPC-68 or MPC-68FF, a comparison of source terms is performed. Table 5.2.8 of *Revision 0* of the HI-STORM FSAR indicates that the source term for the LaCrosse design basis fuel assembly in the 1.0-1.5 MeV range is  $6.34\text{E}+13$  photons/sec for 10 years cooling, assuming a 144-inch active fuel length. This is equivalent to  $4.31\text{E}+15$  photons/sec/cask. At 13 years cooling, the fuel source term in that energy range decreases to  $4.31\text{E}+13$  photons/sec, which is equivalent to  $2.93\text{E}+15$  photons/sec/cask. If the source term from the stainless steel channels is scaled to 144 inches and added to the 13 year fuel source term the result is  $4.30\text{E}+15$  photons/sec/cask ( $2.93\text{E}+15$  photons/sec/cask +  $4.94\text{E}+13$  photons/sec/channel x 144 inch/83 inch x 16 channels/cask). This number is equivalent to the 10 year  $4.31\text{E}+15$  photons/sec/cask source used in the shielding analysis. Therefore, it is concluded that the storage of 16 stainless steel channels in an MPC-68 is acceptable.

This discussion is provided in Section 5.2.8 of proposed FSAR *Revision 1* provided in Attachment 6.

### Criticality Evaluation

The criticality calculations presented in Chapter 6 of the HI-STORM FSAR for BWR fuel array/classes 10x10D and 10x10E have been performed using Zircaloy as the material for the flow channels. Stainless steel, which is used for some of these assemblies, has a higher neutron absorption than Zircaloy, which would lead

to a slight reduction in reactivity. The calculations using Zircaloy are therefore bounding for assemblies with stainless steel channels and no further calculations are required.

### **Proposed Change No. 12**

#### **Certificate of Compliance, Appendix B, Sections 2.1.2 and 2.1.3; and Tables 2.1-6 and 2.1-7:**

- a. Subsection 2.1.2 is revised to state that preferential loading is applicable during uniform loading (which is also defined) and to state that regionalized loading meets the intent of preferential loading.
- b. *A footnote is added to Section 2.1.3 to clarify the intended purpose of new Figures 2.1-1 through 2.1-4.*
- c. New Subsection 2.1.3 and Figures 2.1-1 through 2.1-4 are added to introduce regionalized fuel loading as an option. Specific cooling time, burnup, and decay heat limits for regionalized fuel loading are specified in Tables 2.1-6 and 2.1-7 in the Approved Contents section of Appendix B to the CoC.

#### **Reason for Proposed Change**

- a. Clarification to distinguish between uniform fuel loading and regionalized fuel loading and to clarify that regionalized loading meets the intent of preferential fuel loading.
- b. *The new figures are provided to define the two regions of the MPC basket for regionalized fuel storage. The azimuths and some other design details of the MPC basket are also depicted in the figures. These other details are not intended to be controlled a part of the Certificate of Compliance.*
- c. Regionalized fuel loading, in accordance with Figures 2.1-1 through 2.1-4 and Tables 2.1-6 and 2.1-7, as applicable, allows users to load relatively higher heat emitting fuel assemblies than would otherwise be allowed using uniform fuel loading.

## **Justification for Proposed Change**

- a. Clarification
- b. *The figures depict some MPC details that are not germane to defining the fuel storage regions. Region 1 in each of the figures is defined axisymmetrically. Therefore, the azimuths and other MPC details shown have no bearing on the definition of the regions.*
- c. This change is proposed to allow users a method to store fuel assemblies with higher heat emission rates with those having lower heat emission rates, while remaining within the total heat dissipation capabilities of the storage cask design. The specific technical justification is arranged by affected technical discipline below.

### Thermal Evaluation

In the regionalized fuel loading scenario, a two-region fuel configuration is analyzed. The two regions are defined as an inner region (Region 1) for storing relatively hot fuel, and an outer region (Region 2) physically enveloping the inner region and storing relatively cooler fuel. These regions are specifically defined by fuel storage cell number in Appendix B to the CoC. To permit hot fuel storage in the inner region, a low decay heat rate is specified for fuel in the outer region. The maximum allowable heat load for the inner region fuel is then a function of fuel age-dependent permissible cladding temperatures. The regionalized fuel loading thermal modeling is discussed in detail in proposed FSAR Subsection 4.4.1.1.9 and the results of the analysis are provided in proposed FSAR Subsection 4.4.2 (see Attachment 6).

### Shielding Evaluation

Regionalized loading in the HI-STORM cask system is used to place fuel with higher heat emission rates (higher burnups and shorter cooling times) in the center of an MPC surrounded by fuel with lower heat emission rates (lower burnup and longer cooling time). From a shielding perspective, the older fuel on the outside of the MPC is serving as shielding for the fuel on the center of the MPC for the dose rates on the side of the casks. The dose rates on the ends of the casks, however, increase as a result of putting hotter fuel on the inside of the MPC. However, this is a localized effect.

Proposed FSAR *Revision 1*, Section 5.4 in Attachment 6 provides a discussion of regionalized fuel loading and its effect on dose rates. Generally, the radial dose rates for uniform loading bound the dose rates for regionalized loading.

### Confinement Evaluation

Regionalized loading allows higher heat emitting fuel (higher burnup fuel at shorter decay times) to be loaded into the HI-STORM cask. From a confinement perspective the newer, high burnup fuel in the center of the cask has an increased radionuclide inventory due to increased fission products. The radionuclide inventories for each of the MPC designs that allow regionalized loading was revised to ensure that bounding source terms are maintained. The resultant doses are presented in Table 7.3.2 through Table 7.3.4 in proposed *Revision 1* of the FSAR (see Attachment 6). Additionally, Table 7.3.8 of proposed *Revision 1* of the FSAR presents bounding doses for casks containing PWR and BWR fuel and compares them directly to the limits of 10CFR72.

### Proposed Change No. 13

#### Certificate of Compliance, Appendix B, Table 2.1-1 (throughout):

- a. Cooling time, burnup, and decay heat limits are presented by array/class designation instead of by cladding material.
- b. The wording in the right side of the table for cooling time, burnup, and decay heat is made consistent.
- c. Fuel assembly weights are clarified to include non-fuel hardware (PWR), channels (BWR), and damaged fuel canisters, as applicable.
- d. The maximum allowed length for standard BWR fuel is increased from 176.2 inches (nominal) to 176.5 inches (nominal).

#### **Reason and Justification for Proposed Change**

- a. With the addition of more fuel types and unique limits for certain Zircaloy clad fuel assemblies, the presentation format became too complex for users to follow. This change simplifies the presentation.
- b. Editorial clarification.
- c. The MPC has been analyzed with a maximum bounding weight assumed and divided among the total number of fuel storage cells. The user must ensure that all components loaded into a storage location, in total, do not exceed that limit. There is no need to distinguish among the components.

- d. Customer feedback indicates some of their BWR fuel assemblies are longer than the current nominal limit of 176.2 inches. The new nominal length limit of 176.5 inches bounds these fuel assemblies and has been evaluated against the MPC height tolerance as well as growth of the limiting length assembly due to irradiation and thermal expansion and found to be acceptable. There is no impact on the structural, thermal, shielding, criticality, or confinement evaluations due to this change.

### **Proposed Change No. 14**

Certificate of Compliance, Appendix B, Section 1.0 Table 2.1-1, and new Table 2.1-8:

*The definition of NON-FUEL HARDWARE is added, MPC-24, Items I.A and C, are revised; new Note 1 is added to Item I, and new Table 2.1-8 is added as shown in the attached marked-up CoC pages to allow storage of non-fuel hardware, including Burnable Poison Rod Assemblies (BPRAs)\*, Thimble Plug Devices (TPDs)\*, Control Rod Assemblies (CRAs), Axial Power Shaping Rods (APSRs), Control Element Assemblies (CEAs), wet annular burnable absorbers (WABAs), rod cluster control assemblies (RCCAs), water displacement guide tube plugs and orifice rod assemblies. Non-fuel hardware is also proposed to be authorized for loading into MPC-24E, MPC-24EF, and MPC-32 and the same limits are specified for those MPC models later in Table 2.1-1.*

### **Reason for Proposed Change**

A large number of PWR plant fuel assemblies are currently stored in spent fuel pools with either BPRAs, TPDs, WABAs, water displacement guide tube plugs, or orifice rod assemblies as integral hardware to the assemblies. A smaller number of PWR assemblies are stored with CRAs, RCCAs or APSRs. This irradiated hardware must be authorized for dry storage with the assemblies to accommodate user needs (particularly for plants who wish to decommission their spent fuel pools) and is therefore proposed to be added to the authorized contents.

### **Justification for Proposed Change**

#### **Structural Evaluation**

There is no effect on the structural evaluation because these changes do not change the fuel assembly geometry or weight used in the structural analyses. The limits on these parameters as stated elsewhere in the CoC fuel tables remain the same and fuel assemblies containing these components must meet these limits.

### Thermal Evaluation

The non-fuel bearing hardware becomes activated as a result of in-core irradiation. In the dry cask storage scenario, this hardware represents a Low Heat Emitting (LHE) source distributed over the length of the fuel assembly. The non-fuel hardware contribution to the total decay heat load burden of a cask is quite small.

The *hardware*, when inserted in the fuel assemblies, displace the gas in the guide tubes and replace them with solid materials (neutron absorbers and metals) which conduct heat much more readily. As a result, dissipation of heat by the fuel assemblies is enhanced by the presence of these components. In the thermal evaluation supporting this amendment request, no credit was taken for this enhanced decay heat dissipation. Thus, the design basis heat load of the HI-STORM cask is conservatively unaltered by this proposed change. To conservatively compute a lower bound value for the permissible burnup and cooling time limits for storage in the HI-STORM cask, the limiting fuel type for the class of PWR fuel (i.e., the one with the highest uranium mass) is utilized. In the CoC, a requirement is specified to comply with these burnup and cooling time limits. In addition, each assembly proposed for storage must be confirmed to have a total heat emission rate less than the design maximum, including the fuel and any non-fuel hardware, as applicable.

The addition of this non-fuel hardware has two effects on the MPC cavity pressures. As discussed in the last paragraph, non-fuel hardware enhances heat dissipation, thus lowering fuel and MPC cavity fill gas temperatures. The gas volume displaced by the mass of the non-fuel hardware lowers the cavity free volume. These two effects, namely, temperature lowering and free volume reduction, have opposing influences on the MPC cavity pressure. The first effect lowers the gas pressure while the second effect raises it. In the HI-STORM thermal analysis, the computed temperature field (with non-fuel hardware *excluded*) provides a conservatively bounding thermal response of the HI-STORM cask. The MPC cavity free space was computed based on displacement by the heaviest fuel (bounding weight) with non-fuel hardware *included*. Thus, the previously computed MPC cavity pressure results remain conservative with respect to gas temperature and free space as affected by the changes proposed in this amendment.

PWR fuel assemblies with BPRAs containing helium gas have been evaluated under the hypothetical accident condition where 100% of the BPRAs rupture, releasing all of the contained helium into the MPC cavity. The maximum helium backfill pressure TS limit for the PWR MPCs is adjusted appropriately so that the resultant post-accident MPC cavity pressure, including BPA gas release, is limited to an acceptable value, within the design pressure of the MPC.

Appropriate discussion has been added to proposed *Revision 1* FSAR Chapters 4 and 11 (see Attachment 6).

#### Shielding Evaluation –BPRAs and TPDs

Burnable Poison Rod Assemblies (including Wet Annular Burnable Absorbers and other similarly designed devices with different names) and Thimble Plug Devices (including orifice rod assemblies, *water displacement* guide tube plugs, and other similarly designed devices with different names) are an integral, yet removable, part of a large portion of PWR fuel. The TPDs are not used in all assemblies in a reactor core, but are re-used from cycle to cycle. Therefore, these devices can achieve very high burnups. In contrast, BPRAs are burned with a fuel assembly in core and are not reused. In fact, many BPRAs are removed after one or two cycles before the fuel assembly is discharged. Therefore, the achieved burnup for BPRAs is not significantly different than fuel assemblies.

TPDs are made of stainless steel and contain a small amount of Inconel. These devices extend down into the plenum region of the fuel assembly but do not extend into the active fuel region with the exception of the Westinghouse 14x14 water displacement guide tube plugs. Since these devices are made of stainless steel, there is a significant amount of Co-60 produced during irradiation. This is the only significant radiation source from the activation of steel and Inconel.

BPRAs are made of stainless steel in the region above the active fuel zone and may contain a small amount of Inconel in this region. Within the active fuel zone, the BPRAs may contain two to 24 rodlets which are burnable absorbers clad in either Zircaloy or stainless steel. The stainless steel clad BPRAs create a significant radiation source (Co-60) while the Zircaloy clad BPRAs create a negligible radiation source. Therefore the stainless steel clad BPRAs are bounding.

SAS2H and ORIGEN-S were used to calculate a radiation source term for the TPDs and BPRAs. These calculations were performed by irradiating the appropriate mass of steel and Inconel using the flux calculated for the design basis B&W 15x15 fuel assembly. The mass of material in the regions above the active fuel zone was scaled by the appropriate scaling factors listed in Table 5.2.10 of the HI-STORM FSAR, *Rev. 0* in order to account for the reduced flux levels above the fuel assembly. The total curies of cobalt and the decay heat load were calculated for the TPDs and BPRAs as a function of burnup and cooling time. For burnups beyond 45,000 MWD/MTU, it was assumed, for the purpose of the calculation, that the burned fuel assembly was replaced with a fresh fuel assembly every 45,000 MWD/MTU. This was achieved in ORIGEN-S by resetting the flux levels and cross sections to the zero burnup condition after every 45,000 MWD/MTU.

Since the HI-STORM 100 cask system is designed to store many varieties of PWR fuel, a bounding TPD and BPRAs had to be determined for the purposes of the analysis. This was accomplished by analyzing all of the fuel containing BPRAs and TPDs (Westinghouse and B&W 14x14 through 17x17) found in FSAR references [5.2.5] and [5.2.7] listed in Section 5.6 of the FSAR to determine the TPD and BPRAs which produced the highest Co-60 source term and decay heat for a specific burnup and cooling time. The bounding TPD was determined to be the Westinghouse 17x17 guide tube plug and the bounding BPRAs was actually determined by combining the higher masses of the Westinghouse 17x17 and 15x15 BPRAs into a single hypothetical BPRAs. The masses of this TPD and BPRAs are listed in Table 5.2.30 of the proposed *Revision 1* of the HI-STORM FSAR (see Attachment 6). As mentioned above, FSAR reference [5.2.5] describes the Westinghouse 14x14 water displacement guide tube plug as having a steel portion that extends into the active fuel zone. This particular water displacement guide tube plug was analyzed and determined to be bounded by the design basis TPD and BPRAs.

Once the bounding BPRAs and TPD were determined, the Co-60 source from the BPRAs and TPD were specified: 50 Curies for each TPD, and 831 Curies for each BPRAs. Table 5.2.31 of the proposed *Revision 1* of the HI-STORM FSAR shows the Curies of Co-60 that were calculated for BPRAs and TPDs in each region of the fuel assembly (e.g., incore, plenum, top). An allowable burnup and cooling time, separate from the fuel assemblies, is used for the BPRAs and TPDs themselves. These burnup and cooling times assure that the Co-60 activity remains below the allowable levels specified above. It should be noted that at very high burnups (greater than 200,000 MWD/MTU) the Co-60 source for a given cooling time actually decreases as the burnup continues to increase. This is due to a decrease in the Co-60 production rate as the initial Co-59 impurity is depleted. Conservatively, a constant cooling time has been specified for burnups from 180,000 to 630,000 MWD/MTU for the TPDs.

#### Shielding Evaluation – CRAs and APSRs

Control Rod Assemblies (CRAs) and Axial Power Shaping Rods (APSRs) are an integral portion of many PWR fuel assemblies going into dry storage. These devices are utilized for many years (upwards of 20 years) prior to discharge into the spent fuel pool. The manner in which the CRAs are utilized varies from plant to plant. Some utilities maintain the CRAs fully withdrawn during normal operation while others may operate with a bank of rods partially inserted (approximately 10%) during normal operation. Even when fully withdrawn, the ends of the CRAs are present in the upper portion of the fuel assembly since they are never fully removed from the fuel assembly during operation. The result of the different operating styles is a variation in the source term for the CRAs. In all

cases, however, only the lower portion of the CRAs will be significantly activated. Therefore, when the CRAs are stored with the PWR fuel assembly, the activated portion of the CRAs will be in the lower portion of the cask. CRAs are fabricated of various materials. The cladding is typically stainless steel, although Inconel has been used. The absorber can be a single material or a combination of materials. Silver-Indium-Cadmium (Ag-In-Cd) is possibly the most common absorber, although B<sub>4</sub>C in aluminum is used, and hafnium has also been used. Ag-In-Cd produces a noticeable source term in the 0.3-1.0 MeV range due to the activation of Ag. The source term from the other absorbers is negligible, therefore the Ag-In-Cd CRAs are the bounding CRAs.

APSRs are used to flatten the axial power distribution during normal operation and, as a result, these devices achieve a considerably higher activation than CRAs. There are two types of B&W stainless steel clad APSRs: gray and black. According to FSAR reference [5.2.5], the black APSRs have 36 inches of Ag-In-Cd as the absorber while the gray ones use 63 inches of Inconel as the absorber. Because of the Cobalt-60 source from the activation of Inconel, the gray APSRs produce a higher source term than the black APSRs and therefore are the bounding APSR.

Since the level of activation of CRAs and APSRs can vary, the quantity that can be stored in an MPC is being limited to four CRAs and/or APSRs. These four devices are required to be stored in the inner four locations in the MPC-24, MPC-24E, MPC-24EF, and MPC-32 as specified in Appendix B to the CoC.

In order to determine the impact on the dose rates around the HI-STORM 100 System, source terms for the CRAs and APSRs were calculated using SAS2H and ORIGEN-S. In the ORIGEN-S calculations the cobalt-59 impurity level was conservatively assumed to be 0.8 gm/kg for stainless steel and 4.7 gm/kg for Inconel. These calculations were performed by irradiating 1 kg of steel, Inconel, and Ag-In-Cd using the flux calculated for the design basis B&W 15x15 fuel assembly. The total curies of cobalt for the steel and Inconel and the 0.3-1.0 MeV source for the Ag-In-Cd were calculated as a function of burnup and cooling time to a maximum burnup of 630,000 MWD/MTU. For burnups beyond 45,000 MWD/MTU it was assumed, for the purpose of the calculation, that the burned fuel assembly was replaced with a fresh fuel assembly every 45,000 MWD/MTU. This was achieved in ORIGEN-S by resetting the flux levels and cross sections to the 0 MWD/MTU condition after every 45,000 MWD/MTU.

The sources were then scaled by the appropriate mass using the flux weighting factors for the different regions of the assembly to determine the final source term. Two different configurations were analyzed for both the CRAs and APSRs with an additional third configuration analyzed for the APSRs. The configurations, which are summarized below, are described in Tables 5.2.32, of

the proposed *Revision 1* of the FSAR, for the CRAs and Table 5.2.33, of the proposed *Revision 1* of the FSAR, for the APSR. The masses of the materials listed in these tables were determined from a review of FSAR reference [5.2.5] with bounding values chosen. The masses listed in Tables 5.2.32 and 5.2.33 do not match exact values from FSAR reference [5.2.5] because the values in the reference were adjusted to the lengths shown in the tables.

### **Configuration 1: CRA and APSR**

This configuration had the lower 15 inches of the CRA and APSR activated at full flux with two regions above the 15 inches activated at a reduced power level. This simulates a CRA or APSR which was operated at 10% insertion. The regions above the 15 inches reflect the upper portion of the fuel assembly.

### **Configuration 2: CRA and APSR**

This configuration represents a fully removed CRA or APSR during normal core operations. The activated portion corresponds to the upper portion of a fuel assembly above the active fuel length with the appropriate flux weighting factors used.

### **Configuration 3: APSR**

This configuration represents a fully inserted gray APSR during normal core operations. The region in full flux was assumed to be the 63 inches of the absorber.

Tables 5.2.34 and 5.2.35 of proposed *Revision 1* of the FSAR present the source terms that were calculated for the CRAs and APSRs, respectively. The only significant source from the activation of Inconel or steel is Co-60 and the only significant source from the activation of Ag-In-Cd is in the range of 0.3-1.0 MeV. The source terms for CRAs, Table 5.2.34, were calculated for a maximum burnup of 630,000 MWD/MTU and a minimum cooling time of 5 years. Because of the significant source term in APSRs that have seen extensive in-core operations, the source term in Table 5.2.35 was calculated to be a bounding source term for a variable burnup and cooling time as outlined in Appendix B to the CoC. The very large Cobalt-60 activity in Configuration 3 in Table 5.2.35 is due to the assumed Cobalt-59 impurity level of 4.7 gm/kg. If this impurity level was similar to the assumed value for steel, 0.8 gm/kg, this source would decrease by approximately a factor of 5.8.

## Shielding Summary

Section 5.4.6 of proposed *Revision 1* of the HI-STORM FSAR provides the dose rate increase due to the inclusion of BPRAs, TPDs, CRAs, and APSRs. The data in this section indicate that BPRAs result in the highest dose rate increase on the radial surfaces of the cask while the APSRs result in the largest dose rate increase in the bottom of the cask. The increase in the dose rates at the bottom of the cask will not significantly affect occupational exposure. Therefore, the additional dose rate from the BPRAs was included in the design basis analysis presented in Section 5.1 and in the dose rates calculated in Section 5.4 of the proposed *Revision 1* of the HI-STORM FSAR found in Attachment 6. The occupational exposure estimates provided in Chapter 10 of the FSAR were also revised to include the dose rate contribution from BPRAs. These new values can be found in proposed *Revision 1* of Chapter 10 in Attachment 6. The controlled area boundary dose rate analysis provided in Chapter 5 of *Revision 0* of the FSAR was not revised to include the effect of BPRAs because this analysis had been performed with a bounding burnup and cooling time of 52.5 GWD/MTU and 5 year cooling.

In conclusion, the shielding analysis has been revised to include the additional dose rate from non-fuel hardware. While the dose rates around the HI-TRAC have increased as a result of including this non-fuel hardware, the safety of the system has not been compromised.

## Criticality Evaluation

For MPCs filled with pure water, the reactivity of any PWR assembly with non-fuel hardware inserted into the guide tubes is bounded by (i.e. lower than) the reactivity of the same assembly without the inserts. This is due to the fact that the inserts reduce the amount of moderator, while the amount of fissile material remains unchanged. In the presence of soluble boron in the water, especially for higher soluble boron concentrations, it is possible that the non-fuel hardware in the PWR assembly results in an increase of reactivity. This is due to the fact that the insert not only replaces water, but also the neutron absorber in the water. To account for this effect, analyses with and without non-fuel hardware in the assemblies have been performed for higher soluble boron concentrations (see Tables 6.4.6 and 6.4.10 of Proposed *Rev. 1* of the FSAR). The highest reactivities for either case are used as the basis of the criticality evaluation.

## **Proposed Change No. 15**

### **Certificate of Compliance, Appendix B, Table 2.1-1:**

Item II.A.2 is revised to authorize a broader range of BWR damaged fuel, beyond the currently authorized Dresden Unit 1 and Humboldt Bay damaged fuel. The additional damaged fuel must be loaded into the new generic BWR DFC for loading into the MPC-68. Further, the damaged fuel is only authorized for loading into the 16 peripheral fuel storage locations, called out numerically in revised Item II.B.3. Damaged fuel assemblies meeting the same specifications are also proposed to be authorized for loading into the MPC-68FF as discussed later in this section.

### **Reason for Proposed Change**

Most users have at least some fuel assemblies destined for dry storage that would be classified as damaged fuel assemblies in accordance with the CoC. The current CoC only authorizes damaged fuel from Dresden Unit 1 and Humboldt Bay for storage. The CoC needs to be expanded to accommodate customer needs.

### **Justification for Proposed Change**

#### **Structural Evaluation**

The only structural requirements on the contents of a BWR or PWR fuel basket are that the total weight per cell does not exceed the design basis weight (700 lbs for BWR assemblies and 1,680 lbs for PWR assemblies), and that loading of these assemblies does not alter the temperature limits used in the design basis analyses. The damaged fuel assemblies covered by this change, together with the appropriate DFC, satisfy these restrictions, so that no additional structural evaluation is necessary.

#### **Thermal Evaluation**

The thermal performance characteristics of the most heat resistive Zircaloy and stainless steel clad BWR fuel assemblies, encased in the proposed DFC design, have been evaluated in support of this amendment. The interruption of thermal radiation heat exchange between the fuel assembly and the fuel basket by the DFC renders the DFC configuration more restrictive than the non-DFC configuration. The thermal performance characteristics of MPC-68s loaded entirely with fuel assemblies in BWR DFCs were evaluated, using the same methods employed to evaluate the previously approved MPC-68 with Dresden Unit 1 and Humboldt Bay damaged fuel, and appropriate decay heat loads determined. It is noted that this amendment only requests loading of 16 BWR

DFCs, so the thermal evaluations of MPCs completely loaded with fuel in DFCs is highly conservative.

#### Shielding Evaluation

See the shielding evaluation for Proposed Change Number 10.

#### Criticality Evaluation

Criticality calculations have been performed for an MPC-68 loaded with intact and damaged fuel/fuel debris (up to 16 damaged fuel assemblies placed in DFCs) and maximum enrichments of up to 4.0 wt%  $^{235}\text{U}$  for the damaged fuel/fuel debris and up to 3.7 wt%  $^{235}\text{U}$  for the intact fuel. The calculations use a bounding approach to account for the possible wide variation of fuel distribution inside the DFC, based on the analysis of arrays of bare fuel rods. Also, typical damaged fuel conditions such as missing rods or collapsed assemblies are analyzed for selected array/classes. The analyses are presented in Section 6.4.4.2 of proposed *Revision 1* of the FSAR (see Attachment 6). The maximum calculated  $k_{\text{eff}}$  is 0.9328, which demonstrates that the cask system is in compliance with the regulatory requirement of  $k_{\text{eff}} < 0.95$  for all BWR fuel array/classes.

#### Proposed Change No. 16\*

##### Certificate of Compliance, Appendix B, Table 2.1-1:

New Items II.A.5 and III.A.7 are added to Table 2.1-1 for MPC-68 and MPC-68F as shown in the attached marked-up pages of the CoC table to allow storage of one Dresden Unit 1 (D-1) Thoria Rod Canister in these MPC models. Drawings of the D-1 Thoria Rod Canister were provided in LAR 1008-1 submitted to the NRC in November, 1999 for the HI-STAR 100 System (Docket 72-1008). Figure 2.1.2A is added to the FSAR showing key dimensions and major fabrication details for the Thoria Rod Canister (see Attachment 6). Conforming revisions are also made to Appendix B, Items II.B and III.B.

##### **Reason for Proposed Change**

Dresden Unit 1 needs to place one Thoria Rod Canister into dry storage to support plant decommissioning.

## **Justification for Proposed Change**

### Structural Evaluation

The Dresden Unit 1 Thoria Rod Canister has been structurally evaluated by Holtec International and found to meet all required design requirements for storage in the HI-STORM 100 system. The details of this evaluation are contained in proposed *Revision 1* FSAR Appendix 3.AR, included in Attachment 6 to this letter. All required safety margins are greater than zero or, in other words, the factors of safety are greater than 1.0.

### Thermal Evaluation

The Thoria Rod Canister is designed to hold a maximum of 20 fuel rods arrayed in a 5x4 configuration. Eighteen rods are actually in the canister. The fuel rods contain a mixture of enriched  $\text{UO}_2$  and thorium oxide in the fuel pellets. The fuel rods were originally constituted as part of an 8x8 fuel assembly and used in the second and third cycle of Dresden-1 operation. The maximum fuel burnup of these rods is quite low ( $< 16,000$  MWD/MTIHM). The Thoria Rod Canister internal design is a honeycomb structure formed from 12 gage stainless steel plates. The rods are loaded in individual square cells and thus are isolated from each other by the cell walls. The few number of rods (18 per assembly) and very low burnup of fuel stored in these Dresden-1 canisters render them as miniscule sources of decay heat. The canister all-metal internal honeycomb construction serves as an additional means of heat dissipation in the fuel cell space. In accordance with preferential fuel loading requirements imposed in the Approved Contents section of Appendix B to the CoC, low burnup fuel is required to be loaded toward the basket periphery (i.e., away from the hot central core of the fuel basket). All these considerations provide ample assurance that these fuel rods will be stored in a benign thermal environment and therefore remain protected during long-term storage.

### Shielding Evaluation

The Dresden Unit 1 Thoria Rod Canister contains 18 thoria rods that have obtained a relatively low burnup, 16,000 MWD/MTIHM. These rods were removed from two 8x8 fuel assemblies that contained 9 rods each. The irradiation of thorium produces an isotope that is not commonly found in depleted uranium fuel. Th-232, when irradiated, produces U-233. The U-233 can undergo an (n,2n) reaction that produces U-232. The U-232 decays to produce Tl-208 that produces a 2.6 MeV gamma during beta decay. This results in a significant source in the 2.5-3.0 MeV range that is not commonly present in depleted uranium fuel. Therefore, this single DFC container was analyzed to determine if it was bounded by the current shielding analysis.

A radiation source term was calculated for the 18 thoria rods using SAS2H and ORIGEN-S for a burnup of 16,000 MWD/MTIHM and a cooling time of 18 years. Table 5.2.36 of proposed *Revision 1* of the HI-STORM FSAR (Attachment 6) describes the 8x8 fuel assembly that contains the thoria rods. Table 5.2.37 and 5.2.38 of proposed *Revision 1* of the HI-STORM FSAR shows the gamma and neutron source terms, respectively, that were calculated for the 18 thoria rods in the Thoria Rod Canister. Comparing these source terms to the design basis 6x6 source terms for Dresden Unit 1 fuel in FSAR Tables 5.2.7 and 5.2.18 clearly indicates that the design basis source terms bound the thoria rod source terms in all neutron groups and in all gamma groups except the 2.5-3.0 MeV group. As mentioned above, the thoria rods have a significant source in this energy range due to the decay of Tl-208.

It is obvious that the neutron spectrum from the 6x6 fuel assembly bounds the thoria rod neutron spectra with a significant margin. In order to demonstrate that the gamma spectrum from the single Thoria Rod Canister is bounded by the gamma spectrum from the design basis 6x6 fuel assembly, the gamma dose rate on the outer radial surface of the 100-ton HI-TRAC transfer cask and the HI-STORM overpack was estimated conservatively assuming an MPC-68 filled with Thoria Rod Canisters. This gamma dose rate was compared to an estimate of the dose rate from an MPC full of design basis 6x6 fuel assemblies. The gamma dose rate from the 6x6 fuel was higher for the 100-ton HI-TRAC and only 17% lower for the HI-STORM overpack than the dose rate from an MPC full of Thoria Rod Canisters. This, in conjunction with the significant margin in neutron spectrum and the fact that only one thoria rod canister is proposed to be authorized for storage in the HI-STORM 100 System clearly demonstrates that the Thoria Rod Canister is acceptable for storage in the MPC-68 or the MPC-68F.

#### Criticality Evaluation

The Thoria Rod Canister is similar to a DFC with an internal separator assembly containing 18 fuel rods. The configuration is illustrated in proposed *Revision 1* FSAR Figure 6.4.19 (see Attachment 6). The  $k_{\text{eff}}$  value for an MPC-68/68F filled with Thoria Rod Canisters is calculated to be 0.18. This low reactivity is attributed to the relatively low content in  $^{235}\text{U}$  (equivalent to  $\text{UO}_2$  fuel with an enrichment of approximately 1.7 wt%  $^{235}\text{U}$ ), the large spacing between the rods (the pitch is approximately 1", the cladding outside diameter is 0.412"), and the absorption in the separator assembly. Together with the maximum  $k_{\text{eff}}$  values listed in FSAR Tables 6.1.7 and 6.1.8 this result demonstrates that the  $k_{\text{eff}}$  for a Thoria Rod Canister loaded into the MPC-68 or the MPC-68F together with other approved fuel assemblies or DFCs will remain well below the regulatory requirement of  $k_{\text{eff}} < 0.95$ .

### Confinement Evaluation

The HI-STORM confinement analyses have been revised to account for several new isotopes associated with the Thoria Rod Canister. These isotopes (Bi-212, Pb-212, Po-216, Ra-224, Rn-220, Th-228 and U-232) had a negligible effect on the resulting doses because only one Thoria Rod Canister is authorized for loading in an MPC-68 or -68F with 67 other design basis BWR assemblies. Therefore, the Thoria Rod isotopes are not included in the presentation of the confinement analysis inputs or results in the FSAR.

### Proposed Change No. 17\*

#### Certificate of Compliance, Appendix B, Table 2.1-1

New Items II.D and III.D are added as shown in the attached marked-up CoC pages to authorize Dresden Unit 1 fuel assemblies containing up to one antimony-beryllium neutron source in the assembly lattice for storage.

#### **Reason for Proposed Change**

Dresden Unit 1 needs to place fuel assemblies containing antimony-beryllium neutron sources into dry storage to support plant decommissioning.

#### **Justification for Proposed Change**

##### Structural Evaluation

The structural evaluation is not affected because the fuel assembly parameters used in the design basis structural evaluations are not affected by this change. The neutron sources have no impact on component temperatures or fuel assembly size and weight.

##### Thermal Evaluation

The substitution of antimony-beryllium sources in a fuel assembly in lieu of heat emitting fuel rods is bounded by the existing thermal analyses, which assume decay heat production from the replaced fuel rods.

##### Shielding Evaluation

Dresden Unit 1 has antimony-beryllium neutron sources that are placed in the water rod location of their fuel assemblies. These sources are steel rods that contain a cylindrical antimony-beryllium source that is 77.25 inches in length.

The steel rod is approximately 95 inches in length. Information obtained from Dresden Unit 1 characterizes these sources in the following manner: "About one-quarter pound of beryllium will be employed as a special neutron source material. The beryllium produces neutrons upon gamma irradiation. The gamma rays for the source at initial start-up will be provided by neutron-activated antimony (about 865 curies). The source strength is approximately  $1\text{E}+8$  neutrons/second."

As stated above, beryllium produces neutrons through gamma irradiation and, in this particular case, antimony is used as the gamma source. The threshold gamma energy for producing neutrons from beryllium is 1.666 MeV. The outgoing neutron energy increases as the incident gamma energy increases. Sb-124, that decays by beta decay with a half-life of 60.2 days, produces a gamma of energy 1.69 MeV that is just energetic enough to produce a neutron from beryllium. Approximately 54% of the beta decays for Sb-124 produce gammas with energies greater than or equal to 1.69 MeV. Therefore, the neutron production rate in the neutron source can be specified as  $5.8\text{E}-6$  neutrons per gamma ( $1\text{E}+8/865/3.7\text{e}+10/0.54$ ) with energy greater than 1.666 MeV or  $1.16\text{E}+5$  neutrons/curie ( $1\text{E}+8/865$ ) of Sb-124.

With the short half life of 60.2 days, all of the initial Sb-124 is decayed and any Sb-124 that was produced while the neutron source was in the reactor is also decayed since these neutron sources are required to have the same minimum cooling time as the Dresden 1 fuel assemblies (array classes 6x6A, 6x6B, 6x6C, and 8x8A) of 18 years. Therefore, there are only two possible gamma sources that can produce neutrons from this antimony-beryllium source. The first is the gammas from the decay of fission products in the fuel assemblies in the MPC. The second gamma source is from Sb-124 that is produced in the MPC from neutron activation by neutrons from the decay of fission products.

MCNP calculations were performed to determine the gamma source as a result of decay gammas from fuel assemblies and Sb-124 activation. The calculations explicitly modeled the 6x6 fuel assembly described in Table 5.2.2 of *Revision 0* of the HI-STORM FSAR. A single fuel rod was removed and replaced by a guide tube. In order to determine the amount of Sb-124 that is activated from neutrons in the MPC it was necessary to estimate the amount of antimony in the neutron source. The O.D. of the source was assumed to be the I.D. of the steel rod encasing the source (0.345 in.). The length of the source is 77.25 inches. The beryllium is assumed to be annular in shape encompassing the antimony. Using the assumed O.D. of the beryllium and the mass and length, the I.D. of the beryllium was calculated to be 0.24 inches. The antimony is assumed to be a solid cylinder with an O.D. equal to the I.D. of the beryllium. These assumptions are conservative since the antimony and beryllium are likely encased in another material that would reduce the mass of antimony. A larger mass of antimony is

conservative since the calculated activity of Sb-124 is directly proportional to the initial mass of antimony.

The number of gammas from fuel assemblies with energies greater than 1.666 MeV entering the 77.25 inch long neutron source was calculated to be  $1.04\text{E}+8$  gammas/sec that would produce a neutron source of 603.2 neutrons/sec ( $1.04\text{E}+8 * 5.8\text{E}-6$ ). The steady state amount of Sb-124 activated in the antimony was calculated to be 39.9 curies. This activity level would produce a neutron source of  $4.63\text{E}+6$  neutrons/sec ( $39.9 * 1.16\text{E}+5$ ) or  $6.0\text{E}+4$  neutrons/sec/inch ( $4.63\text{E}+6/77.25$ ). These calculations conservatively neglect the reduction in antimony and beryllium that would have occurred while the neutron sources were in the core and being irradiated at full reactor power.

Since this is a localized source (77.25 inches in length) it is appropriate to compare the neutron source per inch from the design basis Dresden Unit 1 fuel assembly, 6x6, containing an Sb-Be neutron source to the design basis fuel neutron source per inch. This comparison, presented in Table 17.1 below, demonstrates that a Dresden Unit 1 fuel assembly containing an Sb-Be neutron source is bounded by the design basis fuel.

As stated above, the Sb-Be source is encased in a steel rod. Therefore, the gamma source from the activation of the steel was considered assuming a burnup of 120,000 MWD/MTU which is the minimum burnup assuming the Sb-Be source was in the reactor for the entire 18-year life of Dresden Unit 1. The cooling time was assumed to be 18 years that is the minimum cooling time for Dresden Unit 1 fuel. The source from the steel is bounded by the design basis fuel assembly. In conclusion, storage of a Dresden Unit 1 Sb-Be neutron source in a Dresden Unit 1 fuel assembly is acceptable and bounded by the current analysis.

**Table 17.1  
 Comparison of Neutron Source per Inch per Second for  
 Design Basis 7x7 Fuel and Design Basis Dresden Unit 1 Fuel**

Assembly	Active fuel length (inches)	Neutrons per sec per inch	Neutrons per sec per inch with Sb-Be source	Reference for neutrons per sec per inch
7x7 design basis	144	9.17E+5	N/A	Table 5.2.17 <i>Rev. 1</i> HI-STORM FSAR 40 GWD/MTU and 5 year cooling
6x6 design basis	110	2.0E+5	2.6E+5	Table 5.2.18 <i>Rev. 0</i> HI-STORM FSAR
6x6 design basis MOX	110	3.06E+5	3.66E+5	Table 5.2.23 <i>Rev. 0</i> HI-STORM FSAR

Criticality Evaluation

The reactivity of a fuel assembly is not affected by the presence of a neutron source (other than by the presence of the material of the source, which is discussed later). This is true because in a system with a  $k_{eff}$  less than 1.0, any given neutron population at any time, regardless of its origin or size, will decrease over time. Therefore, a neutron source of any strength will not increase reactivity, but only the neutron flux in a system, and no additional criticality analyses are required. Sources are inserted as rods into fuel assemblies, i.e., they replace either a fuel rod or water rod (moderator). Therefore, the insertion of the material of the source into a fuel assembly will also not lead to an increase of reactivity.

**Proposed Change No. 18**

Certificate of Compliance, Appendix B, Table 2.1-1

Items III.A.1.f, g, and h are revised as shown in the attached CoC markups to correct these dimensional limits to match the dimensions for Zircaloy fuel assembly array/classes 6x6A, 6x6C, 7x7A, and 8x8A (Dresden Unit 1 and Humboldt Bay). Only these array/classes (and 6x6B MOX fuel) are authorized for loading into the MPC-68F. This is simply an editorial change because fuel

assemblies exceeding the correct dimensional limits would not be able to be inadvertently loaded as they would not fall into the above-mentioned array/classes.

### **Reason and Justification for Proposed Change**

Editorial corrections.

### **Proposed Change No. 19**

#### **Certificate of Compliance, Appendix B, Table 2.1-1**

New Item IV is added to the table for MPC-24E. See also, proposed Change Number 29.

#### **Reason for Proposed Change**

The MPC-24E provides for storage of higher enriched fuel than the MPC-24 through the optimization of the storage cell layout. In addition, storage of damaged PWR fuel assemblies in generic PWR DFC is authorized. This change is required to meet customers' needs for storage of higher enriched fuel and damaged fuel. The MPC-24E has been analyzed for storage of two ranges of enrichment for PWR fuel. The lower of the two ranges has been analyzed with unborated water in the MPC during wet loading and unloading operations and the higher range has been analyzed with credit taken for soluble boron in the MPC water (see associated changes to Table 2.1-2 and Proposed Change Number 3).

#### **Justification for Proposed Change**

The MPC-24E is a very close variant of the previously approved MPC-24. Holtec's engineers and analysts have taken advantage of optimizing the fuel storage cell configuration, flux trap sizes, and <sup>10</sup>B loading in the Boral, while still meeting subcriticality requirements. The basic honeycomb basket structure remains unchanged. The structural and thermal characteristics of the basket are virtually the same as the MPC-24. There is an effect on the confinement analysis due to the addition of damaged fuel. A detailed discussion of this change is provided below, arranged by technical discipline.

#### **Structural Evaluation**

A finite element model of the MPC-24E fuel basket was prepared in the same manner that was used for the previously approved MPC-24 and MPC-68 fuel baskets. The analyses of the MPC-24E fuel basket under applied inertia loads,

simulating a handling accident, have been carried out to obtain primary stresses in the fuel basket structure and in the MPC shell. The safety factors, after applying the appropriate dynamic amplifier, exceed 1.0 and are reported in the proposed FSAR revision in appropriate tables in Chapter 3, Subsection 3.4. Text in Chapter 3 of the FSAR has been appropriately modified to reflect the addition of this new fuel basket. All other structural analyses currently approved have been reviewed to ensure that the bounding loads used as input for the specific structural analyses remained bounding. The bounding weights used as input for the FSAR analyses were not changed by the addition of this new basket; therefore, previously reported safety factors in the FSAR are not altered by this new fuel basket. See Attachment 6 for proposed FSAR changes.

#### Thermal Evaluation

With respect to thermal performance, the MPC-24E configuration is slightly different (symmetric basket layout) from the previously approved MPC-24, but employs the same general construction (integral honeycomb basket) and the same heat rejection mechanisms. The thermal performance of the MPC-24E design has been evaluated, in support of this amendment request, using the analysis methods employed to determine the performance of the previously approved MPC-24 and MPC-68. The substantial conservative assumptions embedded in the evaluations of the MPC-24 and MPC-68 designs have also been incorporated in the evaluations of the MPC-24E. Allowable decay heat loads have been determined for design-basis (DB) intact Zircaloy clad, damaged Zircaloy clad, and stainless steel clad fuel that ensure safe long-term storage of SNF in the MPC-24E. The HI-STORM temperature field for the MPC-24E loaded with design-basis heat emitting fuel was calculated and is reported in proposed revisions to HI-STORM FSAR Chapter 4 (see Attachment 6).

#### Shielding Evaluation

From a shielding perspective, the new MPC-24E is identical to the MPC-24 and therefore was not explicitly analyzed. The different fuel cell pitch in the MPC-24E, compared to the MPC-24, will have little impact on the dose rates outside the overpack. In addition, all of the steel fuel cell walls in the MPC-24E are 5/16 inch thickness and provide somewhat more shielding compared to the MPC-24 (which utilizes both 9/32 and 5/16 inch walls). The analysis of the MPC-24 in Chapter 5 of the proposed *Revision 1* of the HI-STORM FSAR conservatively bounds the allowable contents for both the MPC-24 and the MPC-24E.

### Criticality Evaluation

In order to increase the maximum permissible fuel enrichment for the MPC-24E compared to the MPC-24, the following changes were introduced into the MPC-24E:

- The fuel storage cells and flux traps are arranged in a fully symmetric manner, which allows moving some cells further away from the center of the basket. This results in increased flux traps in some areas of the basket.
- The  $^{10}\text{B}$  loading of the Boral is increased from 0.0267 (minimum) to 0.0372 g/cm<sup>2</sup> (minimum). This requires a change in the Boral thickness from 0.082 inches to 0.101 inches.
- The cell pitch is slightly increased.

Additionally, four of the peripheral cells have an increased cell ID to accommodate PWR Damaged Fuel Containers. This results in decreased flux traps for these cells.

Overall, this design allows an increase in the maximum permissible fuel enrichment of 0.4 wt%  $^{235}\text{U}$  for most fuel classes, while maintaining the same level of margin toward the regulatory requirement of  $k_{\text{eff}} < 0.95$ . The maximum  $k_{\text{eff}}$  for the bounding assembly in each class is listed in Table 6.1.3 in Section 6.1 of the proposed *Revision 1* of the FSAR (see Attachment 6).

Additionally, the MPC-24E is analyzed with credit taken for soluble boron present in the water during wet loading and unloading operations. With a minimum soluble boron concentration in the water of 300 ppmb, a maximum enrichment of 5.0 wt%  $^{235}\text{U}$  for all assembly classes is permissible. To ensure that the actual  $k_{\text{eff}}$  is always below the maximum calculated  $k_{\text{eff}}$ , the following additional conservative assumptions are applied in the calculations with soluble boron.

- The pellet to clad gap is assumed to be flooded with pure, unborated water.
- The water above and below the active regions is assumed to be pure, unborated water.

The maximum  $k_{\text{eff}}$  for the bounding assembly in each class for this condition is listed in Table 6.1.4 in Section 6.1 of the Proposed *Rev. 1* of the FSAR.

### Confinement Evaluation

From a confinement perspective, the evaluation for the MPC-24 and MPC-24E are identical with the exception of the minimum free volume in the MPC cavity. The MPC-24E minimum free volume is slightly less than the MPC-24 due to increased thickness of the basket cell walls and the presence of more basket cell walls. This increases the concentration of radionuclides slightly due to the smaller dilution volume. The resultant doses from the MPC-24E are presented in FSAR Table 7.3.2 in proposed *Revision 1* of the FSAR and bound the doses from the MPC-24 (see Attachment 6).

### Proposed Change No. 20

Certificate of Compliance, Appendix A, Table 3-1 and Appendix B, Table 2.1-1

New Item V is added to the table for MPC-32.

#### **Reason for Proposed Change**

The MPC-32 allows users to place PWR fuel into dry storage using one third fewer casks due to its increased storage capacity over the MPC-24 and MPC-24E. Fewer casks to load decreases the probability of cask handling mishaps, reduces the overall occupational exposure for the fuel loading campaign, and reduces customer cost.

#### **Justification for Proposed Change**

The MPC-32 basket design is very similar to the previously approved BWR MPC-68. However, unlike the MPC-24 series PWR basket, no flux traps are used. As such, credit for soluble boron is taken in the MPC-32 criticality analyses for all authorized fuel enrichments. Two ranges of enrichment, with two separate minimum boron concentration requirements have been analyzed (see associated changes to Table 2.1-2 and Proposed Change Number 3). A detailed discussion of this change is provided below, arranged by technical discipline.

### Structural Evaluation

The structural analysis of the MPC-32 was considered in the initial versions of the HI-STAR TSAR (Docket 72-1008). The review of the structural analysis of the MPC-32 fuel basket was performed by the NRC staff and all structural questions from the NRC staff resolved. Prior to final approval of the HI-STAR TSAR, however, the MPC-32 basket was removed from the submittal to permit final resolution of some outstanding non-structural issues without a delay in the CoC

approval process. The MPC-32 was also removed from the HI-STORM FSAR submittal at the same time.

The re-introduction of the MPC, from a structural point of view, required only the addition back into the text and appendices previously reviewed calculations and results. To that end, all FSAR text, tables, and appendices have been reviewed and updated to include the MPC-32 input data and structural results. The finite element model of the MPC-32 fuel basket was originally prepared at the same time and in the same manner as the currently reviewed and approved MPC-24 and MPC-68 fuel baskets. The analyses of the MPC-32 fuel basket under applied inertia loads, simulating a handling accident was carried out to obtain stresses in the fuel basket structure and in the MPC shell. The safety factors, previously reviewed, after applying the appropriate dynamic amplifier, exceed 1.0 and are re-introduced into the FSAR document in the appropriate tabular form. Since the MPC-32 was (and still is) the heaviest MPC when fully loaded, there has been no change in the bounding loads used as input for other calculations. Appropriate text and tables in Section 3 of the FSAR have been updated to reflect the presence of this new fuel basket (see Attachment 6). The changes to the MPC-32 drawings as described in Section III of this attachment, were reviewed and found to be insignificant with respect to the structural evaluation. No new structural evaluations have been introduced into the FSAR as a result of restoring the MPC-32.

#### Thermal Evaluation

With respect to thermal performance, the MPC-32 design for PWR fuel is akin to the previously approved MPC-68 for BWR fuel in that the same general construction and the same heat rejection mechanisms are present. The thermal performance of the MPC-32 design has been evaluated, in support of this amendment, using the analysis methods employed to determine the performance of the previously approved MPC-24 and MPC-68. The substantial conservative assumptions embedded in the evaluations of the MPC-24 and MPC-68 designs have also been incorporated in the evaluations of the MPC-32. Allowable decay heat loads have been determined for design-basis (DB) intact Zircaloy and stainless steel clad fuel that ensure safe long-term storage of SNF in the MPC-32. The HI-STORM temperature field for the MPC-32 loaded with design-basis heat emitting fuel was calculated and is reported in proposed revisions to HI-STORM FSAR Chapter 4 (see Attachment 6). This analysis demonstrates substantial cladding thermal margins.

#### Shielding Evaluation

The MPC-32 was explicitly analyzed in Chapter 5 of the proposed *Revision 1* to the HI-STORM FSAR (see Attachment 6). The dose rates around the HI-STORM

overpack were conservatively analyzed at a burnup of 45,000 MWD/MTU and 5 year cooling for the MPC-32. Only the 100-ton HI-TRAC was analyzed with the MPC-32 since those dose rates bound the dose rates from the 125-ton HI-TRAC. The burnup and cooling times used for the HI-TRAC analysis are consistent with the burnup and cooling times specified in the proposed changes to the Approved Contents section of Appendix B to the CoC. Since the specified burnups and cooling times for the MPC-32 are considerably lower than the MPC-24, the MPC-24 was still used for the site-boundary evaluation to demonstrate compliance with 10CFR72.104. In addition, because of the differences in burnup and cooling times between the MPC-32 and the MPC-24, the radial dose rates from the MPC-24 are typically higher than for the MPC-32. Therefore, the MPC-24 was still used for the dose rate evaluations in Chapter 10.

Sections 5.1 and 5.4 of proposed *Revision 1* of the HI-STORM FSAR report the calculated dose rates for the MPC-32 and Section 5.2 reports the source terms used for the MPC-32 evaluations.

#### Criticality Evaluation

The MPC-32 is analyzed with credit for soluble boron present in the water during wet loading and unloading operations. Two soluble boron concentrations are used in the analysis, 1900 ppmb and 2600 ppmb. With a minimum soluble boron concentration in the water of 1900 ppmb, a maximum enrichment of 4.1 wt%  $^{235}\text{U}$  for all authorized fuel assembly array/classes is permissible. At 2600 ppmb, a maximum enrichment of 5.0 wt%  $^{235}\text{U}$  for all authorized fuel assembly array/classes is permissible. Consistent with the analysis for the MPC-24E, the following additional conservative assumptions are applied to ensure that the actual  $k_{\text{eff}}$  is always below the maximum calculated  $k_{\text{eff}}$ .

- The pellet to clad gap is assumed to be flooded with pure, unborated water.
- The water above and below the active regions is assumed to be pure, unborated water.

The maximum  $k_{\text{eff}}$  for the bounding assembly in each class for the two soluble boron levels is listed in Tables 6.1.5 and 6.16 in Section 6.1 of the Proposed *Rev. 1* of the FSAR (see Attachment 6).

#### Confinement Evaluation

The MPC-32 is explicitly analyzed in Chapter 7 of proposed *Revision 1* of the HI-STORM FSAR. The radionuclide inventories were conservatively calculated assuming the design basis assembly at a burnup of 70,000MWD/MTU at a 5 year cooling time. The fuel specifications in the Approved Contents section of

Appendix B to the CoC limit the fuel assembly burnup to well below 70,000 MWD/MTU for 5-years cooling time, ensuring that this inventory exceeds that of the actual fuel acceptable for loading into the MPC-32. The resultant doses are summarized in Table 7.3.3 of proposed *Revision 1* of the FSAR (see Attachment 6).

## **Proposed Change No. 21**

### **Certificate of Compliance, Appendix B, Table 2.1-1**

New Item VI is added to the table for MPC-68FF.

### **Reason for Proposed Change**

The MPC-68FF allows users to place BWR fuel debris into dry storage where this was previously not authorized beyond Dresden Unit 1 and Humboldt Bay Fuel. User feedback on fuel condition indicates that some fuel assemblies destined for dry storage would be classified as fuel debris in accordance with the CoC.

### **Justification for Proposed Change**

The MPC-68FF combines the thickened top portion of the previously approved MPC-68F shell with the maximized  $^{10}\text{B}$  loading in the Boral neutron absorbers of the standard MPC-68, to allow storage of a wide range of damaged BWR fuel or fuel debris, loaded into DFCs. A detailed discussion of this change is provided below, arranged by technical discipline.

### **Structural Evaluation**

With the exception of the thickened top portion of the MPC shell, the MPC-68FF is identical to the previously approved MPC-68F. The thickening of the MPC shell is limited to the closure lid region, and has already been evaluated for structural integrity and approved as part of the HI-STAR 100 Part 71 SAR.

### **Thermal Evaluation**

With the notable exception of the thickened top portion of the MPC shell, the MPC-68FF is identical to the previously approved MPC-68. The thickening of the MPC shell is limited to the closure lid region, and has no impact on the thermal performance of the MPC. The thermal performance of the MPC-68FF is, therefore, identical to that of the previously approved MPC-68.

### **Shielding Evaluation**

The MPC-68FF is identical to the MPC-68 from a shielding perspective. Therefore the analysis of the MPC-68, including damaged fuel, in Chapter 5 of proposed *Revision 1* of the HI-STORM FSAR is applicable for the MPC-68FF and no explicit analysis of the MPC-68FF is required.

#### Criticality Evaluation

The basket structure in the MPC-68FF is identical to the basket structure inside the MPC-68. More specifically, all dimensions relevant for the criticality analysis such as pitch, basket wall thickness and <sup>10</sup>B loading in the Boral are identical between MPC-68 and MPC-68FF. Therefore, all criticality results obtained for the MPC-68 are valid for the MPC-68FF and no further analyses are necessary. With regard to the analyses of damaged fuel and fuel debris, see Proposed Change No. 5, Holtec Generic BWR DFC.

#### Confinement Evaluation

The MPC-68FF confinement analysis is bounded by the evaluation of the MPC-68. The MPC-68FF has a larger MPC lid-to-shell weld, which is necessary for storage and transportation of fuel debris. The smaller MPC lid-to-shell weld in the MPC-68 conservatively overestimates the leakage rate from the MPC-68FF. Therefore, no separate explicit analysis of the MPC-68FF is required.

### Proposed Change No. 22

#### Certificate of Compliance, Appendix B, Table 2.1-1

New Item VII is added to the table for MPC-24EF.

#### **Reason for Proposed Change**

The MPC-24EF allows users to place PWR fuel debris into dry storage where this was previously not authorized. User feedback on fuel condition indicates that some fuel assemblies destined for dry storage would be classified as fuel debris in accordance with the CoC.

#### **Justification for Proposed Change**

The MPC-24EF combines the thickened top portion of the previously approved MPC-68F shell with the newly proposed optimized MPC-24E fuel basket arrangement, to allow storage of a wide range of damaged PWR fuel or fuel

debris, loaded into DFCs. A detailed discussion of this change is provided below, arranged by technical discipline.

#### Structural Evaluation

With the exception of the thickened top portion of the MPC shell, the MPC-24EF is identical to the proposed MPC-24E design discussed elsewhere in this section (Proposed Change No. 19). The thickening of the MPC shell is limited to the closure lid region, and has already been evaluated for structural integrity and approved as part of the HI-STAR 100 Part 71 SAR.

#### Thermal Evaluation

With the notable exception of the thickened top portion of the MPC shell, the MPC-24EF is identical to the proposed MPC-24E design discussed elsewhere in this section (Proposed Change No. 19). The thickening of the MPC shell is limited to the closure lid region, and has no impact on the thermal performance of the MPC. The thermal performance of the MPC-24EF is, therefore, identical to that of the previously approved MPC-24. The evaluations of thermosiphon (MPC convection) and high burnup fuel for the MPC-24E are applicable to the MPC-24EF.

#### Shielding Evaluation

The MPC-24EF is identical to the MPC-24E from a shielding perspective. Therefore the shielding evaluation for Proposed Change No.19 is applicable here.

#### Criticality Evaluation

The basket structure in the MPC-24EF is identical to the basket structure inside the MPC-24E. More specifically, all dimensions relevant for the criticality analysis such as pitch, basket wall thickness and  $^{10}\text{B}$  loading in the Boral are identical between MPC-24E and MPC-24EF. Therefore, all criticality results obtained for the MPC-24E are valid for the MPC-24EF and no further analyses are necessary. With regard to the analyses of damaged fuel and fuel debris, see Proposed Change No. 10, Holtec Generic PWR DFC.

#### Confinement Evaluation

The MPC-24EF confinement analysis is bounded by the evaluation of the MPC-24. The MPC-24EF has a larger MPC lid-to-shell weld, which is necessary for storage and transportation of fuel debris. The smaller MPC lid-to-shell weld in the MPC-24 conservatively overestimates the leakage rate from the MPC-24EF. Therefore, no separate explicit analysis of the MPC-24EF is required.

### **Proposed Change No. 23**

#### Certificate of Compliance, Appendix B, Table 2.1-2:

Table 2.1-2 is revised to indicate two ranges of enrichment for PWR fuel to be stored in the MPC-24, MPC-24E, and MPC-24EF, with and without soluble boron in the MPC water (see also Proposed Change Numbers 5, 19 and 22).

#### **Reason for Proposed Change**

This change is proposed to allow higher enriched PWR fuel to be stored in the MPC-24, MPC-24E, and MPC-24EF with credit taken for soluble boron in the MPC water during wet loading and unloading operations.

#### **Justification for Proposed Change**

##### Criticality Evaluation

The MPC-24, MPC-24E, and MPC-24EF are all analyzed with credit taken for the soluble boron present in the water during wet loading and unloading operations. With a minimum soluble boron concentration in the water of 400 ppmb in the MPC-24 or 300 ppmb in the MPC-24E and MPC-24EF, a maximum enrichment of 5.0 wt% <sup>235</sup>U for all authorized fuel assembly array/classes is permissible. To ensure that the actual  $k_{eff}$  is always below the maximum calculated  $k_{eff}$ , the following additional conservative assumptions are applied in the calculations with soluble boron.

- The pellet to clad gap is assumed to be flooded with pure, unborated water.
- The water above and below the active regions is assumed to be pure, unborated water.

The maximum  $k_{eff}$  for the bounding assembly in each class for this condition is listed in Tables 6.1.2 (MPC-24) and 6.1.4 (MPC-24E and MPC-24EF) in Section 6.1 of proposed *Revision 1* of the FSAR (see Attachment 6).

### **Proposed Change No. 24**

#### Certificate of Compliance, Appendix B, Tables 2.1-2 and 2.1-3

Notes at the end of Tables 2.1-2 and 2.1-3 are revised/added as shown in the attached marked-up pages of the CoC. Pointers to these notes in the tables are also revised accordingly.

- a. Note 3 in both tables is revised to clarify the intent.\*
- b. New Note 5 is added to Table 2.1-2.
- c. New Note 6 is added to Table 2.1-2.
- d. New Note 7 is added to Table 2.1-2
- e. Note 4 in Table 2.1-3 is revised to increase the allowable weight percent of U-235 in the MOX rods of fuel assembly array/class 6x6B from 0.612 to 0.635. This note is also clarified to state that the weight percentages are to be calculated based on the total fuel weight (i.e., uranium oxide plus plutonium oxide).\*
- f. Notes 6 and 7 in Table 2.1-3 are swapped.
- g. New Note 11 is added to Table 2.1-3.\*
- h. New Note 12 is added to Table 2.1-3.\*
- i. New Note 13 is added to Table 2.1-3.\*
- j. New Note 14 is added to Table 2.1-3.

#### **Reason for Proposed Changes**

- a. As currently worded, it is unclear whether implementation of the tolerance offered by Note 3 allows adjusting the documented value of the as-delivered uranium mass for a fuel assembly, or adjusting the uranium mass limit specified in the table for comparison against users' fuel records. The intent is to adjust the uranium mass limit up (within the prescribed tolerance), as necessary, for comparison against users fuel records. This eliminates a potential poor practice of users adjusting uranium mass values found on fuel records.
- b. This note is required to connect the enrichment level for PWR fuel to be loaded with the LCO for the required boron concentration in the MPC water.
- c. This note is necessary to recognize that this array/class (representing only the Indian Point Unit 1 fuel assembly) includes two different fuel rod pitches.

- d. This note is required due to the addition of damaged PWR fuel to the authorized contents.
- e. User feedback indicates that there are fuel assemblies with MOX rods containing less than 1.578 weight percent fissile plutonium in natural uranium. To bound this situation, the uranium content in the MOX rods is increased slightly. The second change to Note 4 is proposed to improve clarity regarding the intent of the note.
- f. These notes are swapped for consistency between the HI-STAR and HI-STORM for these same notes.
- g. New Note 11 is proposed in response to user feedback that some assemblies may include non-fuel rods which are filled with zirconium or an alloy of zirconium material in lieu of water.
- h. New Note 12 is proposed to be added for information on this new array/class.
- i. New Note 13 is proposed to address a situation for the 9x9E fuel assembly array/class where one assembly type in the class (SPC 9x9-5) contains rods of different dimensions within the array.
- j. New Note 14 addresses an issue related to the criticality analyses for stainless steel clad fuel from the LaCrosse plant.

#### **Justification for Proposed Changes**

- a. None. The tolerance in the mass limit allowed by this note is in the current, approved CoC.
- b. This note provides required logic for proper implementation of the CoC requirements.
- c. The Indian Point Unit 1 (IP-1) fuel assembly is unique and has been analyzed separately to account for the two different pitches. Only the IP-1 assembly fits into this array/class. The criticality analysis for the IP-1 fuel assembly is performed based on the actual configuration with different pitches in different sectors of the assembly. However, as this assembly class does not bound any assemblies other than the IP-1, the pitches are not listed in *the body of* Table 2.1-2.
- d. The addition of damaged fuel and fuel debris in the PWR MPC-24E and MPC-24EF requires that the maximum enrichment of all fuel assemblies

in the MPC be no greater than the maximum enrichment for the damaged fuel and fuel debris to preserve the assumptions of the criticality analyses. In the criticality analysis for damaged fuel in the generic PWR damaged fuel container, both intact and damaged fuel loaded into the same MPC are modeled at an enrichment of 4.0 wt%  $^{235}\text{U}$ . The results of the analysis demonstrates that this ensures compliance with the regulatory requirement of  $k_{\text{eff}} < 0.95$ . Therefore, limiting the maximum initial enrichment to 4.0 wt% for this loading situation is a requirement to ensure regulatory compliance.

- e. All criticality calculations for the 6x6B (MOX) fuel assembly array/class were re-performed (see proposed revised FSAR Table 6.2.38 in Attachment 6). The change in reactivity for this change is small (less than  $2\sigma$ ). This demonstrates that the maximum  $k_{\text{eff}}$  remains below 0.95 with the increased uranium concentration. The second change is proposed for clarity.
- f. Editorial.
- g. Replacing water with a non-fissile zirconium material will reduce the amount of moderator without increasing the amount of fissile material. This results in a decreased reactivity. This situation is comparable to the overall reduction of water density analyzed in Section 6.4.2.1 of the FSAR, which shows a decrease of reactivity with decreasing water density (i.e. decreasing the amount of water in the cask). The existing calculations assuming water in the water rods are therefore bounding for rods with non-fissile material in lieu of water.
- h. New fuel assembly array/class 8x8F represents a unique fuel assembly type known as the QUAD+. New Note 12 is proposed to describe the unique water rod features of this assembly.
- i. The SPC 9x9-5 fuel assembly is configured with two types of fuel rods having differing dimensions. Accordingly, the criticality analyses have been performed considering the varying fuel rod dimensions in the SPC 9x9-5 fuel type. Bounding all fuel rods in the assembly with one set of rod dimensions is not feasible because of excessive dimensional overlap.
- j. In the criticality analysis for damaged fuel in the generic BWR damaged fuel container, intact and damaged fuel/fuel debris loaded into the same MPC are modeled at enrichments of 3.7 wt%  $^{235}\text{U}$  (intact) and 4.0 wt%  $^{235}\text{U}$  (damaged/debris). The results of the analysis demonstrate that this ensures compliance with the regulatory requirement of  $k_{\text{eff}} < 0.95$ . Therefore, limiting the maximum initial enrichment of the intact fuel to

3.7 wt% for this loading situation is a requirement to ensure the assumptions of the criticality analyses are preserved.

### **Proposed Change No. 25\***

#### **Certificate of Compliance, Appendix B, Tables 2.1-2 and 2.1-3 :**

The maximum allowed design initial uranium masses for selected fuel assemblies are increased as shown in the marked-up CoC tables. This affects PWR fuel assembly array/classes 14x14A, 14x14B, 14x14C, 15x15A, 16x16A, 17x17A, 17x17B, and 17x17C in Table 2.1-2 and BWR fuel assembly array/classes 6x6A, 6x6B, 6x6C, 8x8B, 8x8C, 8x8D, 8x8E, 9x9A, 9x9B, 9x9C, 9x9D, 9x9E, 9x9F, 10x10A, 10x10B, and 10x10C in Table 2.1-3.

#### **Reason for Proposed Changes**

To respond to user feedback describing certain fuel assemblies which have uranium masses slightly above the specified limit (including the tolerance allowed by Note 3 included with Tables 2.1-2 and 2.1-3) for the applicable fuel assembly array/class. These changes are required to ensure users can load all of the fuel they plan to place into dry storage.

#### **Justification for Proposed Changes**

##### **Structural Evaluation**

There is no effect on the existing structural evaluation. The increased uranium masses do not cause an increase in the overall assembly weight limits in the CoC. These weights (or greater) were used in the structural evaluation. Since the allowed assembly weights are not being changed, the structural evaluation is unaffected.

##### **Thermal Evaluation**

There is no effect on the existing thermal evaluation. This is because the allowed heat load for the cask is computed based on the heat transfer characteristics of the cask system and permissible peak cladding temperatures. The increase in uranium mass does not impact any assumption made in determining the heat transfer characteristics of the cask system.

### Shielding Evaluation

The uranium mass limit is a value that is determined from the shielding analysis. An increase in the mass of uranium will result in an increase in the neutron and gamma source term and decay heat load for a specified burnup and cooling time. The current CoC developed from the analyses in *Revision 0* of the HI-STORM FSAR provides some margin between the analyzed mass of uranium and the approved mass of uranium as listed in the CoC. The allowable burnup and cooling times in the CoC were developed by comparing the calculated decay heat for the design basis assemblies to the allowable decay heat load as determined in the thermal analysis. The decay heat values that are compared against the limits were calculated using the mass of uranium listed in Chapter 5 of the HI-STORM FSAR for the design basis fuel assemblies. Since a lower mass of uranium will result in a lower decay heat, it is conservative, and provides margin, to specify the allowable mass of uranium in the current CoC for the design basis fuel assemblies (B&W 15x15 and 7x7) lower than the values analyzed in FSAR Chapter 5.

As discussed in Section 5.2.5 of the HI-STORM FSAR *Revision 0*, the design basis assembly was chosen by comparing the source terms for many different types of assemblies. All of the assemblies were shown to have a lower source term than the design basis fuel assemblies. For additional conservatism, the mass of uranium specified in the current CoC for these non-design basis fuel assemblies is also specified lower than the mass used in the comparison in Chapter 5 of FSAR *Revision 0*. This level of conservatism is unnecessary since the decay heat load used to determine the allowable burnup and cooling times for all assemblies was the decay heat load from the design basis fuel assemblies. Therefore, there was already a significant amount of conservatism for the non-design basis fuel assemblies included by using the design basis decay heat to determine the allowable burnup and cooling times. Section 5.2.5.3 of *Revision 0* of the HI-STORM FSAR provides an indication of the level of conservatism associated with using the design basis decay heat for the non-design basis fuel assemblies.

The proposed change in the CoC is to increase the mass of uranium for the non-design basis fuel assemblies up to the value that was used in the analysis in Chapter 5 of the HI-STORM FSAR to determine the design basis fuel assembly. In order to permit a slightly larger increase in the uranium mass loadings relative to *Revision 0* of the HI-STORM FSAR, the analysis in Sections 5.2.5.2 and 5.2.5.3, specifically Tables 5.2.26 and 5.2.28, has been modified to use a slightly larger uranium mass loading for the 8x8, 9x9, and 10x10 assemblies. As mentioned above, this change eliminates unnecessary over-conservatism while still maintaining a significant degree of conservatism and margin for the non-design basis fuel assemblies. The design basis fuel assemblies and the allowable mass loading for the design basis fuel assemblies remains unchanged. Therefore, the proposed change does not affect the shielding analysis presented in *Revision 0*

of the HI-STORM FSAR. Additional clarification has been added to the proposed *Revision 1* of the HI-STORM FSAR to discuss this issue (see Attachment 6).

#### Criticality Evaluation

The criticality analyses are not affected by the proposed changes to the maximum allowed design uranium masses shown in the Certificate of Compliance (CoC). The uranium mass limits in the CoC are determined from the shielding analysis, and are specified as bounding values for groups of fuel classes (e.g. all B&W 15x15). The criticality analyses are based on an independent bounding assumption of a fuel stack density of 96.0% of the theoretical fuel density of 10.96 g/cm<sup>3</sup>. The fuel stack density is approximately equal to 98% of the pellet density. Therefore, while the pellet density of some fuels might be slightly greater than 96% of theoretical, the actual stack density will be less. For some fuel classes, this density assumption results in a uranium mass for the criticality analyses that is below the value shown in the CoC. However, this only indicates the conservatism of the shielding analysis for these classes. The criticality analyses are still valid and bounding for all classes, due to the density assumption stated above, which is valid for current and future fuel assemblies.

#### Confinement Evaluation

As described in the shielding evaluation, the values of uranium mass used in the shielding analyses have not changed. These proposed changes simply increase the allowed uranium masses for non-design basis fuel assemblies to those used in the analysis for the design basis fuel assembly. The source terms used in the confinement analyses were taken from the design basis source terms used in the shielding analyses. Therefore, the existing confinement evaluation is still bounding for the proposed new uranium mass limits.

#### **Proposed Change No. 26\***

##### Certificate of Compliance, Appendix B, Tables 2.1-2 and 2.1-3:

Certain fuel assembly parameter limits are revised as shown in the attached marked-up CoC tables. This affects PWR fuel assembly array/class 14x14C in Table 2.1-2 and BWR fuel assembly array/classes 6x6A, 6x6B, 7x7A, 7x7B, 8x8A, 8x8B, 8x8D, 9x9B, 9x9D, 9x9E, 9x9F, and 10x10C in Table 2.1-3.

## **Reason for Proposed Changes**

To respond to user feedback describing certain fuel assemblies that have parameters outside of the limits in the existing CoC Tables. These changes are required to ensure users can load all of the fuel they plan to place into dry storage.

## **Justification for Proposed Changes**

### Structural Evaluation

The proposed changes to fuel parameter limits for some of the existing fuel assembly array/classes have no impact on the structural evaluation because the design basis weights used in the analyses (and provided as limits elsewhere in the CoC) are not changed, the design basis temperatures are not changed, and the geometry of the fuel assemblies (also limited by the CoC) are not changed.

### Thermal Evaluation

The active fuel length for array/classes 6x6A and 6x6B is proposed to be increased to 120 inches to bound an earlier variant of Dresden-1 fuel. Among the fuel assemblies included in the 6x6A array/class, one particular fuel type was determined to be fabricated with a thinner cladding (0.026 in.) relative to other fuel in this class (minimum 0.030 in. cladding). In the 7x7A array/class of fuel assemblies, minor adjustments to the fuel parameters<sup>4</sup> was necessary to bound Humboldt Bay fuel. Changes to the 7x7B and 8x8B array/classes were necessary to bound the fuel types at Oyster Creek plant. Accordingly, the thermal analyses for these fuel types were evaluated in support of this amendment and additional analyses performed, as required.

A review of the Oyster Creek fuel parameters against the fuel parameters of other fuel types in the same array/classes has revealed no significant differences. The Oyster Creek 7x7 fuel rod mechanical parameters are identical to an existing member of the 7x7B class. The relatively larger pellet diameter (from 0.491 vs. 0.488 in) necessitates an adjustment to the uranium weight limit for this array/class. The Oyster Creek 8x8 fuel rod diameter is slightly larger than other members in the 8x8B class and has a thicker cladding.

An 8x8 fuel assembly used at Browns Ferry and a 9x9 fuel assembly from Grand Gulf, have been evaluated in support of this amendment request to modify the BWR fuel parameters. Likewise, a Millstone Unit 2 14x14 fuel assembly has been evaluated to support modification of the PWR fuel tables. As explained below, these PWR and other BWR fuel have been evaluated in accordance with

---

<sup>4</sup> Cladding thickness change from 0.033 inch to 0.0328 inch and active fuel length from 79 in to 80 in.

the NRC-approved HI-STORM thermal analysis methodologies to confirm that the HI-STORM 100 temperature field is bounded by the design basis analyses.

The overall HI-STORM thermal analysis methodology is partitioned into two evaluations. The first evaluation pertains to determining the appropriate peak cladding temperature limits for long term dry storage for each proposed fuel type. For this purpose, theoretical bounding rod gas pressures for the PWR and BWR classes of fuel are employed. In the second evaluation, the temperature field in the HI-STORM 100 cask is computed and the resulting cladding temperatures demonstrated to be below the respective temperature limits. The analytical evaluations for BWR fuel are further sub-divided in two groups of fuel assemblies classified as Low Heat Emitting (LHE) fuel assemblies and Design Basis (DB) fuel assemblies. The LHE fuel assemblies are characterized by low burnup, long cooling time and short active fuel lengths. Consequently, their heat loads are dwarfed by the full active length DB fuel assemblies. The additional Dresden-1 and Humboldt Bay fuel assemblies in the 6x6A and 7x7A array/classes belong to the LHE group of fuel, while the additional Oyster Creek, Browns Ferry, and Grand Gulf fuel assemblies are included in the DB group.

In accordance with the PNL-6189 methodology, peak fuel cladding temperature limits are specified as a function of cladding stress and age of fuel. The cladding stress calculations for the additional fuel are documented in proposed revised FSAR Tables 4.3.2, 4.3.3, 4.3.5 and 4.3.6 in Attachment 6 to this letter. The cladding stress in the additional DB fuel types is bounded by the limiting cladding stress computed previously. An adjustment to the 10x10 SVEA-96 fuel parameters (an O.D. change by 0.001 inch) is insignificant for the cladding stress evaluation as it is bounded by the design basis cladding stress. Consequently, the age-dependent peak fuel cladding temperature limits do not require changes to accommodate the additional fuel. For the LHE fuel group, the thin-clad Dresden-1 fuel type is determined to be the limiting fuel resulting in a downward shift in the applicable fuel cladding temperature limit. The revised temperature limits for LHE and DB fuel are summarized in proposed revised FSAR Tables 4.3.7 and 4.3.8.

The second evaluation pertaining to computation of the HI-STORM 100 cask temperature field is functionally dependent upon the effective conductivity of fuel assemblies loaded in the MPC-68 fuel cells. The LHE fuel assemblies are further analyzed under the assumption that they are loaded while encased in stainless steel DFCs. Due to interruption of radiation heat exchange between the fuel assembly and the fuel basket by the DFC boundary, this configuration is bounding for the thermal evaluation. Two DFC designs are evaluated - a previously approved Holtec design (FSAR Figure 2.1.1) and an existing TN/D-1 DFC in which some of the Dresden-1 fuel is currently stored (FSAR Figure 2.1.2) (see Proposed Change Number 5). The most resistive fuel assembly determined by

analytical evaluation is considered for the HI-STORM 100 cask thermal evaluation. The results of the evaluation of additional fuel types performed in support of this amendment request are summarized in proposed revised Table 4.4.6 for LHE and DB fuel (see Attachment 6).

In both groups investigated, the thermal conductivity of the additional fuels is bounded by the limiting fuel types in each group. For the DB group of fuel assemblies, it is shown that the peak cladding temperature limits for the limiting fuel type adequately cover the additional fuel. The most resistive fuel characteristics also bound the additional fuel in the list of DB fuel types authorized for storage in the HI-STORM 100 System. Thus, the design basis thermal analysis envelopes the HI-STORM 100 System thermal response when loaded with the additional BWR and PWR fuel. For the LHE group of assemblies, the low decay heat load burden on the HI-STORM 100 cask (~ 8kW) guarantees large thermal margins to permit safe storage of Dresden-1 and Humboldt Bay fuel. Nevertheless, a conservative analysis was performed and is described in the proposed *Revision 1* FSAR and the temperature field determined and reported Subsection 4.4.1.1.13 (see Attachment 6).

#### Shielding Evaluation

The accuracy of the shielding analysis is dependent upon the calculation of the radiation source term. The source term is dependent on the mass of uranium in the fuel assembly. For a specified burnup and cooling time, the radiation source term will increase as the mass of uranium increases (this is addressed in Proposed Change Number 25). The minor changes proposed for the dimensions of the fuel assembly array/classes will have a negligible impact on the radiation source term. Since the allowable uranium mass loadings are not being changed as a result of these changes in dimensions, it is concluded that these changes will have a negligible effect of the shielding analysis and therefore are not explicitly considered in *Revision 1* of Chapter 5 of the HI-STORM FSAR.

#### Criticality Evaluation

For the criticality evaluation, the fuel assemblies are grouped into assembly array/classes. The proposed CoC modifications to fuel assemblies already included are reflected in proposed revised FSAR Table 6.2.1 (see Attachment 6). For each assembly array/class, a theoretical bounding assembly is defined. The characteristics of the bounding assembly for each affected array/class was amended to reflect the additional fuel types within an array/class.

Criticality calculations were performed for the changed fuel types and the bounding assembly in each array/class to account for the modified dimensions. Table 26.1 below shows the comparison between the maximum  $k_{eff}$  for each of

the affected array/classes and the corresponding current values (i.e. FSAR *Rev. 0*). The FSAR table number containing the detailed results is also listed. The comparison demonstrates that, apart from the 10x10C assembly class, the maximum  $k_{eff}$  of each affected class only changes slightly as a result of the changes in the fuel assembly characteristics.

For the 10x10C assembly class, the changes are larger due to a change in the material of the internal structures (water tubes) inside the assembly. The initial calculation assumed stainless steel for these structures, whereas the actual material is a zirconium alloy. This results in an increase in reactivity, as the zirconium alloy shows a lower neutron absorption compared to stainless steel. Additionally, some dimensions in the model (Channel ID and sub-assembly spacing) deviated from the fuel manufacturers specification available for this assembly. Adjustment of these values leads to an additional small reduction in reactivity. Overall, for the same initial planar average enrichment of 4.2 wt%  $^{235}U$ , the reactivity of this assembly increases, but still remains below 0.95. Therefore, with the proposed changes, the cask system is still in compliance with the regulatory requirement of  $k_{eff} < 0.95$  for all authorized fuel assembly array/classes.

**Table 26.1**  
**Comparison of Maximum  $k_{eff}$  for FSAR Rev. 0 and Proposed Rev. 1**

<b>Assembly Array/Class</b>	<b>Maximum <math>k_{eff}</math> FSAR Rev. 0</b>	<b>Table Number in FSAR Rev. 0</b>	<b>Maximum <math>k_{eff}</math> FSAR Proposed Rev. 1</b>	<b>Table Number in Proposed Rev. 1 of the FSAR</b>
6x6A	0.7602	6.2.35	0.7888	6.2.41
6x6B	0.7611	6.2.36	0.7824	6.2.42
7x7A	0.7973	6.2.38	0.7974	6.2.44
7x7B	0.9375	6.2.19	0.9386	6.2.23
8x8A	0.7685	6.2.39	0.7697	6.2.45
8x8B	0.9368	6.2.20	0.9416	6.2.24
8x8D	0.9366	6.2.22	0.9403	6.2.26
9x9B	0.9388	6.2.25	0.9436	6.2.30
9x9D	0.9392	6.2.27	0.9394	6.2.32
9x9E	0.9406	6.2.28	0.9401	6.2.33
9x9F	0.9377	6.2.29	0.9401	6.2.34
10x10C	0.8990	6.2.32	0.9433	6.2.38
14x14C	0.9361	6.2.6	0.9400	6.2.8

Confinement Evaluation

There is no effect of these proposed changes on the confinement evaluation because the source terms used in the confinement analysis are not changed.

**Proposed Change No. 27**

**Certificate of Compliance, Appendix B, Tables 2.1-2 and 2.1-3:**

Four new fuel assembly array/classes, 14x14E and 15x15H\* (PWR); and 8x8F\* and 9x9G (BWR) are added to Appendix B, Tables 2.1-2 and 2.1-3, respectively, as shown in Tables 27.1 and 27.2 below and in the attached marked-up CoC tables. Items II.A.1.d and e and Items VI.a.1.d and e in Table 2.1-1 are also revised to add separate decay heat, cooling time, and burnup limits for the 8x8F array/class (QUAD+ assembly).

**Table 27.1  
 New PWR Fuel Assembly Array/Classes 14x14E and 15x15H**

Fuel Assembly Array/Class	14x14E	15x15H
Clad Material	SS	Zr
Design Initial U (kg/assy.)	≤ 206	≤ 475
Initial Enrichment (wt % <sup>235</sup> U)		
MPC-24 without soluble boron credit	≤ 5.0	≤ 3.8
MPC-24E/24EF without soluble boron credit	≤ 5.0	≤ 4.2
Any PWR MPC with soluble boron credit	≤ 5.0	≤ 5.0
No. of Fuel Rod Locations	173	208
Fuel Clad O.D. (in.)	≥ 0.3145	≥ 0.414
Fuel Clad I.D. (in.)	≤ 0.3175	≤ 0.3700
Fuel Pellet Dia. (in.)	≤ 0.3130	≤ 0.3622
Fuel Rod Pitch (in.)	0.441 and 0.453	≤ 0.568
Active Fuel Length (in )	≤ 102	≤ 150
No. of Guide and/or Instrument Tubes	0	17
Guide/Instrument Tube Thickness (in.)	N/A	≥ 0.0140

**Table 27.2**  
**New BWR Fuel Assembly Array/Classes 8x8F and 9x9G**

Fuel Assembly Array/Class	8x8F	9x9G
Clad Material	Zr	Zr
Design Initial U (kg/assy.)	≤ 191	≤ 179
Maximum PLANAR-AVERAGE INITIAL ENRICHMENT (wt.% <sup>235</sup> U)	≤ 4.0	≤ 4.2
Initial Maximum Rod Enrichment(wt.% <sup>235</sup> U)	≤ 5.0	≤ 5.0
No. of Fuel Rod Locations	64	72
Fuel Clad O.D. (in.)	≥ 0.4576	≥ 0.4240
Fuel Clad I.D. (in.)	≤ 0.3996	≤ 0.3640
Fuel Pellet Dia. (in.)	≤ 0.3913	≤ 0.3565
Fuel Rod Pitch (in.)	≤ 0.609	≤ 0.572
Design Active Fuel Length (in.)	≤ 150	≤ 150
No. of Water Rods	N/A	1
Water Rod Thickness (in.)	≥ 0.0315	≥ 0.320
Channel Thickness (in.)	≤ 0.055	≤ 0.120

### Reason for Proposed Changes

Based on user feedback, additional fuel assemblies were identified that did not fit into any of the existing fuel assembly array/classes. Four new assembly array/classes are required to assure all user fuel types can be loaded. The 14x14E array/class represents only Indian Point Unit 1 fuel. The 15x15H includes the B&W Mark B11 fuel design. The 8x8F represents only the "QUAD+" assembly. The 9x9G array/class represents the ANF-9X fuel assembly.

### Justification for Proposed Changes

#### Structural Evaluation

The addition of new fuel types permitted to be stored in the HI-STORM 100 System can have an effect on the structural analyses performed in Chapter 3 if, and only if, one or more of the following occurs because of the new fuel types:

1. The design basis weights of 700 lbs (BWR) or 1680 lbs. (PWR), including non-fuel hardware, channels, and DFCs, as applicable, are exceeded.

2. The design basis temperatures are exceeded because of the presence of the new fuel types.
3. The lengths of the new fuel assemblies cause an increase in the length of the Holtec fuel spacers.

Section 3.0 of the HI-STORM FSAR contains a compliance matrix showing how the structural review requirements of NUREG 1536 have been satisfied by the totality of analyses currently reviewed and reported in Chapter 3. To ascertain whether any of the proposed amendment items require a re-visiting of any or all of the currently approved analyses reported in Chapter 3, the Compliance Matrix was reviewed and the following conclusions reached.

1. The weights of the proposed new fuel types do not exceed the limiting (i.e., design basis) weights specified in Table 2.1-1 of Appendix B to the CoC. Therefore, no structural analysis currently approved needs to be re-visited.
2. The design basis temperatures of all components have not exceeded the values currently licensed. Therefore, no structural analyses or free thermal expansion analyses currently approved needs to be revisited.
3. The lengths of the proposed new fuel types are longer than the minimum length of the fuel assemblies currently approved for the HI-STORM 100. Therefore, the fuel spacer stability analysis in the FSAR remains bounding. The lengths of the proposed new fuel types are also less than the maximum lengths specified in Table 2.1-1 of Appendix B to the CoC.

#### Thermal Evaluation

The Indian Point Unit 1, B&W Mark B11, QUAD+, and ANF-9X fuel types have been evaluated along with the changes to the existing 8x8 and 15x15 fuel assembly array/classes as described in Proposed Change No. 26 above.

The B&W Mark B11 and ANF-9X fuel assemblies are bounded by the existing design basis thermal analyses. The QUAD+ fuel assembly is included in the LHE group of BWR fuel assemblies and has been found acceptable for safe storage in proposed *Revision 1* of the HI-STORM FSAR Subsection 4.4.1.1.13. The Indian Point Unit 1 fuel assembly is included in the stainless steel group of PWR fuel assemblies and has been found acceptable for safe storage in proposed *Revision 1* of the HI-STORM FSAR Subsection 4.4.1.1.13.

Shielding Evaluation

The accuracy of the shielding analysis is dependent upon the calculation of the radiation source term. The source term is dependent on the mass of uranium in the fuel assembly. For a specified burnup and cooling time, the radiation source term will increase as the mass of uranium increases. Minor variations in the dimensions of a fuel assembly will have a negligible impact on the radiation source term if the mass of uranium remains constant. The additional fuel assemblies proposed for the CoC are not significantly different than the currently licensed fuel assemblies to require an assembly-specific source term calculation. These new fuel assemblies are bounded by the current design basis fuel assemblies. In addition, the allowable uranium mass loadings for these new fuel assemblies is specified consistent with similar fuel assemblies in the CoC thereby assuring that these assemblies are bounded by the current design basis fuel assemblies. Therefore, these additions will have a negligible effect on the shielding analysis and therefore are not explicitly considered in proposed *Revision 1* of Chapter 5 of the HI-STORM FSAR.

Criticality Evaluation

Criticality calculations were performed for all four new fuel array/classes. The results for these classes in the MPC-24 and MPC-68 are summarized in Table 27.3 below. The two PWR assemblies (14x14E and 15x15H) are also permitted in the MPC-24E, MPC-24EF, MPC-32 and the MPC-24 with credit for soluble boron. Maximum  $k_{eff}$  values for these baskets are similar to the values listed in Table 21.3 below, and can be found in Tables 6.1.2 through 6.1.6 in Section 6.1 of the Proposed *Rev. 1* of the FSAR (see Attachment 6). For all new PWR and BWR fuel assemblies, the maximum  $k_{eff}$  is below 0.95. Therefore, with the proposed changes, the cask system is still in compliance with the regulatory requirement of  $k_{eff} < 0.95$  for all authorized fuel assembly array/classes.

**Table 27.3**  
**Maximum  $k_{eff}$  for new PWR and BWR Fuel Assembly Array/Classes**

Fuel Assembly Array/Class	Basket Type	Maximum $k_{eff}$	Table Number in Proposed <i>Rev. 1</i> of the FSAR
14x14E	MPC-24	0.7715	6.2.10
15x15H	MPC-24	0.9411	6.2.18
8x8F	MPC-68/68FF	0.9411	6.2.28
9x9G	MPC-68/68FF	0.9309	6.2.35

### Confinement Evaluation

The source terms used for the existing confinement analysis bound those of the new fuel assembly array/classes. Therefore, there is no impact on confinement.

### **Proposed Change No. 28**

#### Certificate of Compliance, Appendix B, Approved Contents, Tables 2.1-4 through 2.1-7:

The per-assembly limits on fuel burnups, cooling time, and decay heat have been modified to reflect thermosiphon (convection inside the MPC) heat transfer and to allow loading of high burnup fuel (> 45,000 MWD/MTU) into the MPC.

#### **Reason for Proposed Changes**

To take appropriate account for a naturally-occurring method of heat transfer inside the MPC vessel that was previously not credited. User feedback indicates a growing inventory of fuel burned to greater than 45,000 MWD/MTU that must be authorized for loading into dry storage casks.

#### **Justification for Proposed Changes**

##### Structural Evaluation

The thermosiphon effect inside the MPC (now included in Chapter 4 thermal evaluations) results in an alteration in the MPC/overpack temperature distributions. The free thermal expansion evaluations, summarized in Subsection 3.4.4.2.1 for the "hot" MPC in HI-STORM or HI-TRAC and in Subsection 3.4.5 for the "hot" MPC inserted into a "cold" overpack have been revisited using the new temperature distributions from Chapter 4. The summary tables have been updated and the applicable appendices showing detailed calculations (Appendices 3.U, 3.V, 3.W, 3.I, 3.AF, and 3.AQ) have been revised to reflect the new temperatures. The revised calculations continue to demonstrate that there is no restraint of free thermal expansion between the fuel basket and the MPC canister, and between the MPC and the HI-STORM or HI-TRAC overpacks.

##### Thermal Evaluation

In the previous HI-STORM licensing analyses, the thermal models were run with the MPC internal convection heat transfer completely suppressed. Benchmarking studies performed by Holtec on full-size cask data and submitted to the NRC as a topical report showed that a complete neglect of the thermosiphon effect has the result of grossly over-predicting the peak fuel cladding temperature by as much as

200°F. Recent independent work performed by PNNL on the thermal simulation of the HI-STORM 100 System using the COBRA-SFS code has confirmed large conservatisms in the peak cladding temperature results of the current HI-STORM 100 thermal model that does not recognize internal convection in the honeycomb basket-equipped MPC. Including MPC internal convection heat dissipation in the HI-STORM 100 thermal models is found to yield conservative results when compared with the full-scale cask data. However, the extent of the conservatism is not inordinately large.

Accordingly, in the revised thermal model, the effect of internal convection is incorporated. However, to impute added conservatism, the conduction heat transfer contribution of the "aluminum heat conduction elements" (located in the peripheral spaces between the fuel basket and the MPC wall) is neglected. A detailed discussion of the revised thermal model is included in the proposed Chapter 4 FSAR *Revision 1* changes.

#### Shielding Evaluation

The shielding evaluation in Chapter 5 has been revised to reflect the increased permissible heat loads and the increased burnups beyond 45 GWD/MTU. The increased heat loads result in a decreased cooling time for a specific burnup. The increased heat loads in conjunction with higher burnups result in increased dose rates around the HI-STORM 100 System including the HI-TRAC transfer casks. These dose rates are evaluated in Chapter 5 and their effect on occupational exposure are evaluated in Chapter 10. As a result of the increased dose rates, the dose rate limits specified in the LCOs have been increased (see Proposed Change Nos. 3 and 4). While the dose rates and occupational exposure both increased, the HI-STORM 100 system is still in compliance with 10CFR72.104 and 10CFR72.106. The increases in the very conservatively estimated occupational exposures do not pose an ALARA concern, as the user may employ various forms of temporary shielding to reduce the dose rates.

#### Criticality Evaluation

All criticality analyses are performed assuming fresh fuel, i.e. no credit is taken for the reduction in reactivity due to the burnup of the fuel. An increase of the allowable fuel burnup will therefore increase the inherent safety margin in the criticality evaluation and no further analyses are necessary.

#### Confinement Evaluation

The confinement evaluation has been modified to account for the increased fuel burnup limits per-assembly. The source terms for the MPC-24, MPC-24E, MPC-24EF, MPC-32, MPC-68 and MPC-68FF have been chosen to ensure that a

bounding inventory is chosen for determining the dose due to a leak in the confinement boundary. The inventory for the MPC-24, MPC-24E, MPC-24EF and MPC-32 was conservatively based on the B&W 15x15 fuel assembly with a burnup of 70,000 MWD/MTU, 5 years of cooling time, and an enrichment of 4.8%. The inventory for the MPC-68 and MPC-68FF was based on the GE 7x7 fuel assembly with a burnup of 60,000 MWD/MTU, 5 years of cooling time, and 4.4% enrichment. The CoC limits the fuel assembly burnup below 60,000 MWD/MTU for both BWR and PWR fuel at 5 years of cooling time. This ensures that the inventory used in this calculation exceeds that of the fuel authorized for storage. Additionally, the leakage rate for normal, off-normal and hypothetical accident conditions has been updated to reflect the increased MPC pressure and temperature.

For storage of spent fuel assemblies with burnups in excess of 45 GWD/MTU the source term from the assumed rod breakage fractions of ISG-5 were augmented by the source term from 50% of the rods having peak cladding oxide thicknesses greater than 70 micrometers. *ISG-15* recommends that for high burnup fuel assemblies the releasable source term from ISG-5 for normal and off-normal conditions be increased by an additional factor. Therefore, the source term available for release has been revised from 1.0% to 2.5% for normal conditions and from 10.0% to 11.5% for off-normal conditions.

Additionally, the confinement analysis has incorporated the assumption that only 10% of the fines released to the MPC cavity from a cladding breach remain airborne long enough to be available for release from the MPC. It is conservatively assumed that 100% of the volatiles, crud and gases remain airborne and available for release.

### **Proposed Change No. 29**

#### **Certificate of Compliance, Appendix B, Design Features Section 3.2:**

New design features important for criticality control are added for the MPC-24E, MPC-24EF, MPC-68FF and the MPC-32.

#### **Reason and Justification for Proposed Changes**

These changes are conforming changes in support of the addition of these MPC models to the CoC. The values for Boron-10 loading and flux trap size are consistent with their respective design drawings, including tolerances.

**Proposed Change No. 30\***

**Certificate of Compliance, Appendix B, Table 3-1:**

The entry in the "Exception, Justification & Compensatory Measures" column for the exception to Code Section NB-5230 for the closure ring, vent, and drain cover plate welds is clarified as shown in the attached marked-up CoC table to recognize welds which may be single pass welds.

**Reason for Proposed Change**

To provide clarification and as a conforming change to a proposed drawing change (see *Attachment 5*).

**Justification for Proposed Change**

Small welds, such as 1/8 inch will likely be completed in one pass, with no root.

**Proposed Change No. 31**

**Certificate of Compliance, Appendix B, Design Features Section 3.4.3:**

Revisions are made to these requirements to distinguish between free-standing casks and casks for deployment in high seismic regions.

**Reason for Proposed Changes**

Under the current CoC, the seismic acceleration limits for free-standing casks do not envelop the seismic spectra for plants located in so-called "high seismic" regions. The new overpack variant called HI-STORM 100A is designed for use at ISFSIs in high seismic regions. The key design features proposed to be included in the CoC are essential for ensuring deployment of the HI-STORM 100A System is performed within the design and analysis basis for the system.

**Justification for Proposed Changes**

This is purely a structural design issue. The thermal, shielding, criticality, and confinement evaluations are unaffected by these design changes. The details of the structural evaluation may be found in the proposed Chapter 3 FSAR revisions in Attachment 6.

**Proposed Change No. 32\***

Certificate of Compliance, Appendix B, Design Features Section 3.4.6:

Re-format and revise Design Features Section 3.4.6 to remove the specific ISFSI pad and subgrade design parameters and to distinguish between free-standing overpacks and the HI-STORM 100A. New Design Features Sections 3.4.6.a and 3.4.6.b establish ISFSI pad requirements for the free-standing and HI-STORM 100A overpacks, respectively, as shown in the attached marked-up CoC pages.

**Reason for Proposed Change**

The current CoC requires that all ISFSI pads be designed to meet a single set of design parameters, including pad thickness, concrete compressive strength, reinforcing bar yield strength, and subgrade modulus of elasticity. This proposed change allows the necessary flexibility for utility licensees to design their ISFSI pads according to their site-specific needs and geological characteristics.

**Justification for Proposed Change**

The deceleration limit of 45-g's for the HI-STORM 100 System provides assurance that the cask system, including contents, will remain intact and retrievable after a postulated drop event and non-mechanistic tipover event. Therefore, the 45-g deceleration limit is the appropriate safety limit to be included in the CoC, while the specific pad design parameters may be left to the discretion of the general licensee. Any site-specific drop and tipover analyses are required to be performed in accordance with the methodologies described in the HI-STORM FSAR.

To assist the licensee in designing their ISFSI pad, Holtec has added a second set of "pre-approved" ISFSI pad and subgrade design parameters to FSAR Table 2.2.9. These design parameters were developed using the approved FSAR methodologies for cask drop and tipover analyses. Licensees may choose to design their ISFSI pads using either the Set "A" or Set "B" ISFSI pad and subgrade design parameters in FSAR Table 2.2.9, or design their own pad. Any ISFSI pad design is acceptable provided it is a structurally competent pad for which cask deceleration limits are shown to be met (if required).

## SECTION II – PROPOSED CHANGES TO THE FSAR

Nearly all of the proposed FSAR changes included in Attachment 6 are in support of CoC changes discussed in Section I. The changes to Chapters 3 through 7 are referred to in the technical justifications in Section I, as required, and are not listed again as changes here in Section II. However, several FSAR changes have also been included in this LAR for NRC review due to their overall magnitude or potential significance. These changes are listed below by subject (e.g., HI-STORM 100S) or grouped by Chapter. Throughout the proposed *Rev. 1* FSAR, text revisions may be found that correct editorial inconsistencies or support other changes not proposed for NRC review and approval (i.e., are being processed under 10 CFR 72.48). These text revisions are left in the chapter sections provided with this submittal for continuity of the chapter content by our chapter authors and are not proposed as changes requiring NRC review and approval.

In summary, if a FSAR change is not referred to from the change justifications in Section I or explicitly listed below, we intend to process the change under 10 CFR 72.48 and NRC review and approval is not requested as part of this LAR. Further, some of the changes below which are submitted for NRC approval may be implemented under 10 CFR 72.48 in parallel with NRC review to meet users' needs (i.e., *HI-STORM 100S, without the outlet air ducts rotated*).

### Proposed Change No. 33

#### HI-STORM 100S

The text, tables, and figures are revised throughout the FSAR and new licensing drawing 3669 (including a Bill-of-Material) (is included in Attachment 5. *HI-STORM 100S is being implemented by at least one Holtec client, with two exceptions:*

1. *The overpack lid is not rotated and the inlet and outlet air ducts remain in vertical alignment as shown in current technical specification Figure 3.2.3-1.*
2. *The current, more restrictive HI-STORM 100 overpack dose rate limits specified in LCO 3.2.3 will be complied with.*

*While the outlet air ducts in technical specification Figure 3.2.3-1 are shown as being located in the overpack body, this figure is illustrative is not a necessary detail for ensuring compliance with the LCO as supported by current Bases B 3.2.3 in FSAR Appendix 12.A (see also Proposed Change No. 4). Therefore, a change to the technical specifications is not required to implement the HI-STORM 100S as described above. Further, all issues identified in the NRC RAI regarding the HI-STORM 100S design have been resolved for the version being*

*implemented under 72.48.* The technical evaluations of HI-STORM 100S contained in the proposed FSAR changes in Attachment 6 are summarized by affected technical discipline below:

#### Structural Evaluation

The HI-STORM 100S overpack is a slightly shortened version of HI-STORM 100 overpack that is approximately 12,000 lb. lighter. The weight reduction has been achieved by reduction in the height of the concrete pedestal supporting the MPC and by the shortening of the overpack inner, outer, and shield shell, and the contained concrete. The weight of the HI-STORM 100S lid, however, is increased. Section 3.2 provides the specifics of the weights and center of gravity locations for the HI-STORM 100S loaded with the different MPCs. Detailed evaluations are performed in Chapter 3 to justify that nearly all analysis results previously performed and approved for the HI-STORM 100 bound results for the HI-STORM 100S and need not be repeated. Where justifications could not be provided, the detailed evaluations specific to the HI-STORM 100S are performed. All new safety factors specific to the HI-STORM 100S are greater than 1.0. Where required to perform specific evaluations for the short HI-STORM, new appendices have been added to Chapter 3. Attachment 6 details all changed text and calculations specific to the introduction of the HI-STORM 100S into the FSAR.

#### Thermal Evaluation

From the standpoint of thermal performance, the HI-STORM 100S overpack is nearly identical to HI-STORM 100. HI-STORM 100S features a slightly smaller inlet duct-to-outlet duct separation and a *different* gamma shield cross plate (which acts as a flow straightener) than its older counterpart. *The rotation of the outlet air ducts by 45 degrees has no consequence on the thermal performance or modeling of the HI-STORM system. Of the two gamma shield cross plate designs (discussed in the shielding evaluation below), the optional design creates more flow resistance and provides the limiting case for the thermal evaluation. With these changes considered,* the HI-STORM 100S peak fuel cladding temperatures are bounded by the HI-STORM 100 thermal solution. Therefore, HI-STORM 100S and HI-STORM 100 are considered to be interchangeable from the thermal-hydraulic standpoint.

#### Shielding Evaluation

The HI-STORM 100S overpack is quite similar to the current HI-STORM overpack. The only significant difference from a shielding perspective is that the MPC has been moved closer to the upper and lower air ducts. This results in an increase in the local dose rate at the opening of the ducts. In addition, the lid

design has been changed by moving the concrete shielding from below the 4 inch thick steel to above the 4 inch steel plate in the top lid. The radial shielding is identical between the HI-STORM 100 and the HI-STORM 100S overpacks.

Chapter 5 of proposed *Revision 1* of the HI-STORM FSAR specifically analyzes the HI-STORM 100S with the MPC-32 and the MPC-68. The MPC-24 analysis in the HI-STORM 100 overpack was unchanged. A comparison of the dose rates between the MPC-32 and MPC-24 indicates that the dose rate at the duct openings has increased in the HI-STORM 100S. This increase in the dose rate does not pose an ALARA concern and does not alter the HI-STORM 100 System's capability of meeting 10CFR72.104 requirements. Since the only significant change in the dose rate between the HI-STORM 100 and the HI-STORM 100S is at the duct opening, the previous analysis of the controlled area boundary dose rates using the HI-STORM 100 overpack was maintained.

*There are mandatory gamma shield cross plates, shown on the drawings, that must be installed in the HI-STORM 100S during storage operations. The mandatory design has been modeled in the shielding analysis.* For those users that are especially concerned with the dose rate at the duct openings, the HI-STORM 100S offers an optional gamma shield cross plate *design (described on the licensing drawings)* that has more metal than the *mandatory gamma shield cross plates* and would therefore further reduce the dose rates at the duct openings.

### **Proposed Change No. 34**

#### **Changes to FSAR Chapter 1**

- a. The text and figures in Sections 1.0, 1.1, 1.2, and *Appendix 1.D* have been revised throughout to address the new MPC models, HI-STORM 100S, HI-STORM 100A, new DFC designs, the increased heat duty of the cask, and other CoC changes from Section I.
- b. Table 1.0.1, Section 1.2, and Appendix 1.B have been revised to clarify the text regarding our Holtite-A neutron shielding material, consistent with our docketed correspondence dated August 18, 2000.
- c. Several definitions in Table 1.0.1 have been modified or added in support of other proposed changes in the CoC and FSAR document.
- d. Section 1.4 has been revised to clarify the requirements for cask spacing and make them more consistent with the thermal analysis basis.

### **Proposed Change No. 35**

#### Changes to FSAR Chapter 2

- a. The text and figures in Sections 2.0, 2.1, 2.2, and 2.3 have been revised throughout to address the new MPC models, HI-STORM 100S, HI-STORM 100A, new DFC design, the increased heat duty of the cask, and other CoC changes from Section I.
- b. *A footnote has been added to the accident temperature limit column in Table 2.2.3 to clarify the applicable temperature limit for steel components. Under accident conditions with only thermal and no mechanical loading, the ASME Code allows a temperature limit of 700°F. This change was required as part of the response to RAI Question 4.12.*
- c. Table 2.3.1 is revised to be consistent with the latest language in 10 CFR 72.104 and 72.106.

### **Proposed Change No. 35A**

#### Changes to FSAR Chapter 3

- a. *Appendices 3.N through 3.T, which contain only finite element node definitions and analysis output data, are deleted and the information re-located to the structural calculation package. This type of voluminous numerical data, with no accompanying explanatory text is more appropriately archived in the calculation package and not in the FSAR. Cross -references to these appendices in the chapter text have been appropriately revised.*
- b. *Appendices 3.AO and 3.AP, included as proposed new appendices in LAR 1014-1, Rev. 1 are no longer used. They contained detailed calculational information that is more appropriately re-located to the structural calculation package.*
- c. *Figures 3.A.19 through 3.A.30 are deleted from the FSAR and relocated to the structural calculation package. This information (time-history plots) is more appropriately located in the calculation package.*

### **Proposed Change No. 36**

#### **Changes to FSAR Chapter 7**

In addition to being revised to support high burnup fuel and other changes to the CoC, the confinement analyses have been revised to reflect new regulations at 10 CFR 72.104 and the revised review guidance in ISG-5 and ISG-15.

### **Proposed Change No. 37**

#### **Changes to FSAR Chapter 8**

- a. The operating procedures have been revised throughout to include lessons learned from cask loadings at Dresden Unit 1 and Plant Hatch and other enhancements.
- b. The chapter introduction has been revised to provide clarification regarding the need for users to develop and implement site-specific procedures that meet the intent of Chapter 8. *Mandatory and optional procedural steps and sequences have been noted in response to RAI Question 8.1.*
- c. The ITS categories for several ancillary components are clarified based on lessons learned from the ongoing engineering and manufacturing phase for these components.

### **Proposed Change No. 38**

#### **Changes to FSAR Chapter 9**

- a. Subsection 9.1.5.1 is revised regarding Holtite-A testing to re-define the frequency of testing to be every manufactured lot instead of every mixed batch.\*
- b. Subsection 9.1.5.1 is revised to allow the option of installing the lead shielding in the HI-TRAC transfer cask as pre-cast sections in lieu of pouring molten lead. This is for fabrication flexibility. Appropriate cautions are also added to minimize gaps if pre-cast sections are used.
- c. Subsection 9.1.5.2 is revised to allow gamma scanning of the HI-TRAC shielding prior to, or after the installation of the water jacket. This is fabrication flexibility.

- d. *Subsection 9.1.5.3 has been modified in response to RAI Question 9.1 to discuss neutron absorber visual inspection requirements.*

### **Proposed Change No. 39**

#### **Changes to FSAR Chapter 10**

- a. The occupational exposure estimates were revised throughout to account for the revised dose rates due to fuel and MPC changes, and the HI-STORM 100S configuration.
- b. Table 10.1.2 has been revised to provide general licensees with the flexibility to decide for themselves whether or not temporary shielding is required based on the particular age and burnup of the fuel being loaded, and the actual dose rates measured. Long cooling time and/or low burnup fuel may yield very low dose rates, even with the HI-TRAC 100, potentially obviating the need for any temporary shielding. Users' radiation protection programs will govern the use of temporary shielding.
- c. *The term "thermocouples" is changed to "temperature elements" throughout to be consistent with changes elsewhere in the document.*

### **Proposed Change No. 40**

#### **Changes to FSAR Chapter 11**

- a. The events and accidents in Subsections 11.1 and 11.2 have been reanalyzed, as necessary to reflect changes made to the authorized contents and heat loads for the MPC in Section I.
- b. *Subsection 11.2.13.4 has been modified in response to RAI Question 4.12 and to be consistent with new Section 3.4.9 of Appendix B to the CoC.*

### **Proposed Change No. 41**

#### **Changes to FSAR Chapter 12**

The list of technical specifications in Tables 12.1.1 and 12.1.2 and the Bases in Appendix 12.A are revised to match the changes to the technical specifications proposed in Section I.